

POLITECNICO DI MILANO
School of Industrial and Information Engineering
MSc in Energy Engineering – Sistemi per l'energia e l'ambiente



UNIVERSIDAD PONTIFICIA BOLIVARIANA
Escuela de Ingenierías
Maestría en Ingeniería - Grupo de Investigación en Energía y Termodinámica
Centro de Investigación, Desarrollo y Calidad en Refrigeración y Climatización – CIRCLI



PERFORMANCE ANALYSIS OF SOLAR-POWERED AIR-CONDITIONING SYSTEM
USING ABSORPTION REFRIGERATION CYCLE AND HIGH EFFICIENCY COOLING
TECHNOLOGIES INSTALLED IN COLOMBIA

SUPERVISOR
Paolo Silva

AUTHOR
Caterina Fella
841917

CO-SUPERIVSOR
Cesar Isaza Alejandro Rolán

July 2017

1 INDEX

2	Summary	3
	Sommario	3
3	Introduction	5
4	Chapter 1.....	9
4.1	System description.....	9
4.1.1	Evacuated heat pipe tube collectors (ETCs).....	12
4.1.2	Absorption refrigeration chiller	18
4.1.3	Pressurized water storage tanks	26
4.1.4	Auxiliary heater	27
4.1.5	Closed circuit adiabatic cooler	28
4.1.6	Water capillary mats	32
4.1.7	Water pipeline including five pumps	34
4.1.8	The coolerado	37
4.1.9	Air duct for the coolerado.....	43
4.1.10	Auxiliary and measurement components.....	45
5	Chapter 2.....	46
5.1	Performance analysis	46
5.1.1	Absorption Chiller performance analysis.....	46
5.1.2	Collectors performance analysis	64
5.1.3	Coolerado performance analysis	69
5.2	Economic analysis	74
5.2.1	Fixed Costs	74
5.2.2	Variable Costs.....	76
6	Conclusions	80
7	Annex	83
8	Figure list.....	88
9	Table list.....	90
10	Glossary.....	91
11	References.....	94

2 SUMMARY

In this work is presented an analysis of the performance of solar absorption air-cooling system installed to a building office of the Bolivarian Pontifical University (UPB) of Medellín in Colombia. The solar powered, single-effect Li-Br absorption cooling system using evacuated heat pipe collectors, has a nominal capacity of 11,5 kW and it is implemented with a 17,6 kW indirect evaporative cooler, responsible to improve the energy efficiency and to renovate the air in the building, for a total cooling capacity of more than 29 kW (more than 8 refrigeration tons). A system of chilled water capillary mats is implemented for air conditioning, where the heat transfer takes place through a radiant ceiling, reducing recirculation airflow and increasing the temperature of chilled water supplied, allowing a reduction in energy consumption by airflow and an improvement in energy efficiency of the solar-powered absorption cooling system.

Once defined the system in all of its part the further step is to perform its operation in different conditions. The performance are evaluated for three main subsystem composing the air conditioning system: the absorption chiller, the heat pipe evacuated tube collectors and the indirect evaporative cooler, called Coolerado.

The analysis is carried out through experimental test-measurements (TMs), whose intent is to evaluate the use of new technologies used in Colombia ambient conditions. A series of TMs are carried out varying the value of one or more particular parameters that affects the performance. Indeed the operational parameters in terms of temperatures of the flux involved and instant power consumption are measured during the whole period of TMs. Some indicators, which describe the performance, are calculated and compared, so an evaluation of the different TMs is provided. In more is presented an economic comparison with a conventional scheme in order to assess the potential energy savings of the system, the simple payback period of the investment is calculated for different size and cooling demand of the system presented for both Colombian and Italian case.

Keywords: Solar Cooling system; absorption chiller; heat pipe evacuated tube collectors; indirect evaporative cooler; performance analysis; experimental test-measurements; simple payback period

SOMMARIO

In questo elaborato è presentata una analisi delle prestazioni di un sistema solare di aria condizionata installato per un edificio amministrativo della Università Pontificia Bolivariana (UPB), a Medellín, COLOMBIA.

La macchina frigorifera ad assorbimento a singolo effetto a miscela binaria H₂O/BrLi ha una capacità nominale di 11,5 kW ed è accoppiata a pannelli solari a tubi evacuati. Il sistema è implementato con un condizionatore d'aria per raffreddamento evaporativo indiretto che ha una capacità nominale di 17,6 kW, per una totale capacità frigorifera superiore a 29 kW. Quest'ultimo è responsabile nel rinnovare l'aria nell'edificio e migliorare l'efficienza energetica del sistema di tubi capillari di acqua gelata, installato sulla parete dell'edificio così da creare un tetto radiante, responsabile della climatizzazione nel locale. Il tetto radiante scambia calore con l'ambiente per radiazione assorbita dalle superfici emittenti e convezione naturale di correnti d'aria (quest'ultimo favorito dalla presenza del Coolerado), pertanto rispetto alle tradizionali fun-coil, riduce l'aria di ricircolo e la climatizzazione risulta efficace anche a temperatura dell'acqua refrigerante maggiori, permettendo una riduzione nel consumo energetico e quindi un miglioramento nell'efficienza energetica del sistema solare di aria condizionata.

Una volta definito il sistema in tutte le sue parti, lo step successivo è testare il suo funzionamento in differenti condizioni di operazione. Le prestazioni sono state valutate per i tre grandi sottosistemi che compongono il sistema solare di aria condizionata: la macchina frigorifera ad assorbimento, i collettori solari a tubi evacuati e il condizionatore per raffreddamento evaporativo indiretto, chiamato Coolerado.

Con l'intento di valutare l'uso delle nuove tecnologie sopra citate, nelle condizioni ambientali della Colombia una serie di prove sperimentali sono state effettuate variando i parametri che incidono sulle prestazioni del sistema. Le prestazioni del sistema in differenti condizioni di operazione sono valutate attraverso l'uso di coefficienti di prestazione, estrapolati attraverso la misurazione dei parametri operativi caratterizzanti il sistema, in termini di temperature dei flussi coinvolti e dei consumi istantanei di potenza.

Inoltre è presentata una comparazione dei costi rispetto ad una macchina frigorifera che sfrutta il tradizionale ciclo a compressione di vapore, attraverso il calcolo del periodo di ammortamento dell'investimento, per differenti taglie dell'impianto e differenti fabbisogni di raffreddamento, così da valutare il potenziale risparmio economico nel tempo che ne deriva dal sistema solare di aria condizionata.

Parole Chiave: sistema solare di aria condizionata; macchina frigorifera ad assorbimento; pannelli solari a tubi evacuati; condizionatore per raffreddamento evaporativo indiretto; analisi delle prestazioni; prove sperimentali; periodo di ammortamento dell'investimento

3 Introduction

Buildings represents a fundamental impact in people life and planet's sustainability. In developed Country, Buildings produce high CO₂ emissions as they consume almost 40% of worldwide energy [1], more than 65% of electricity and more than 10% of the water and are responsible for the depletion of Earth resources [2]. In developing Country, like Colombia, the use of these resources and its impact on the ambient could be even more relevant, because of the obsolete technology used for the construction and operation. This situation provoke that several institutions, associations, governments and business company interest on implementation of measurements that goes to rationalise the use of natural resources in the building construction and make this buildings more environmentally friendly like government policies and tax incentives that aimed at efficient energy management to reduce CO₂ emissions [1]. In this contest, was defined the concept of sustainable building or green building, as a standard given by evaluation of the environmental performance about building cycle-life. [3]. According with U.S. Green Building Council (USGBC), to accomplish the requirement for being labelled as "sustainable building", six chapter of evaluation have been created, and one of the most important, being a chapter which gives a lot of points, is "Energy and Mass", which consider the minimum energy performance, the chlorofluorocarbons (CFC) reduction and heating, ventilation, air-conditioning and refrigeration equipment. In this way is possible to evaluate the use of renewable energy and constantly to measure energy consumption and efficiency in the time.

In Colombia the way and the construction processes caused big impact on the environment. The buildings represent a big part of this problem and it is clear the impact of them over its surroundings and over the population [4]. To reach a state of "sustainable building" a big effort is needed in term of money and technology development, existing actually a scarcity in experiences and a low number of success cases in the Country (www.cccs.org.co). Anyway, the Colombian Government has started to move toward the direction in implementing the energy efficiency's knowledge grid, instituting programmes and investing in projects whose aim is to improve the production's system and to drive the productivity and the competitiveness of industry sector towards a major efficiency of thermal and electrical systems, so to work with more sustainable power systems in term of environmental resources depletion and emissions. In Colombia still doesn't exist an established normative which promote and estimate the energy consumption of the buildings, anyway, Green building and Net Zero Energy building are promoted through different agency and institutions like US Green Building Council (USGBC), European University Association (EUA) and "Colombian Council of Security"(CCCS), that through national and international regulations certificate a building. ASHRAE contributes with several norms and instructions thought guide USGBC to determinate the prerequisites and the modality to assign point. One of these guide are:

- "Guía 0-2005 El proceso de Puesta en Marcha" (Iniciacion process)
- "Guía 1-1996 El Proceso de la Puesta en Marcha de Sistema de Aire Acondicionado y Ventilación (Initiation process of Cooling and Ventilation Systems)
- "Norma 100-1995 Conservación de Energía en Edicios Existentes" (Energy Saving of existing buildings)

Which will constitute the basic references for the project that is going to be presented. [2]

A remarkable percentage of the energy consumed by a building is used for achieving thermal comfort conditions, both in heating and cooling. Refrigeration Cycle working by electrical energy contribute to the energy and fossil fuel consumption significantly. Thermal comfort is one of the first priorities, as it represents around 65% of building energy consumption [13]. The International Institute of Refrigeration (IIR) estimated that 15% of total energy produced in the world is employed for refrigeration and air-cooling purposes. Even though the air conditioning system working by electric energy have reached relative high standards in term of energy consumption, still require high quantity of electricity and cause significant pick loads to the electrical network. Additionally, the conventional cooling systems employ working fluids as chlorofluorocarbons (CFC), hydro-chlorofluorocarbons (HCFC) and hydro-fluorocarbons (HFC) considered as the cause of depletion of

ozone- layer of our planet and favour the greenhouses effect and in some way the incrementing of medium global temperature (Wuebbles, 1994). From the Montreal Protocol of 1987, where depletion ozone potentials and trends of the refrigerants were stabilized, international treatise was firm for the reduction in emissions of these refrigerants. Colombia has part of these treatise since the approbation of the Ley 29 of 1992. The Intergovernmental Panel of Climate Change (IPCC) in its 4th Assessment Report 2007 introduce the Global Warming Potential of refrigerant gases used into conventional systems [5]. During recent years several investigation have been concentrated in developing the technology which can provide a reduction in energy consumption, in load peak of energy demand and in energy costs without damaging desired levels of thermal comfort conditions. Principles and strategies of energy savings and efficient energy use have been established with a strong character of sustainability. With the prospective of an growing market of air-conditioning system and considering the saturation grade of electric network of the Countries, a lot of Institutions, enterprises and energy companies are carrying out big effort in introducing in the global market new air cooling technologies with an higher energy efficiency and a rational use of different energy sources. Among the different strategy in achieving thermal comfort reducing energy consumption and environmental impact in the buildings, new thermally operated air-conditioning systems exist. One alternative is absorption refrigeration cycle, which can operate with renewable energy, as solar energy, that is the most widely renewable energy all over the World [4]. Solar power is sufficient to cover the thermal comfort demands in medium and low latitude regions, and it is not a fortuity that a solar-powered absorption cooling system has been projected in Medellín, whose latitude is 6° 15' 6 N. Among the various solar air-conditioning alternatives, the absorption cooling system appears to be one of the most promising methods [6], because of the fact that the pick concentration of solar energy coincides with the hours when the cooling is required (Figure 1).

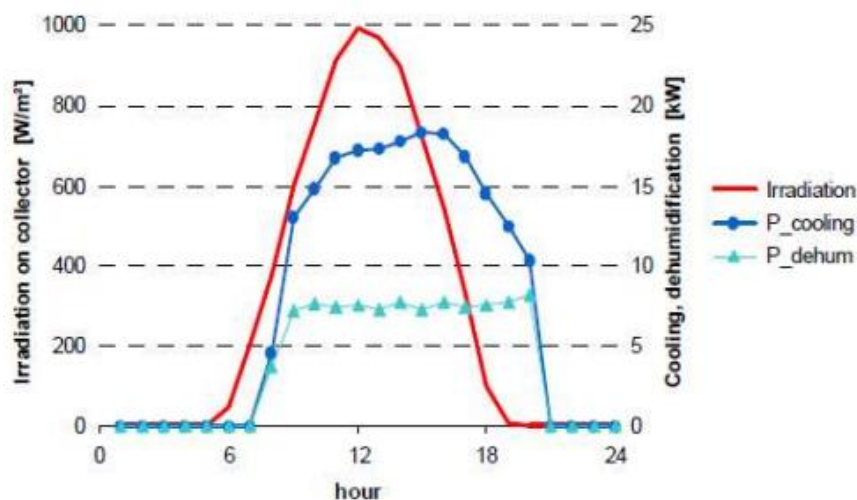


Figure 1: Irradiation on collector surface and cooling demand over a day.

The use of solar refrigeration is not recent; from 1935 installation of air-conditioning solar system exists in USA and since that period a big number of project of solar refrigeration and air-conditioning have been planned all over the World.

Several public and private initiatives have been carry out with the aim to promote the development of solar refrigeration and air conditioning systems. Some of these initiatives have been directed to spread out knowledges come from experiments and investigations of the technology, and other to raise the users' awareness of the importance of clean technologies that contribute to improve environmental conditions and energy savings. Finally, manufacturing consortium and technology development centres succeeded in producing equipment that now are commercially available.

International Energy Agency (IEA) sponsored Task 25 (Solar Assisted Air Conditioning Buildings, www.iea-shc-task25.org) and IEA SHC Task 38 (Solar Air-Conditioning and Refrigeration, www.iea-shc.org), whose objective is the application of measurement in order to introduce in the market solar air-conditioning and refrigeration systems. It is still involved in organizing activities of developing and testing of the equipment, preparing reports about experiences of pilot projects and demonstrations, building up simulation tools for the modelling and the simulation of analysis of the systems. IEA published "Solar-Assisted Air-Conditioning in Buildings A Handbook

for Planners”, that constitute one of the principal information source for the sector.

In the context of the project SOLAIR (Solair Poject 2008, www.solar-project.eu), the solar refrigeration or the solar air-conditioning are used for contributing to:

- Replace the energy demand from fossil fuel and conventional energy source with thermal solar energy.
- Reduce the greenhouses gases emissions.
- Support the electric network stability reducing the electric energy consumption and peak demand.
- Optimize the use of thermal solar energy through combined solar heating space/water and refrigeration system.

In the October 2007, for the 2nd International Conference of Solar Air Conditioning, in Tarragona – Spain, among European Countries, remarkable project are located in France, Germany, Belgium, Italy, Spain, Portugal, Grece, Danmark and Russia (HIGH-COMBI, SOLCO, SAHC, Medisco, ROCOCO, KeepCool, SACE). The Solar Energy Technologies Program make USA, Mexico, Cuba and Brasil stand out in America. In Asian Country stands out the participation of Japan, Australia and Oceania and among Middle-East Country, Israel and Turkey. In Africa two important projects were developed in Nigeria and Egypt. These Countries permit a wide diffusion of solar cooling technologies, reporting 81 successful cases at global level, whose 73 are localised in Europe, 7 in Asia and 1 in North America, in particular in Mexico. 60% of these installations are dedicated to office buildings, 10% to factories, 15% to laboratories and education centers, 6% to hotels and the left percentage to buildings with different final use (hospitals, canteen, sport center, etc). Fifty-six (56) installation operate with technology using absorption cycle (LiBr/Water), ten (10) with adsorption system and seventeen (17) with dessicant evaporative cooling systems (DEC). Among the DEC installations, only 2 systems use a liquid regenerator (DEC liquid). The overall cooling capacity of the solar thermally driven chillers amounts to 9 MW, 31% of it is installed in Spain, 18% in Germany and 12% in Greece[7] (Figure 2)

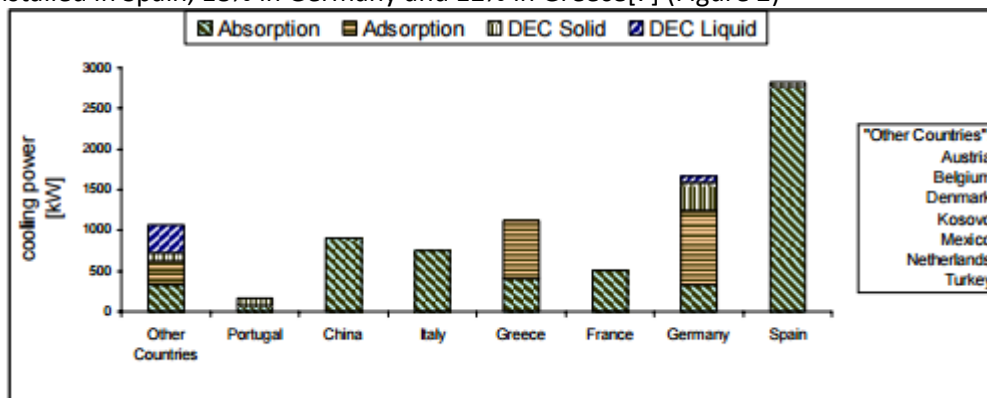


Figure 2: Worldwide distribution of the cooling power assisted by solar energy and type of thermally driven chillers applied in the different countries [7].

In Iberoamérica the principal initiative that rise up in 2001 with the spirit of promoting and diffusing the technologies that produce cooling with solar energy, was RIRAAS grid (Red Iberoamericana de Refrigeración y Aire Acondicionado Solar, www.riraas.net). It was co-financed by “Ciencia y Tecnología para el desarrollo”(CYTED) and by the National Council of Mexico of Science and Development” (CONACYT), until the 2004. Basically, nowadays in Latin-America is counted of one installation of air-conditioning solar system in Mexico and several university prototypes in Universities and Centre of investigation for the investigation and development of varies technologies for the solar cooling. (Best 1998, RIRAAS 2004).

In Colombia after a first period of isolated experience of the technology of absorption cooling system in the Atlantic Cost, the technology has seemed to be completely abandoned because of no successful endurance over time of these plants that caused a diffused bad reputation among the users involved, that has brought the markets to a standstill. The introduction of new technology, in fact, require organized plans that guarantee an adaptation of the new systems to the Country’s conditions. Anyway, today, reacting to this fact, many Colombian enterprises are again going to pay attention to the absorption refrigeration systems. In part this phenomenon has been marked by the multinationals, since, at global level, the absorption refrigeration system has experimented a vertiginous growth thanks to the technology improvements, the training programmes for the technicians and promotional campaigns of high efficient and environmentally friendly technologies previously mentioned. Anyway, a cooling absorption system which exploit a totally free and renewable energy,

indeed the solar energy, never before were experimented in the Country. The project presented is the 7th out of 8 projects belonging to the National Strategic Plan of Energy Management that includes four-years last projects in order to implement energy efficiency of Colombia's electric and thermal energy production systems, reduce the emissions and the environment resources depletion. This project was born as implementation of air-conditioning system for a building office, called Building 24, of UPB by the Li-Br solar absorption cooling system with evacuated tube collectors. The office selected hosts about 50-80 persons and has an area of 239 m², indeed, for improving the energy efficiency of the air conditioning system, an indirect-evaporative air cooler responsible in renovation of the air, was installed, resulting that the air entering is provided at lower temperature than the temperature outside. Employing both system the thermal capacity needed for the office building is satisfied. The peculiarity of this air-conditioning system consists on the use of chilled water capillary mats instead of conventional fan coils. The heat transfer takes place through a radiant ceiling, reducing recirculation airflow and increasing the temperature of chilled water supplied, allowing a reduction in energy consumption by airflow and an improvement in energy efficiency of the solar-powered absorption cooling system.

4 CHAPTER 1

4.1 SYSTEM DESCRIPTION

The project presented is the 7th out of 8 projects belonging to the National Strategic Plan of Energy Management (Programa Estratégico Nacional Sistema de Gestión Integral de Energía SGIE). The National Government of Colombia in 2014 announced the “Call 543- Energy Efficiency in productive sector” which consists on four-years last projects included in a program titled “Consolidation of Colombian knowledge network about Energy Efficiency (Consolidación de la Red Colombiana de Conocimiento en Eficiencia Energética RECIEE)”. The main object of this programme is the implementation of energy efficiency of Colombian electric grid and thermal energy production systems. By means of projects in energy management and theoretical investigations about sustainable systems for energy production, the programme aims to include the industrial sector so to observe important impacts both in the productivity and competitiveness of industrial sector and in the quality of life. The programme also aims to identify an unifying concept between University, Companies and Government (Universidad-Empresa-Estado UEE) and a management model for the continuity and sustainability of the programme’s results and for the strategies for the electric energy of the Country.

This project was born as implementation of air-conditioning system for a building office by Li-Br solar absorption cooling system with evacuated tube collectors, that indeed will exploit renewable energy reducing both the CO₂ emissions and exploitation of natural resources, according to the sustainable initiative that focus the Programme.

The system is installed in Pontifical Bolivarian University (UPB), in Medellín, in the region of Antioquia, in Colombia. The city is also know as the city of eternal spring, presenting full year mostly sunny weather, with diurnal temperature which oscillate between 22°C and 35°C and a relative humidity between 20% and 75%. For this reason, it suits very well with this type of system, having all the year a sunny climate, and for the same reason each month results a cooling season. Its latitude and longitude are 6° 15’ 6 N and 75° 33’ 48 W respectively.

Inside the activity which were planned to do the first were to choose an appropriate building that match with the actual needs and was appropriate for demonstrative installation. “Building 24- Comprehensive Counseling.” of the Pontifical Bolivarian University was chosen for the following reasons:

- The building did not present an air- conditioning system; it was projected to be in a relatively windy area indeed was thought to solve the problem by inserting perforated grids that allow to circulate air from outside to inside creating air currents.
- The building has a peculiarity to be interconnected to all the staff and students of the University, being an office building were bureaucratic procedures are solved.
- The workers inside the building were not in optimal thermal conditions because results that the building hosts in some peak period about 80 persons.

Building 24 is located on the southwestern side of the campus, close to the pedestrian gateway of Nutibara Avenue with Circular 1^a; it presents easy access and great visibility, here below Figure 3, which shows the map of the Building.

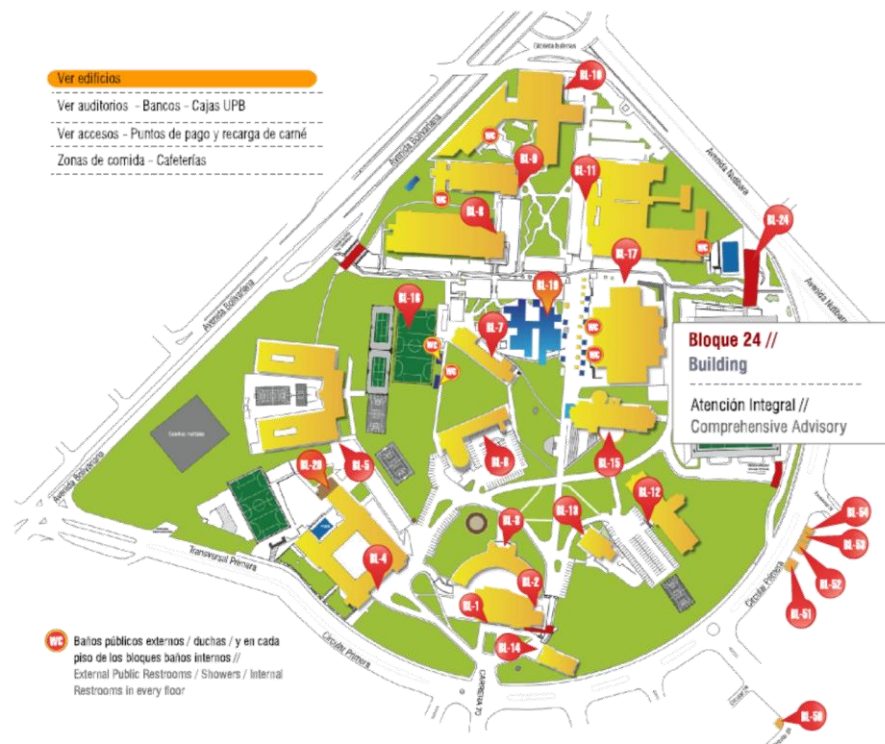


Figure 3: Map of UPB with a focus on Building 24 [8]

The next activity planned were the thermal load calculation, indeed the tons of cooling capacity required for air-condition the building chosen. The calculation were executed dimensioning the system with the pick load that could happen over 3 or 4 months in the year. The following characteristic were considered in order to calculate the thermal load:

- Number of person ordinary occupied the building: among 20 workers
- Number of person occupied the building in peak period: between 50 and 80 hosts
- Volume of the building: $239 \text{ m}^2 \times 4 \text{ m}$
- Border of the building: built in white block wall, roof in thermo-acoustic type metal roof tile, suitable for installing solar collectors in the upper part.

The Figure 4 shows a schematic view of the installation of the heat pipe-tube collector on the roof of the building 24, where there are installed also solar photovoltaic panel for different purposes.

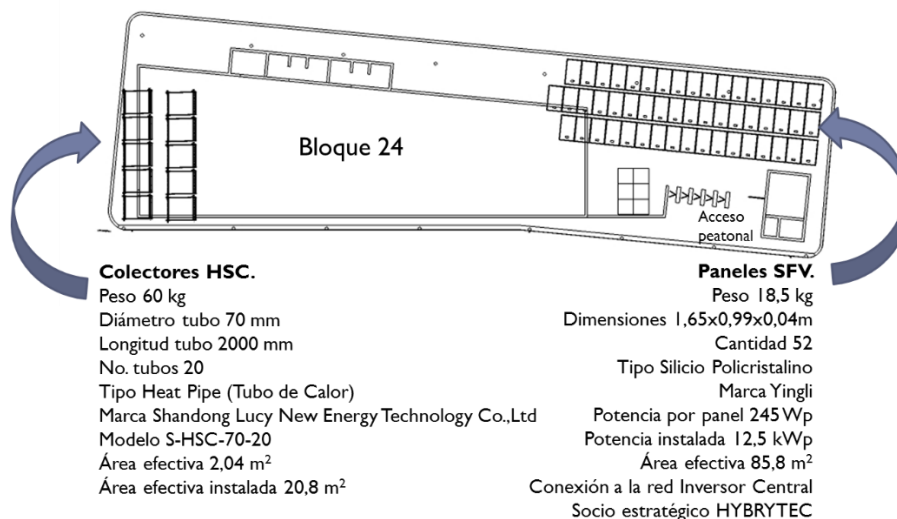


Figure 4: Schematic view of the roof of Building 24 [8]

The appropriate technologies for the installation were finally chosen after an accurate selection of the equipment between several trademarks from America, China and Europe, with the aim to choose the most advanced technologies in the field of the solar absorption air conditioning system. The Figure 5 shows a schematic picture of the system with its principal component by the screen control of the engineering software used in order to test, measure and control the its data. For a good understanding, a description of the most important sub-system that characterize this unique configuration of Li-Br solar absorption air conditioning system, in order to justify the technologic choices that have been taken and focus on the specifications needed for proceed to a performance analysis.

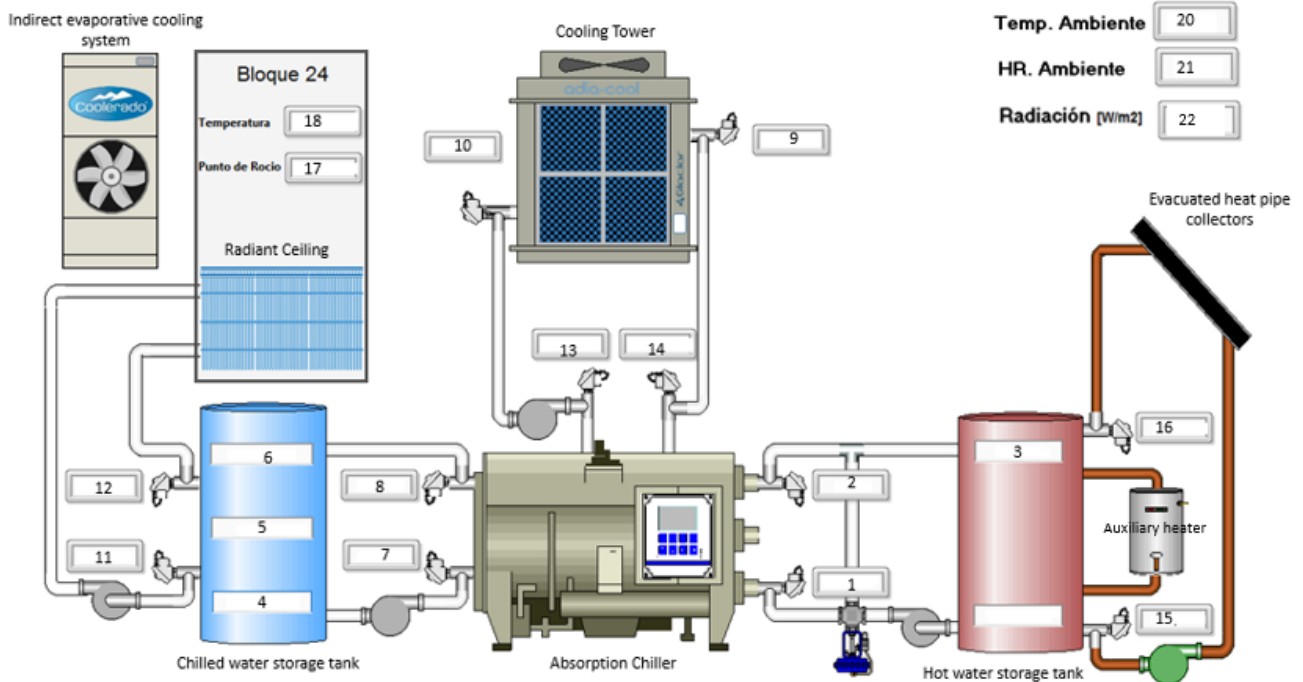


Figure 5: LabView Control screen of the system

4.1.1 Evacuated heat pipe tube collectors (ETCs)

Solar thermal systems use solar heat in order to produce cooling effect. Solar thermal collectors convert sunlight into heat and this heat in turn drives a heat driven refrigeration machine. Solar collectors are available in different types and in a wide range of efficiency.

The collectors selected are evacuated tube collectors (ETCs) and of heat pipe tube type. These solar collectors consist of a heat pipe inside a vacuum-sealed tube, and many tubes are connected to the same manifold. Evacuated tube collectors use liquid-vapour phase change materials to transfer heat at high efficiency. These collectors feature a heat pipe (a highly efficient thermal conductor) encased with a vacuum-sealed tube (a glass cover and insulation material). The pipe, which is a sealed copper pipe, is then attached to a black copper fin that fills the tube (absorber plate). The absorber surface is coated with a selective absorption film (Ti-N-O/Cu) that has a high absorption for the solar spectrum and low emittance for infrared radiation, in more it is high temperature resistant, antiaging and no stripping (Lucy New Energy Tecnology). Protruding from them top of each tube is a metal tip (a manifold made of aluminium alloy inner and red copper outer) attached to the sealed pipe (condenser) (point 4 in Figure 9). The heat pipe contains a small amount of fluid (e.g. methanol) that undergoes an evaporating-condensing cycle. In this cycle, solar heat evaporates the liquid and the vapour travels to the heat sink region, where it condenses and releases its latent heat. The condenser has a much larger diameter than the shaft to provide a large surface over which heat can be transferred to the header. The condensed fluid returns to the solar collector and the process is repeated. The vacuum envelope reduces convection and conduction losses: the space between absorber and glass cover is evacuated to minimize heat loss, so that the collectors can operate at higher temperatures than flate-plate collectors. Like flate-plate collectors, they collect both direct and diffuse radiation. However, their efficiency is higher at low incidence angles. This effect tends to give evacuated tube collectors an advantage over flat-plate collectors in terms of daylong performance.

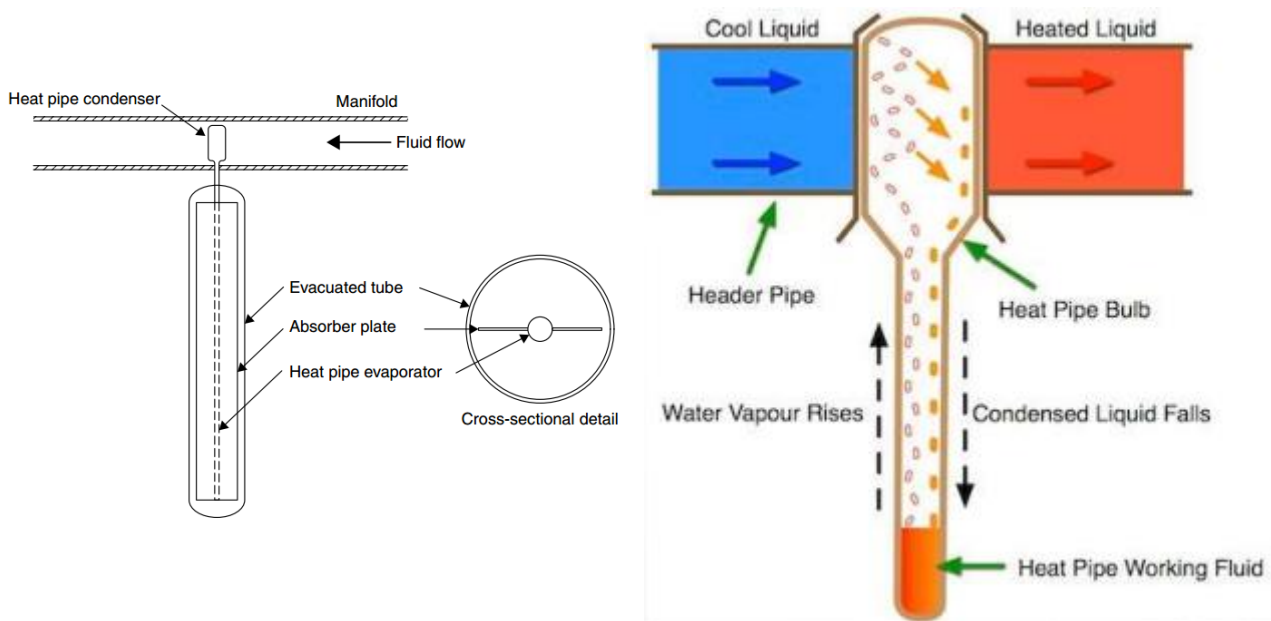


Figure 6: Schematic diagrams of an evacuated tube collector[9]

Have demonstrate that combination of selective surface and an effective convection suppressor can result in a good performance at high temperatures. Because no evaporation or condensation above the phase-change temperature is possible, the heat pipe offers inherent protection from freezing and overheating. This self-limiting temperature control is a unique feature of the ETCs. [10]

A comparison of the efficiency of various collectors at irradiance levels of 500 W/m^2 and 1000 W/m^2 is shown in Figure 7. Five representative collector types are considered: Flat-plate collector (FPC); Advanced flat-plate collector (AFP); Stationary compound parabolic collector (CPC); Evacuated tube collector (ETC); Parabolic trough collector (PTC).

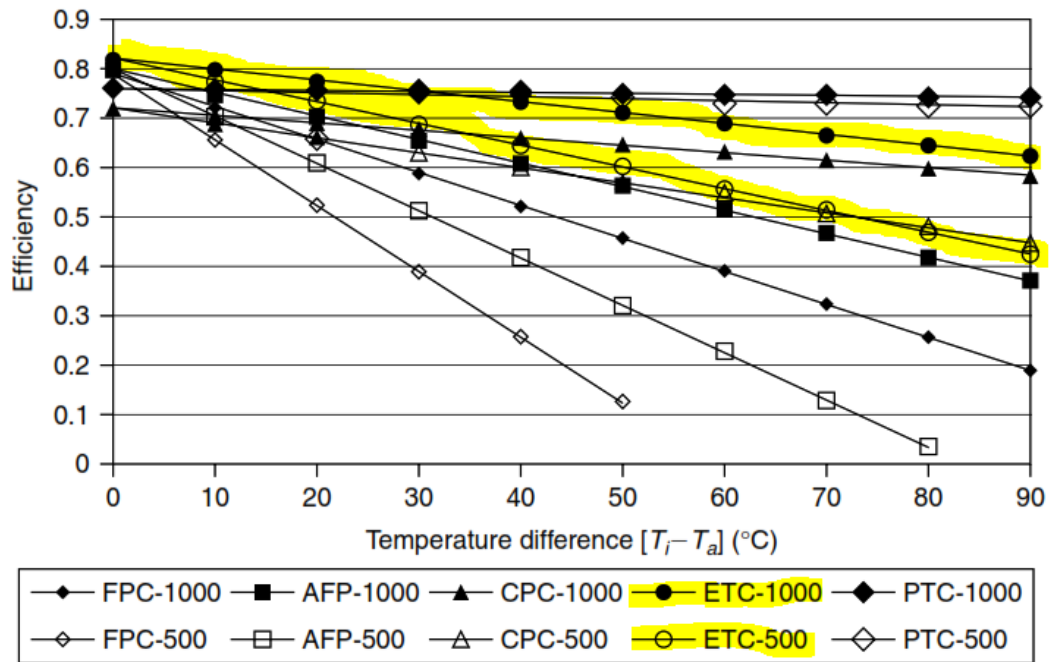


Figure 7: Comparison of the efficiency of various collectors at two irradiance levels: 500 W/m² and 1000 W/m² [10]

As seen in Figure 7, the higher the irradiance level, the better is the efficiency, and the higher-performance collectors, such as the CPC, ETC, and PTC, retain high efficiency, even at higher collector inlet temperatures. It should be noted that the radiation levels examined are considered as global radiation for all collector types except the PTC, for which the same radiation values are used but considered as beam radiation.

The ETCs present some negativities: the quality of the heat transport also can be seriously affected if the heat pipe contains too much condensable gasses. They can form a pocket of air in the top of the heat pipe. This has the effect of moving the heat pipe's hottest point downward away from the condenser.

For the project were chosen a Chinese brand heat pipe tube. It should be noted that the operating temperature of the hot water supplied to the generator of the LiBr-water absorption chiller, as is shown from its specifications reported on Table 3, is between 70°C and 90°C. The lower temperature limit is imposed from the fact that hot water must be at a temperature sufficiently high (at least 68°C) to be effective for boiling the water off the solution in the generator. [9] For a number of 20 tubes for 10 collectors, the effective lighting area installed resulted of 20,4 m². The ETCs are connected directly to a hot water storage tank [10]. The collectors were installed on the roof of the building 24. Although it is recommended to incline the collector according to the latitude of the place, in order to catching the most direct radiation of the sun, it resulted that didn't permit the natural cleaning of the collectors by the rain and for this reason an inclination of 10° was chosen, that is still very near to that of Medellin. Being the collectors installed in north hemisphere, they are directed to the South.



Figure 8: direction and inclination of the collectors

Technical specification of the whole collector		Technical specification of evacuated heat pipe tube	
Brand	Shandong Lucy New Energy Technology Co., Ltd	Manifold inner (n 3 of Figure 9 and n 5 of Figure 12)	Red copper, 1,5 mm
Model	S-HSC-70-20	Manifold outer (n 8 of Figure 9 or n 6 of Figure 12)	Aluminum alloy, 2,5 mm
Type	Heat pipe	Length of tube (Figure 10)	2000 mm
Collector's Width	1860 mm	Diameter of tube (Figure 10)	70 mm
Collector's length	2000 mm	Material of conducting strip (6 of Figure 9)	Copper
Weight of vacuum	60 kg	Length of conduction strip	1700 mm
Number of tubes for collector	20	Width of conducting strip	60 mm
Number of collectors	10	Thickness of conducting strip	0,12 mm
Effective lighting (absorber) areas per collector (20 tubes)	2,04 m ²	Glass type	Borosilicate
Effective lighting area installed	20,4 m ²	Glass thickness	2 mm
Orientation (azimuth)	South (0°)	Transparency	95%
Inclination angle	10°	Absorber material (A3 Figure 12)	TI-N-O/Cu
Collector's gross area	3,72 m ²	Solar absorption	≥96 % (≥90 % in winter)
Total gross area installed	37,2 m ²	Heat emission	≤4 %
Max pressure	12 bar	Heat pipe thickness (6 of Figure 9)	1 mm
Stagnation temperature	280 °C	Heat pipe condensation diameter (2 of Figure 9)	24 mm
		Heat pipe condensation length	90 mm
		Glass tube vacuum grade (D3 of Figure 11)	1.0× 10 ⁻⁴ bar
		Heat pipe vacuum grade (B3 of Figure 11)	1.0× 10 ⁻¹⁰ bar
		Heat Pipe Anti-freezing	≥- 35 °C

Table 1: Specifications of the evacuated tube collectors (ECTs)

In order to speak of performance of the system is necessary to study how to measure the efficiency of the collectors installed in Building 24, indeed with respect to Medellín weather conditions. Here below is presented a study of the efficiency of this type of solar collector presented in Solar Engineering of Thermal Process by Duffy at all. [11], with the aim to further apply this mathematical model with the ECTs chosen in the solar absorption air-conditioning system. Under steady-state conditions, the rate of useful heat delivered by a solar collector is equal to the rate of energy absorbed by the heat transfer fluid minus the direct or indirect heat losses from the surface to the surroundings.

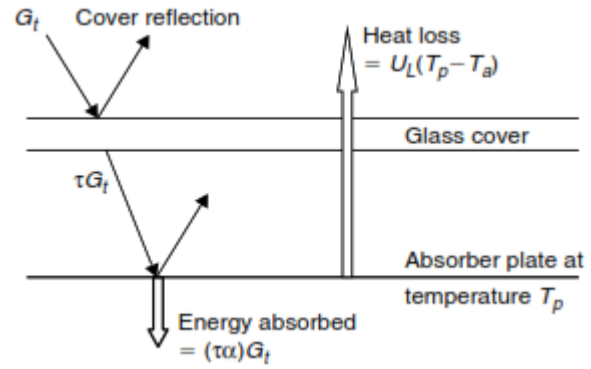
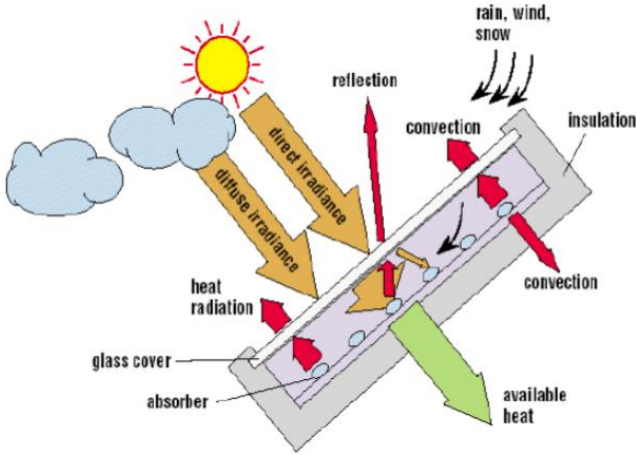


Figure 13: Energy losses in a solar collector (Peter Lund, 2016) Figure 14: Radiation input and heat loss from a collector[10]

The absorbed solar radiation is equal to $G_t(\tau\alpha)$, (where $\tau\alpha$ is the transmittance-absorptance product, describing the properties of the glass and the absorber) and thermal energy lost from the collector to the surroundings by conduction, convection, and infrared radiation is represented by the product of the overall heat loss coefficient, U_L , times the difference between the collector average temperature, $T_{col,av}$, and the ambient temperature, T_a . Therefore, in a steady state, the rate of useful energy collected from a collector of area A_c can be obtained from

$$Q_u = A_c [G_t(\tau\alpha) - U_L(T_{av,col} - T_a)] = \dot{m}c_p [T_o - T_i] \quad (I)$$

This equation can also be used to give the amount of useful energy delivered in joules (not rate in watts), if the irradiance G_t [W/m^2] is replaced with irradiation I_p [J/m^2] and we multiply U_L [$W/m^2 \cdot ^\circ C$], by 3600 to convert to joules per square meter in degrees Centigrade ($J/m^2 \cdot ^\circ C$) for estimations with step of 1 h.

It is usually desirable to express the collector total useful energy gain in terms of the fluid inlet temperature. To do this the collector heat removal factor needs to be used. Heat removal factor represents the ratio of the actual useful energy gain that would result if the collector-absorbing surface had been at the local fluid temperature. Expressed symbolically:

$$F_R = \frac{\text{Actual output}}{\text{Output for tube temperature = Fluid inlet temperature}} \quad (II)$$

and mathematically:

$$F_R = \frac{\dot{m}c_p(T_{f,o} - T_{f,i})}{A_c(S - U_L(T_{f,i} - T_a))} \quad (III)$$

Where S is absorbed solar radiation per unit area (J/m^2); Seebeck coefficient.

If we replace the nominator of Equation (III) with Q_u and S with $G_t(\tau\alpha)$ of the equation (I) than the following equation is obtained:

$$Q_u = A_c F_R [G_t(\tau\alpha) - U_L(T_i - T_a)] \quad (IV)$$

This is the same of previous equation with the difference that the inlet fluid temperature T_i replaces the average tube temperature ($T_{av,tube}$) with the use of F_R . The temperature of the inlet fluid, T_i , depends on the characteristics of the complete solar heating system and the hot water demand or heat demand of the building. However, F_R is affected only by the solar collector characteristics, the fluid type, and the fluid flow rate through the collector.

Indeed, to measure a performance of a the solar collectors the following parameters need to be measured:

1. Global solar irradiance at the tube, $G_t \frac{W}{m^2}$.

2. Diffuse solar irradiance at the collector aperture.
3. Air speed above the collector aperture.
4. Ambient air temperature, T_a .
5. Fluid temperature at the collector inlet, T_i .
6. Fluid temperature at the collector outlet, T_o .
7. Fluid flow rate, \dot{m} .

The efficiency of a solar collector is primarily determined by its working temperature. At a higher working temperature, the collector loses more heat to ambient and delivers less heat. On the other hand, the heat engine or thermal compressor generally works more efficiently with a higher temperature. A solar thermal system is designed in consideration of these two opposing trends.

The thermal efficiency is obtained by dividing equation (IV) by energy input $A_c * G_t$

$$\eta_{th,coll} = F_R(\tau\alpha) - F_R \frac{U_L(T_i - T_a)}{G_t} \quad (V)$$

In reality, the heat loss coefficient, U_L , is not constant but is function of the collector inlet and ambient temperature. Therefore,

$$F_R U_L = c_1 + c_2(T_i - T_a) \quad (VI)$$

Therefore substituting equation (VI) in the equation (V), it can be written as:

$$\eta_{collector} = F_R(\tau\alpha) - c_1 \frac{(T_i - T_a)}{G_t} - c_2 \frac{(T_i - T_a)^2}{G_t} \quad (VII)$$

And if we denote $\eta_0 = F_R(\tau\alpha)$ and $T_r = \frac{(T_i - T_a)}{G_t}$, then equation (VIII) can be written as:

$$\eta_{th,coll} = \eta_0 - c_1 T_r - c_2 T_r^2 G_t \quad (VIII)$$

It could be possible to express the same equation in term of useful energy delivered in joules: a solar collector receives solar radiation \dot{Q}_s from the sun [product of the surface area, $A_c (m^2)$ and the solar radiation perpendicular to the surface $I_p (kW/m^2)$] and supplies \dot{Q}_g to a heat engine at the temperature T_H . The ratio of supply heat \dot{Q}_g to the radiation \dot{Q}_s is defined as the thermal efficiency of a solar thermal collector,

$$\eta_{th,coll} = \frac{\dot{Q}_g}{I_p * A_c} = \frac{\dot{m} c_p (T_o - T_i)}{A_c * I_p} = \frac{\dot{Q}_g}{\dot{Q}_s} \quad (IX)$$

$\eta_{collector}$ would be 1 if the solar collector is a perfectly insulated black body. In reality, $\eta_{collector}$ is less than 1 due to optical and thermal losses, for this reason, from now it will be referred to this efficiency as "temperature dependence collector efficiency". It could be written also:

$$\eta_{th,coll} = \frac{\dot{Q}_g}{I_p * A_c} = \eta_0 - c_1 T_r - c_2 I_p T_r^2 \quad (X)$$

where $T_r \triangleq \frac{T_{htm,avg} - T_{amb}}{I_p}$

Where the reduced temperature, T_r is the temperature difference between the heat transfer medium in the solar collector and the ambient air divided by the solar radiation, which can be considered as the driving potential of solar collectors heat loss to the ambient. This equation include all important design and operational factors affecting steady-state performance, except collector flow rate.

4.1.2 Absorption refrigeration chiller

The absorption chiller, responsible for the production of the chilled water. With its capacity of 11,5 kW and a standard conditions COP of 0,69 the machine present an electric consume of only 0,3 kW. It is composed by four subcomponents: generator, condenser, evaporator and absorber. The generator is responsible for the evaporation of the water present in the Li-Br solution in an high pressure level (6,4 kPa) at temperature that oscillate between 65°C and 90°C. In order to work the temperature out of the tank should not be lower than 68 °C and the cooling capacity increases with increase of this temperature. The refrigerant steam enter then into condenser and is cooled down by cooling water flowing in the pipes, that passes from about 35°C to about 28°C, and the refrigerant water gathered in condenser enter into the evaporator by throttling. Because of low pressure (0,6 kPa) in the evaporator (obtained thanks to a vacuum pump), the refrigerant water will be evaporated by absorbing the heat of chilled water flowing in pipes, so that to lower the temperature of chilled water and realize the refrigeration: is possible to obtain chilled water from 20°C until 7 °C, depending on the ambient and working conditions. Finally, in the absorber the water and the solution are again mixed and cooled, to avoid the crystallization of Li-Br ready for the next cycle. Its mode of operation is detailed explained below.

In order to explain the concept of absorption system, is necessary to introduce some thermodynamic knowledge, in terms of idealized energy conversion cycles, or to be more accurate, about the combined cycle of two Carnot cycles, that the so-called absorption cycle is based on. Both cycles (the work producing and refrigeration cycle) are combined into one device. [12] This device is an absorption heat pump and it is a three temperature device because works between three values of temperature, and for this reason it is called a trivalent temperature cycle. It is assumed that the amount of work produced by Carnot cycle is identical to the amount of work required by the refrigeration cycle. The device raises the temperature level of heat supplied at T_0 to T_1 by using the thermodynamic availability of the high temperature energy supplied at T_2 . The waste heat of power generation portion of this combined cycle is also rejected at T_1 . Thus the total amount of heat rejected at T_1 has two contributions, Q_1' and Q_1'' . This combined cycle represents a heat-pumping device that is driven by the input of heat only. It is the ideal representation of several different heat-pumping concepts. Examples are an engine-driven vapour compression heat pump, a combination of steam power plant with electrical vapour compression heat pump or the representation of an absorption heat pump [12].

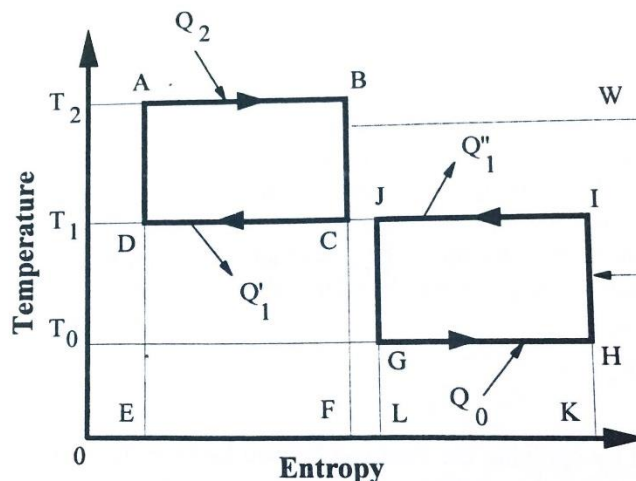


Figure 15: Carnot cycles for a combined heat pumping facility such as an absorption heat [12]

The coefficient of performance for absorption heat pump is customarily defined for cooling or refrigeration applications as

$$COP_{Absorption\ cooling} = \frac{Q_0}{Q_2} \quad (XI)$$

That could also be seen as the product between efficiency of the Carnot cycle and efficiency of the refrigeration

cycle:

$$COP_{Absorption\ cooling} = \eta_{carnot} * \eta_{Carnot\ inverso} \quad (XII)$$

By applying the First and Second Laws and eliminating Q_0 , the equation (XI) can be converted into expressions that depend on temperature only [12].

$$\text{Being} \quad \eta_{carnot} = \frac{W}{Q_2} = \frac{Q_2 - Q_{1'}}{Q_2} \quad (XIII)$$

$$\text{Where:} \quad Q_{1'} = T_1 * \Delta S \quad (XIV)$$

$$Q_2 = T_2 * \Delta S \quad (XV)$$

$$\text{And being} \quad \eta_{Carnot\ inverso} = \frac{Q_0}{W} = \frac{Q_0}{Q_{1''} - Q_0} \quad (XVI)$$

$$\text{Where:} \quad Q_{1''} = T_1 * \Delta S \quad (XVII)$$

$$Q_0 = T_0 * \Delta S \quad (XVIII)$$

$$\text{Indeed:} \quad COP_{Absorption\ cooling} = \frac{T_2 - T_1}{T_2} \frac{T_0}{T_1 - T_0} \quad (XIX)$$

Compared to an ordinary cooling cycle, the basic idea of an absorption system is to avoid compression work by using a suitable working pair[11]. So far the theoretical thermodynamic background, but how practically this device works?

We have a common sense in our daily life: we always feel cool once coating the alcohol on our skin. This is because the alcohol will absorb the skin heat during the evaporation. In fact, it is not limited to the alcohol. Any liquid will absorb the surrounding heat during its evaporation. And it is the same to water evaporation.[13] Porous solids, called adsorbents, can physically and reversibly adsorb large volumes of vapor, called the adsorbate. Though this phenomenon, called solar adsorption, was recognized in 19th century, its practical application in the field of refrigeration is relatively recent. The concentration of adsorbate vapours in a solid adsorbent is a function of the temperature of the pair, i.e., the mixture of adsorbent and adsorbate and the vapour pressure of the latter. The dependence of adsorbate concentration on temperature, under constant pressure conditions, makes it possible to adsorb or desorb the adsorbate by varying the temperature of the mixture. An adsorbent-refrigerant working pair for a solar refrigerator requires the following characteristics:

1. A refrigerant with a large latent heat of evaporation.
2. A working pair with high thermodynamic efficiency.
3. A low heat of desorption under the envisaged operating pressure and temperature conditions.
4. A low thermal capacity.

Absorption systems are similar to vapour compression air-conditioning systems but differ in the pressurization stage. In general, an absorbent, on the low-pressure side, absorbs an evaporating refrigerant. The most usual combinations of fluids are lithium bromide–water (LiBr- H_2O which has been selected in the project), where water vapour is the refrigerant, and ammonia–water (NH_3-H_2O) systems, where ammonia is the refrigerant.[9] Liquid evaporation (boiling) temperature is related to relevant pressure. For instance: the water evaporation temperature is 100°C under one atmospheric pressure, while its evaporation temperature has lowered to 5°C under 0,00891 atmospheric pressure. water evaporation temperature will lower with the pressure reduction. Indeed a space with very low pressure or very high vacuum degree is created in the evaporator and water is evaporated: the low temperature water corresponding to the low pressure can be made. Aqueous solution of lithium bromide has a strong feature of absorption water vapour, and the more concentrated solution concentration, the stronger ability of absorption water vapour, while the lower solution temperature, the stronger ability of absorption water vapour as well. But, the solution temperature will be raised once they have absorbed the water vapour. To maintain the absorption feature, cooling water has to be used to lower the temperature of solution and maintain a certain degree concentration of lithium bromide solution. Lithium bromide absorption chiller just utilizes the above theory (see Figure 16) to evaporate and absorb heat in the evaporator with very low pressure so as to make chilled water with low temperature.



Figure 16: The theory of absorption and evaporation[13]

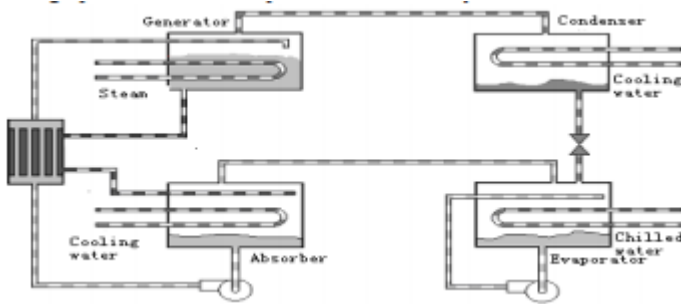


Figure 17: Flow chart of absorption chiller[13]

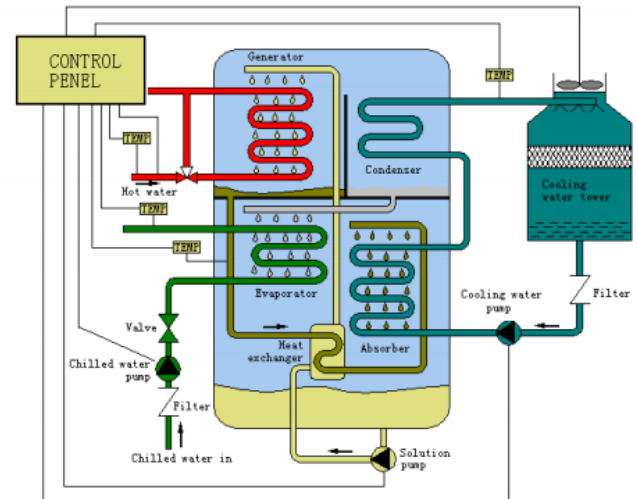


Figure 18: Hot water lithium bromide absorption chiller [13]

Therefore, in order to maintain the evaporation and heat absorption in the evaporator, the evaporated water must be constantly supplemented and evaporated steam shall be taken away. This function is realized just by the features of lithium bromide solution [13]. The main components of an absorption refrigeration system are the generator, absorber, condenser, and evaporator. The following Figure 17 is flow chart of *hot water lithium bromide absorption chiller*. The dilute solution (Li-Br and water) is transmitted by the solution pump in the high pressure generator and is heated up by the hot water flowing in the pipes of the heat exchange, coming from the hot water storage tank connected to the solar collector, in order to produce refrigerant steam and the solution is condensed [13]. The refrigerant steam enter into condenser and cooled down by cooling water flowing in the pipes, and the refrigerant water gathered in condenser enter into the evaporator by throttling. Because of low pressure in evaporator, it will be evaporated by absorbing the heat of chilled water flowing in pipes, lower the temperature of chilled water and the refrigeration is realized. On the other hand, the concentrated solution at the outlet of high pressure generator (dark green coloured in the Figure 18) goes through heat exchanger and enter into absorber to absorb the low temperature refrigerant steam from evaporator and make the evaporator in low-pressure condition, as well as the refrigeration process ongoing. The concentration of concentrated solution is reduced once absorbing the refrigerant steam. Then it is entered into generator by solution pump. The above repeated circulation enables the evaporator to constantly output low temperature chilled water for the cooling operation of air conditioner.[13] The Figure 18 is the structure chart of hot water lithium bromide absorption chiller. This kind of chiller is a packaged one, that is to say, heat exchanger, evaporator, condenser, generator and absorber are all installed in one shell, and it can make almost no leakage possible and the operational reliability. [25]

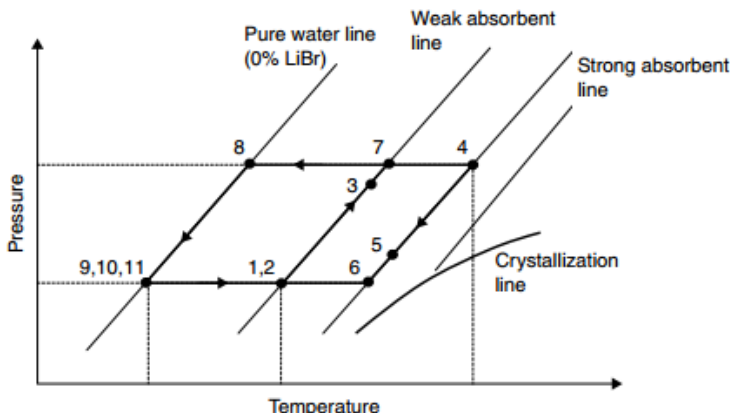


Figure 20 : Duhring chart of the water–lithium bromide absorption cycle[10]

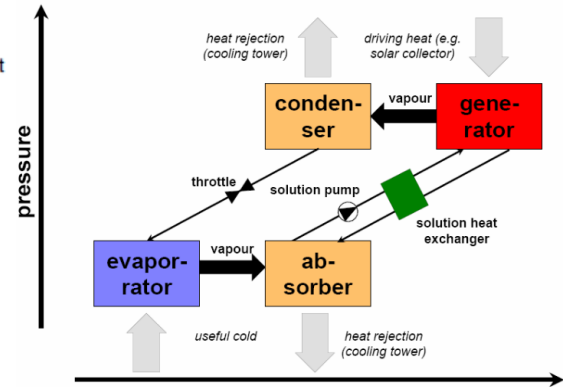


Figure 19: Pressure-temperature diagram of a single effect, lib-water absorption[42]

These charts are called Duhring chart, a pressure temperature graph, where diagonal lines represent constant LiBr mass fraction (concentration equilibrium for $\text{LiBr-H}_2\text{O}$), with the pure water line at the left. At point 1 in Figure 20, the solution is rich in refrigerant and a pump (1–2) forces the liquid through a heat exchanger to the generator. The temperature of the solution in the heat exchanger is increased (2–3). In the generator, thermal energy is added and refrigerant boils off the solution. The refrigerant vapour (7) flows to the condenser, where heat is rejected as the refrigerant condenses. The condensed liquid (8) flows through a flow restrictor to the evaporator (9). In the evaporator, the heat from the load evaporates the refrigerant, which flows back to the absorber (10). A small portion of the refrigerant leaves the evaporator as liquid spillover (11). At the generator exit (4), the steam consists of absorbent-refrigerant solution, which is cooled in the heat exchanger. From points 6 to 1, the solution absorbs refrigerant vapour from the evaporator and rejects heat through an heat exchanger. [9] The pressure in the condenser (8-7-4) and generator is fixed by the condenser fluid coolant temperature and it results to be equal to 6,4 kPa. The pressure in the evaporator and absorber (9-10-11) is fixed by the temperature of cooling fluid to the absorber and results to be among 0,3 kPa. The generation process is one of increasing the concentration from 55 to 60% while the equilibrium temperature of the solution rises from 72 to 82 °C at the pressure of the condenser. In the absorber, the solution concentration drops from 60 to 55% as the solution temperature drops from 48 to 28 °C, all at the evaporator pressure. In the real cycle some sensible heat will have to be transferred in the generator and absorber (the amount dependent on the effectiveness of exchanger HX), there will be pressure changes through the generator due to hydrostatic head, and concentrations with the machine and operation conditions; The maximum solution temperature in the generator is T_4 ; the temperature of the heated fluid to the generator must be above the maximum generator temperature, which is determined by condenser pressure and the concentration of the solution leaving the generator. The generator temperatures must be kept within the limits imposed by the characteristics of heat pipe collectors.[11]

The Figure 19 shows a model in which driving heat is the heat input rate from the heat source to the generator, the heat rejection rates go from condenser and absorber to the heat sinks, the cooling tower and the “useful cold” is the heat input rate from the cooling load to the evaporator.[9]

For the thermodynamic analysis of the absorption system, the principles of mass conservation and the first and second laws of thermodynamics are applied to each component of the system. Each component can be treated as a control volume with inlet and outlet streams, heat transfer, and work interactions. In the system, mass conservation includes the mass balance of each material of the solution. The energy, mass concentrations, and mass balance equations of the various components of an absorption system are given in (Kizilkan et al., 2007).

System components	Mass balance equations	Energy balance equations
Pump	$\dot{m}_1 = \dot{m}_2, x_1 = x_2$	$w = \dot{m}_2 h_2 - \dot{m}_1 h_1$
Solution heat exchanger	$\dot{m}_2 = \dot{m}_3, x_2 = x_3$ $\dot{m}_4 = \dot{m}_5, x_4 = x_5$	$\dot{m}_2 h_2 + \dot{m}_4 h_4 = \dot{m}_3 h_3 + \dot{m}_5 h_5$
Solution expansion valve	$\dot{m}_5 = \dot{m}_6, x_5 = x_6$	$h_5 = h_6$
Absorber	$\dot{m}_1 = \dot{m}_6 + \dot{m}_{10} + \dot{m}_{11}$ $\dot{m}_1 x_1 = \dot{m}_6 x_6 + \dot{m}_{10} x_{10} + \dot{m}_{11} x_{11}$	$Q_A = \dot{m}_6 h_6 + \dot{m}_{10} h_{10} + \dot{m}_{11} h_{11} - \dot{m}_1 h_1$
Generator	$\dot{m}_3 = \dot{m}_4 + \dot{m}_7$ $\dot{m}_3 x_3 = \dot{m}_4 x_4 + \dot{m}_7 x_7$	$Q_G = \dot{m}_4 h_4 + \dot{m}_7 h_7 - \dot{m}_3 h_3$
Condenser	$\dot{m}_7 = \dot{m}_8, x_7 = x_8$	$Q_C = \dot{m}_7 h_7 - \dot{m}_8 h_8$
Refrigerant expansion valve	$\dot{m}_8 = \dot{m}_9, x_8 = x_9$	$h_8 = h_9$
Evaporator	$\dot{m}_9 = \dot{m}_{10} + \dot{m}_{11}, x_9 = x_{10}$	$Q_E = \dot{m}_{10} h_{10} + \dot{m}_{11} h_{11} - \dot{m}_9 h_9$

Table 2: Energy and Mass Balance Equations of Absorption System Components [10]

The equations of Table 2 can be used to estimate the energy, mass concentrations, and mass balance of a LiBr-water system. In addition to these equations, the solution heat exchanger effectiveness is also required, obtained from (Herold et al., 1996):

$$\varepsilon_{SHx} = \frac{T_4 - T_5}{T_4 - T_2} \quad (XX)$$

The useful output energy of the system for the cooling applications is heat extracted from the environment by the evaporator while the input energy is supplied to the generator (Alefeld and Radermacher, 1994; Herold et al., 1996). The cooling coefficient of performance of the absorption system is defined as the heat load in the evaporator per unit of heat load in the generator and can be written as (Herold et al., 1996; Tozer and James, 1997):

$$\begin{aligned} COP_{Absorption\ cooling} &= \frac{Q_E}{Q_G} = \frac{\dot{m}_{10} h_{10} + \dot{m}_{11} h_{11} - \dot{m}_9 h_9}{\dot{m}_4 h_4 + \dot{m}_7 h_7 - \dot{m}_3 h_3} \\ &= \frac{\dot{m}_{18} (h_{18} - h_{19})}{\dot{m}_{12} (h_{12} - h_{13})} \end{aligned} \quad (XXI)$$

where h is the specific enthalpy of working fluid at each corresponding state point (kJ/kg). The second-law analysis can be used to calculate the system performance based on exergy. Exergy analysis is the combination of the first and second laws of thermodynamics and is defined as the maximum amount of work potential of a material or an energy stream, in relation to the surrounding environment (Kizilkan et al., 2007). The exergy of a fluid stream can be defined as (Kotas, 1985; Ishida and Ji, 1999):

$$\varepsilon = (h - h_0) - T_0 (s - s_0) \quad (XXII)$$

where ε is the specific exergy of the fluid at temperature T (kJ/kg).

The terms h and s are the enthalpy and entropy of the fluid, whereas h_0 and s_0 are the enthalpy and entropy of the fluid at environmental temperature T_0 (in all cases absolute temperature is used in Kelvins). The

availability loss in each component is calculated by

$$\Delta E = \sum \dot{m}_i E_i - \sum \dot{m}_o E_o - \left[\sum Q \left(1 - \frac{T_o}{T} \right)_i - \sum Q \left(1 - \frac{T_o}{T} \right)_o \right] + \sum W \quad (\text{XXIII})$$

where ΔE is lost exergy or irreversibility that occurred in the process (kW). The first two terms of the right-hand side of Eq. (XXIII) are the exergy of the inlet and outlet streams of the control volume. The third and fourth terms are the exergy associated with the heat transferred from the source maintained at a temperature, T . The last term is the exergy of mechanical work added to the control volume. This term is negligible for absorption systems because the solution pump has very low power requirements.

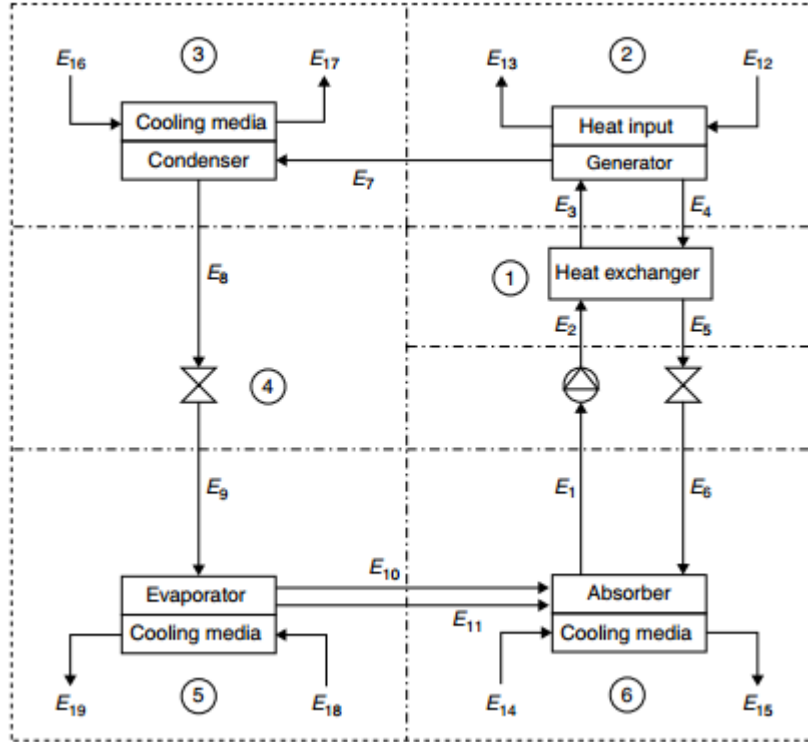


Figure 21: Availability flow balance of the absorption system [10].

The equivalent availability flow balance of the system is shown in Figure 21 (Sencan et al., 2005). The total exergy loss of absorption system is the sum of the exergy loss in each component and can be written as (Talbi and Agnew, 2000):

$$\Delta E_T = \Delta E_1 + \Delta E_2 + \Delta E_3 + \Delta E_4 + \Delta E_5 + \Delta E_6 \quad (\text{XXIV})$$

The second-law efficiency of the absorption system is measured by the exergetic efficiency, η_{ex} , which is defined as the ratio of the useful exergy gained from a system to that supplied to the system. Therefore, the exergetic efficiency of the absorption system for cooling is the ratio of the chilled water exergy at the evaporator to the exergy of the heat source at the generator and can be written as (Talbi and Agnew, 2000; Izquierdo et al., 2000):

$$\eta_{ex} = \frac{\dot{m}_{18}(E_{18} - E_{19})}{\dot{m}_{12}(E_{12} - E_{13})} \quad (\text{XXV})$$

The analysis of mass and energy balance of the absorption chiller done in the Table 2 do not consider the surrounding, but only the chiller as an "isolated box", being not affected by the weather conditions. That is useful in case to perform the behaviour of the absorption chiller not related to a specific system, and indeed useful for the design of the chiller itself. For our purposes, an steady state energy balance inside the absorption chiller, here below presented, is more effective.

The hot water chiller absorption chosen belong to Chinese trademark, the same of evacuated tube collectors,

Shandong Lucy New Energy Technology Co.,Ltd. With its capacity of 11,5 kW and a standard conditions COP of 0,69 the machine present an electric consume of only 0,3 kW. In

Table 3 are presented the technical specifications of the model selected:

Brand		Shandong Lucy New Energy Technology Co.,Ltd		
Model		RXZ – 11,5		
Cooling Capacity		11,5 kW	3.27 USRT	3924.3 BTU/h
Hot water	Flow rate	2.9 m ³ /h	48.3 L/min	12.8 GPM
	Pressure loss	50 kPa	5.10 m	7.25 psi
	Inlet/Outlet temperature	90°C / 85°C		194/185 °F
	Connection diameter	DN40		
	Heat consumption	16.8 kW		
Chilled water	Flow rate	2.5 m ³ /h	41.7 L/min	11.0 GPM
	Pressure loss	40 kPa	4.08 m	5.8 psi
	Inlet/Outlet temperature	14°C / 10°C		57.2/50 °F
	Connection diameter	DN32		
	Cooling capacity	11.65 kW		
	Fouling factor	0.085 m ² C/kW		
	Standard gauge pressure limit	≤ 0.8 MPa		
Cooling water	Flow rate	5 m ³ /h	83,3 L/min	22 GPM
	Pressure loss	50 kPa	5.10 m	7,25 psi
	Inlet/Outlet temperature	30°C / 35°C		86/95 °F
	Connection diameter	DN40		
	Fouling factor	0.085 m ² C/kW		
	Standard gauge pressure limit	≤ 0.8 MPa		
Power Supply		220V	1Phase	60 Hz
Electrical consumption		0.37 kW		
Dimension	Length	1010 mm		
	Width	785 mm		
	Height	1622 mm		
Shipping weight		850 Kg		
COP		0.69		

Table 3: Specifications of RXZ absorption chiller [14]

NOTE: The above technical parameters is based on wet bulb temp 27°C

The unit includes lithium bromide absorption chiller, control box, vacuum pump and hot water adjusting valve.

An overall steady-state energy balance on the absorption cooler indicates that the energy supplied to the generator, Q_G and to the evaporator, Q_E must equal to the energy removed from the machine via the coolant flowing through the absorber Q_A and condenser, Q_C plus whatever net losses may occur to the surroundings.

$$Q_G + Q_E = Q_A + Q_C + Q_{LOSSES} \quad (\text{XXVI})$$

the thermal coefficient of performance cop is defined as the ration of energy into the evaporator, Q_E to the energy into the generator, Q_G

$$COP_{AR} = \frac{Q_E}{Q_G} \quad (\text{XXVII})$$

The coefficient of performance is a useful index of performance in solar cooling, where collector costs (and thus costs of Q_E) are impotent. Usually for LiBr- H_2O machines the COP is nearly constant as the generator temperatures vary over the operating range, as long as the temperature above a minimum. The thermal COP is usually in the rage of 0.6 to 0.8 and the major effect of variation in the solar energy temperature to the generator is to vary Q_E , the cooling rate. Other types of COP can be defined (Mitchell,1986). A COP_e is the

ration of cooling to electrical energy used to provide air and liquid flows, operate controls, etc.

$$COP_e = \frac{Q_E}{\text{Electric input}} \tag{XXVIII}$$

The Coefficient of performance depend on several factor. Here below is shown how the Cooling capacity of the Hot Water Absorption chiller changes in respect to the chilled outlet, cooling inlet and hot inlet temperature respectively:

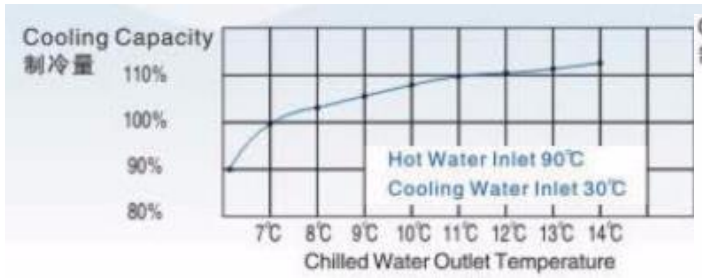


Figure 22: Cooling Capacity versus Chilled Water Outlet Temp [13]

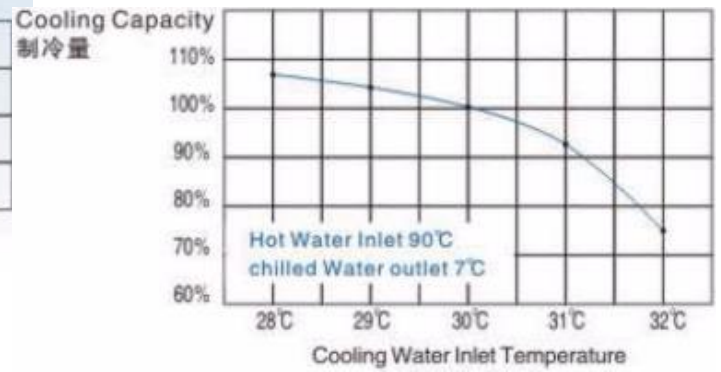


Figure 23: Cooling Capacity versus Cooling Water Inlet Temp [13]

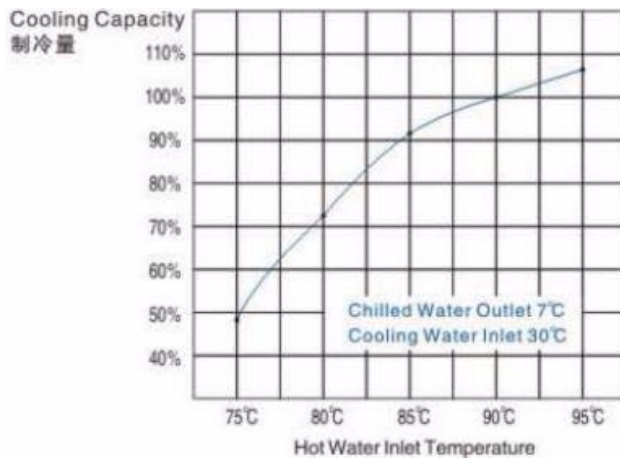


Figure 24 : Cooling Capacity versus Hot Water Inlet Temp [13]

4.1.3 Pressurized water storage tanks

The variations in solar radiation, including day-night and seasonal cycles, require thermal energy storage systems (TES) to adjust the thermal demand to the energy production.[1] Due to the intermittent nature of available solar energy, a hot and a chilled water storage tanks of a capacity of 1000L are installed. The “collected energy” is first stored in the tanks and then used when needed, as an energy source in the generator to heat the strong solution and as refrigerant in the water capillary mats for air-condition the Building 24. Because of the hot-water storage tank, an upper limit of about 98°C is used to prevent water from boiling. The main function of the unpressurized tanks in this system is to storage energy, in order to supply thermal energy to the absorption chiller in case of cloudy weather and to avoid variation on cooling load due to variations in the solar energy input. The tanks chosen belong to Lapesa© and are carbon steel inertia buffer tanks, capable to storage thermal energy insulating the fluid. In fact they are thermally insulated with rigid, mould-injected, 80mm-thick, 130 mm polyurethane (PU) foam ($k=0,04 \text{ W}/(\text{m}\cdot\text{K})$), that minimizes heat losses of stored water. In addition, the tanks are covered by an outer lining for deposit, padded with Polyvinyl chloride (PVC).

Here below the specifications of the tanks selected

Brand	Lapesa
Model	Gaiser Inertia L: G-1000-L
Material	Carbon Steel
Maximum working pressure	0,6 Mpa
Maximum working temperature	100 °C
Capacity	1000 L (1 m^3)
D: external diameter	950 mm
H: overall height	2250 mm
eh: side connection	3 " GAS/F
R: side connection	1M " GAS
tm: probe tube connection for sensors	½ " GAS/F
Empty weight (approx.)	205 kg
Thermal insulation	Rigid, mould-injected PU
Static heat losses EN12897	114 W
Tank for VERTICAL installation on floor	

Table 4: Specifications of water storage tank [15]

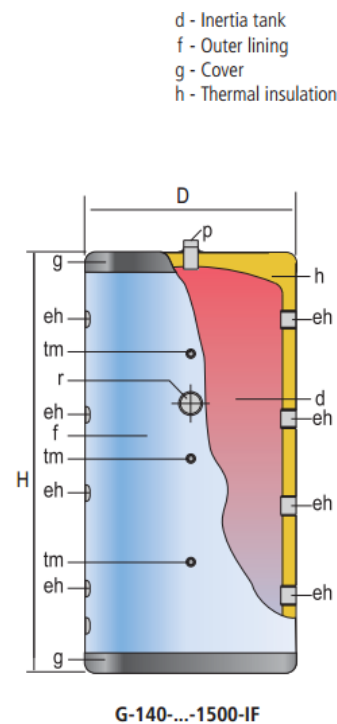


Figure 25: Gaiser inertia buffer tank [15].

4.1.4 Auxiliary heater

The auxiliary heater is used to assure the absorption chiller operation and should be activated whenever the heat pipe collectors' outlet temperature is less than the temperature of the user-specified maximum (T_{set}) (the maximum temperature allowed in the generator of the absorption chiller). For the continuous operation of absorption unit, indeed, the auxiliary heater should automatically operates whenever tank load temperature is below 90°C: in case the temperature sensor indicates that the water is below 90°C, the heater should add hot water at 90°C. The 40 kW auxiliary heater is directly connected to the tank. The auxiliary heater belongs to OKA s.a.s. and here below its specifications:

BRAND		OKA s.a.s.
MODEL		Pilotubular gas heater: L1PB-F7/40
RATED THERMAL LOAD		40 kW
RATED OUTPUT POWER		37 kW
EFFICIENCY AT RATED THERMAL LOAD		>92,2 %
RAED INPUT ELECTRIC POWER		130 W
POWER SUPPLY		a.c. 220/ 60 Hz
NOISE UNDER NORMAL WORKING CONDITIONS		≤42 dB
BOILER NET WEIGHT		55 kg
BOILER SIZE (HxWxTH)		78x54x35 mm
Gas Type & Rated Pressure	(T) NG	2.000 Pa
	(R) Town Gas	1.000 Pa
Hot Water System	Range of output power	40 kW
	Range of water temperature	38- 85 °C
	Rated capacity of hot water ($\Delta t=25$ °C)	21,3 l/min
	Range of water pressure	0,3 - 8 bar
Hot Water System Fitting Dimension	Inlet/outlet pipe diameter of heating (to the tank)	G ¾ inch (mayor diameter: 26,441; minor diameter: 24,117)
	Inlet/outlet pipe diameter of hot water (alimentation)	G ½ inch (mayor diameter: 20,955; minor diameter: 18,631)
	ut diameter of gas	G ¾ inch (mayor diameter: 26,441; minor diameter: 24,117)
Fitting Dimension Smoke vent Dimension	Coaxial pipe	ø60-ø100 mm

Table 5: Specifications of the auxiliary heater [16]

4.1.5 Closed circuit adiabatic cooler

Since in an absorption-refrigeration cycle heat must be rejected from the absorber and the condenser, a cooling water system must be employed in the cycle. Perhaps the most effective way of providing cooling water to the system is to use a cooling tower. Because the absorber requires a lower temperature than the condenser, the cool water from the cooling tower is first directed to the absorber and then to the condenser.[9] Closed circuit cooling towers operate in a manner similar to open cooling towers, except that the heat load to be rejected is transferred from the process fluid (the fluid being cooled) to the ambient air through a heat exchange coil. The coil serves to isolate the process fluid from the outside air, keeping it clean and contaminate free in a closed loop. This creates two separate fluid circuits: an external circuit, in which spray water circulates over the coil and mixes with the outside air, and an internal circuit, in which the process fluid circulates inside the coil. During operation, heat is transferred from the internal circuit, through the coil to the spray water, and then to the atmosphere as a portion of the water evaporates. The closed-circuit assure to minimise energy consumption and water consumption (the nominal power at maximum capacity is of 1,9 kW) and to avoid contamination problem.



Figure 26: Glacier Closed circuit cooling tower [17]

A cooling tower in order to cool the water used the simple principle of evaporative cooling. Evaporative cooling is based on a simple principle: As water evaporates, the latent heat of vaporization is absorbed from the water body and the surrounding air. As a result, both the water and the air are cooled during the process. The evaporative cooling process is shown schematically and on a psychrometric chart in Figure 27. Hot, dry air at state 1 enters the evaporative cooler, where it is sprayed with liquid water. Part of the water evaporates during this process by absorbing heat from the airstream. As a result, the temperature of the airstream decreases and its humidity increases (state 2). In the limiting case, the air leaves the evaporative cooler saturated at state 2'. This is the lowest temperature that can be achieved by this process. The evaporative cooling process is essentially identical to the adiabatic saturation process since the heat transfer between the airstream and the surroundings is usually negligible. Therefore, the evaporative cooling process follows a line of constant wet-bulb temperature on the psychrometric chart. Since the constant-wetbulb-temperature lines almost coincide with the constant-enthalpy lines, the enthalpy of the airstream can also be assumed to remain constant.

That is,

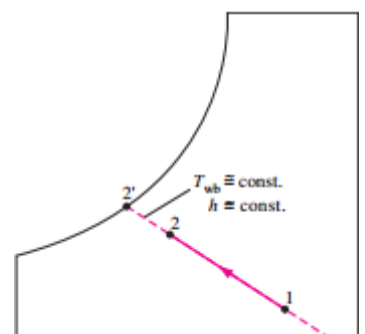


Figure 27: Evaporative cooling process[18]

$$T_{wb} \approx constant \quad (XXIX)$$

and,

$$h \approx constant \quad (XXX)$$

during an evaporative cooling process. This is a reasonably accurate approximation, and it is commonly used in air-conditioning calculations[18].

The closed circuit adiabatic cooler selected is a heat exchanger for cooling liquids in a coil, by means of ambient air. To decrease the air temperature at the coil inlet the cooler is served by an adiabatic cooler wet panel type. With the combination of the closed circuit and the wet panel it is possible to achieve liquid outlet temperatures of 3°C above the wet bulb temperature of the installation area. It has been chosen this particular cooling tower in this process where is necessary that the water does not present problems of contamination and encrustation.

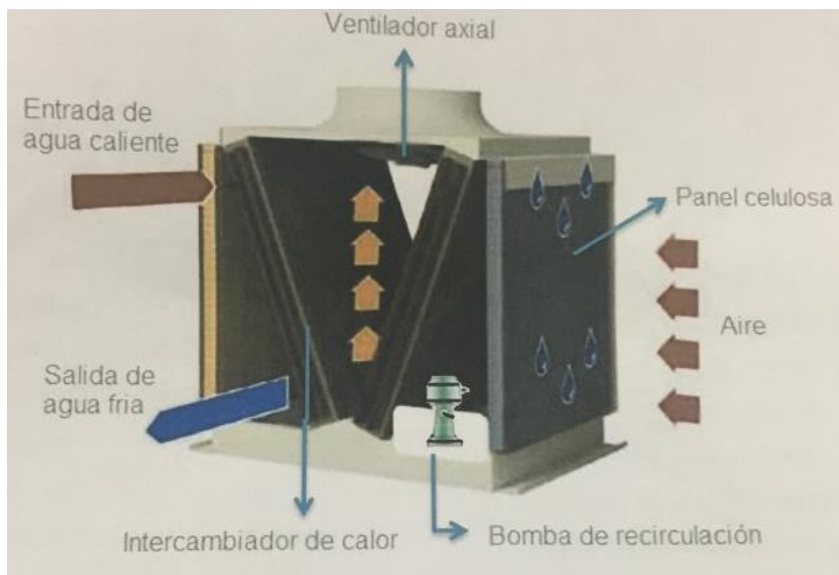


Figure 28: Schematic picture of closed circuit adiabatic cooler[17]

The closed-circuit evaporative cooler is composed by two water-air heat exchanger consists on coils of copper tubes and aluminium fins mechanically attached to the pipes. (Figure 31) installed in V with an axial fan of variable volume installed on its top (see Figure 28). Two evaporative pad CELdek® series (Figure 29), set in a polyester cabinet reinforced with fiberglass are located vertically and in front of the coils and the ensembles have recirculation pump and control panels.

The equipment is manufactured of the size of 10 refrigeration tonnes (35 kW) when cooling 24 gallons por minute (GPM) ($5,45 \text{ m}^3/h$) from 35°C to 30°C with wet bulb temperature of ambient temperature of 23,9 °C[17]. The self-cleaning design and a thickness of 4"(10,6 cm) with crossed channels assure an optimum cooling and saturation efficiency between 84 and 90%. The water distributor system (Figure 30) is made of stainless steel and provides distribution of the water on the evaporative medium with optimum.



Figure 31: Water-air heat exchange[17]



Figure 29: Celdek series[17]



Figure 30: Cooling tower's water distribution[17]

The fan is equipped with an EC type engine of variable speed and efficiency superior to 95%, that permits to regulate the speed of the fan in relationship to the set temperature imposed. In the system $T_{set} = 30^{\circ}\text{C}$, that is mean that when the temperature entering to the cooler is higher the fan switch on. The controller with display governs the speed of the fan with a 0-10VCD signal and the on and off recirculation pump, using the signal of a temperature sensor at the water outlet and the value assigned reference ($T_{set} = 30^{\circ}\text{C}$). The controller allows modification of loop parameters and on / off values of the pump, depending on the fan speed. It also allows the ignition of the pump to confirmation of water level by means of a level switch magnetic. The cooling tower was a donation of a value of 9.000 US dollar, from a Colombian enterprise; in the Table 6 its specifications:

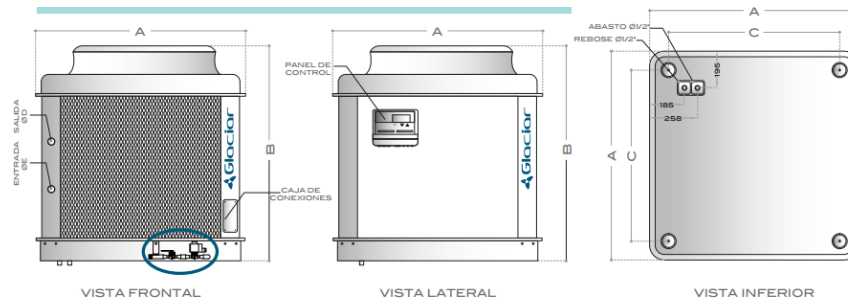


Figure 32: Dimensions of the cooling tower[17]

Brand	Glaciar- Ingeniería s.a.s		
Model	CWEEEX-120-1		
Cooling nominal capacity	35.169 kW	10 USRT	12000 BTU
Nominal flow rate	$6.0409 \text{ m}^3/\text{h}$	100.6809 l/min	26.6 GPM
Pressure drop in the coiling coil	13.152 kPa	4.4 ftH2O	1.34 m
Dimension	Length (A)	1382	
	Width (A)	1382	
	Heigh (B)	1741	
	Internal length/width (C)	1174	
	Water inlet tube diameter	1 ½ inch	
	Water outlet tube diameter	1 ½ inch	
Weight	Net	247 kg	
	In operation	295 kg	
Electric information	Maximum power	1900 W	
	Phases	3	
	Voltage	208-240	
	Full load amperage	7.3-6.5	

Table 6: Closed circuit adiabatic cooling tower specifications[17]

For a cooling tower is not defined a properly efficiency, being the machine an heat exchange. A way to define its performance could be measure the ratio between the thermal gap of inlet and outlet temperature (real heat exchanged) and the maximum thermal gap achievable (the maximum heat that could be exchanged). This relationship is defined by the efficacy of the heat exchange process:

$$\epsilon = \frac{T_i - T_o}{T_i - T_{wb}} \quad (\text{XXXI})$$

Where: T_i = inlet temperature
 T_o = outlet temperature
 T_{wb} = wet bulb temperature of the ambient air

The catalogue of the machine spoke about a temperature gap of 9°C when the wet bulb temperature is at 23,8°C and so the efficacy in that case is 0,45. The table below shows how the machine works at different bulb temperature.

CWEEEX 120-1

CAPACIDAD MÁXIMA DE ENFRIAMIENTO EN GPM		BULBO HÚMEDO (°F)												
		58	60	62	64	66	68	70	72	74	76	78	80	82
TEMPERATURA DE SALIDA DEL AGUA (°F)	70	27.4	23.0	18.2										
	72	31.8	27.6	23.2	18.4									
	74	35.8	31.8	27.8	23.4	18.6								
	76	39.8	36.0	32.0	27.8	23.6	18.8							
	78	43.8	40.0	36.0	32.0	28.0	23.6	19.0						
	80	47.8	44.0	40.0	36.2	32.2	28.0	23.8	20.0					
	82	51.8	47.8	44.0	40.2	36.2	32.2	28.2	24.0	19.4				
	84	55.6	51.8	48.0	44.2	40.2	36.4	32.4	28.2	24.0	19.4			
	85	57.6	53.8	50.0	46.2	42.2	38.4	34.4	30.4	26.2	21.8	17.0		
	86		55.6	51.8	48.0	44.2	40.4	36.4	32.4	28.4	24.2	19.6	14.4	
	87		57.6	53.8	50.0	46.2	42.4	38.4	34.6	30.6	26.4	22.0	17.2	
	88			55.8	52.0	48.2	44.4	40.4	36.6	32.6	28.6	24.2	19.8	14.6
	89			57.8	54.0	50.2	46.2	42.4	38.6	34.6	30.6	26.4	22.2	17.4
	90				55.8	52.0	48.2	44.4	40.6	36.6	32.6	28.6	24.4	19.8

Basado en delta de temperatura de 10°F a 0 psnm

Figure 33: Cooling capacity chart of the Closed adiabatic cooler wrt the ambient conditions and outlet water temperature[17]

The table shows how varies the maximum cooling capacity in gallon per minutes of the tower in respect with the ambient air conditions. Remembering that the wet bulb temperature rise (and also the dewpoint rise) if the relative humidity rises at a certain dry bulb temperature and that it decrease (and also the dewpoint decrease) if ambient temperature decreases, at a certain relative humidity, colder and drier is the air outside the tower (wet bubble temperature low) bigger the capacity. In fact, higher is the temperature of the water to be cooled, bigger is the capacity, so faster is the cooling process, being the flow rate bigger. That because it is higher the temperature difference between them and because the air contain less water, so that to result to be more able to absorb more moisture: high relative humidity slows down heat rejection by evaporation, and low relative humidity speeds it up. In Medellin case, where wet bulb temperature is is about 21,3°C (70°F), if the output temperature of the tower is 30°C (86°F) the maximum cooling capacity is 36,4 gal/min, that corresponds to 8,2 m³/h (these data was provided by the manufacturing being necessary for the calculation of that, knowledge about the efficiency of the machine). In case of working with 28°C as output temperature, the maximum cooling capacity is equal to 28,2 gal/min that corresponds to 6,35 m³/h. This is enough to assure the nominal efficiency if working with a flow rate equal to 5 m³/h in both cases.

4.1.6 Water capillary mats

A system of chilled capillary mats is used for air conditioning, where the heat transfer takes place through a radiant ceiling. They were chosen, instead of conventional fan coils (a combination of ventilator and heat exchanger units, which exchange heat from chilled water and air in the building by convection), because the former results more efficient. The system provides a comfortable and uniform climate in the environments by the effect of thermal radiation/absorption and convection. More in particular, the mats absorb the radiant heat from the people present in the building and also being installed into the ceiling, convective air flow are created because the air cooled falls down and the warmer takes its place. Not even necessary a fan the system does not generate hassle by cold air flow or fan noise [19]. In more, it allows to reduce recirculation airflow and increase the temperature of chilled water supplied (about 7°C or even until 18°C water temperature, against the fan coil's temperature of 5°C), allowing a reduction in energy consumption by airflow and an improvement in energy efficiency of air conditioning, being the heat exchanged results to be effective also a higher temperature of the water out to the system. This system is installed in a superimposed form on the "false ceiling", of the top of building 24, required in order to avoid to damage the ceiling in case of condensation of the water inside the tube. The condensation could happen if the temperature of the water inside the mats equal to the wet bulb temperature of the ambient, that cause "rain" in the building, for this reason is always very important to check the ambient conditions in term of temperature and relative humidity. Water capillary mats belong to ClimaActive International S.A.S, a Germany company, based also in Medellín. Here below some technical features and advantages with respect to the conventional fan coil of the closed hydraulic system implemented:

- The radiant water capillary cooling technology provides air cooling through radiant cooling ceilings where water capillary mats are built-in, and can contain chilled water at temperature until to $-17\text{ }^{\circ}\text{C}$ (The upper limit is not specified because this system can also be used for heating purposes and so containing hot water at temperature of $60\text{ }^{\circ}\text{C}$).
- A ceiling panel acts as a heat exchange element between the indoor air and cooled water in the water capillary mats. The ceiling absorbs heat from the heat sources in the room, exchanging the circulating cooled water.
- The circulating water is continuously pumped to the chiller, cooled and pumped back to the ceiling through the water capillary mats.
- High mechanical resistance - long service life, more than 50 years
- Little space in the installation, max. 15 cm
- Does not produce cold or transports bacteria and viruses
- Saving of maintenance costs, without change of filters, does not require cleaning of pipelines
- Savings in construction materials because transfers high thermal load in little space
- Power saving due to its high efficiency and quiet operation[20].

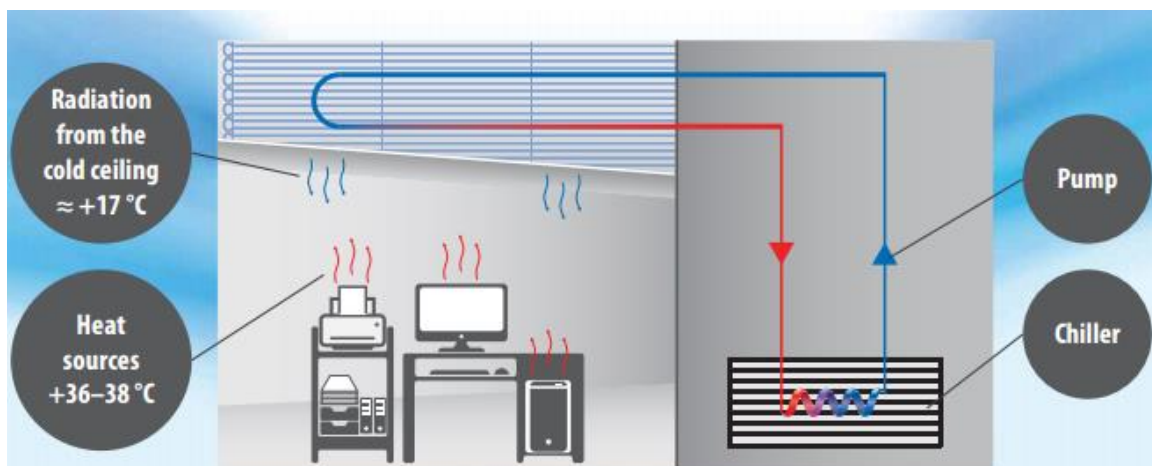


Figure 34: Radiation cooling technology of the water capillary mats [19]

Were installed 20 units of mats in the Building (see Figure 77 in the Appendix). The mats are connected to an hydraulic system: masters tubes and central main branches of PP 63mm (R63) pipe are connected with saddle to 20mm pipe tube in turn connected to the mats. The return is operated by two main branches at the ends of the room by PP 50mm (R50) pipe, also connected with saddle to the 20mm pipe tube of the mats. At the connection to the supply and to the return of each mat is included a shut-off valve.

The mats are made by high quality polypropylene (PP), environmentally friendly and safe plastic with thermal management and elasticity properties. A mat consists of 97 thin tubes ("capillary tube", 4,8 x 0,8 mm) in form of long parallel loops at distances of 10 mm, connected at their ends to two feed tubes (main tubes, 20 x 2 mm), one entrance and one return. Each mat has a width of 1 meter and an extension of 3,20 meters. The means of energy transport is water flowing through the capillaries. The delta temperature between T entering the system for cooling and T of return in general is about between 3 and 4 ° C, with an inlet temperature of cooling water of 10 °C and a return between 13 and 14°C.

In order to connect capillary mats to the PP tube are used connecting pipes and fittings. The system includes the actuators, system performance measurement and control devices. Circulates water under 5 bar pressure. The water capillary mats system operates for both cooling and humidity reduction and they are connected to the chilled water storage tank of the solar cooling absorption system. In table below the specifications are recapitulate:

Brand	Clima Active
Type of mar	GB 10
Polypropylene type	3, PP-R
Heat capacity on active surface	100 - 560 W / m ²
Main tube (inlet / outlet)	20 x 2 mm.
Capillary tube	4,5 x 0,8 mm
Capacity of capillary tube approx	0,640 l / m ²
Capillary tubes gap	10 mm
Number of main tubes per mat	97
Number of capillary tubes per mat	2
Density of mat approx..	860 g / m ²
Capacity of mat approx	2,224 L
Denisty in operation (water+mat)	1.600 g / m ² approx
Presión de operación	< 5 bar (500 kPa)
Prueba de presión en fabricación	20 bar (2000kPa)
Number of mats in Building 24	20
Capacity tot approx	44,480 L

Table 7: Specification of capillary mats installed [20]



Figure 35: Capillary mats assembled in a superimposed form on the "false ceiling", of the top of Building 24

4.1.7 Water pipeline including five pumps

The information of the hydraulic system of the project were taken from the product report realised on the October 2016. Before to establish the type of the five pumps needed in the system, were done calculus for measuring the diameter of the each pipe section. Were built for each section the five Bernoulli's equation by which were found the hydraulic head and the diameter length, known the nominal flow rate required by the machine and the load and minor losses of each section, given by the equipment and the structural frame of the cooling system. Finally, the pump were selected in relation to the speed of working. Here below the five pipe section identified in the system (in relationship to the equipment involved in the pipe section in order to the direction of the flow); each section will be described referring to the following numeration:

1. Hot water storage tank -- Collectors
2. Hot water storage tank – Absorption chiller
3. Chilled water storage tank -- Absorption chiller
4. Chilled water storage tank – Water capillary mats system
5. Closed circuit adiabatic cooler -- Absorption Chiller

The table below shows, at the sections considered, the diameter of the pipeline and the nominal parameters of the pumps selected (the head, the number of step-speed that could be selected and the power with respect to the working speed):

SECTION	DIAMETER internal	HEAD max	SPEEDS	Max POWER INPUT
1 Hot water storage tank - Collectors	0.032 m	10 m	1	245 W
2 Hot water storage tank - Absorption chiller	0.032 m	10 m	1	245 W
3 Chilled water storage tank - Absorption chiller	0.032 m	9 m	3	150-179-196 W
4 Chilled water storage tank - capillary mats	0.063 m	8,5 m	adaptable	9..144 W
5 Cooling tower - Absorption Chiller	0.04 m	27 m	1	740 W

Table 8: Pipeline specifications

1. For this section in Bernoulli's equation was considered load losses because of the roughness of the structure and minor losses due to the collectors and the accessories met in the section, as elbow joint or presence of valves due to equipment of measurement. By EES software were calculated a diameter and the measurement were compared with the ones on the market sale, so a diameter of 0.032 m (commercial pipe of 40 mm 1 ¼") PP PN25.

Taking into account the pressure losses from the evacuated heat pipes until the hot water storage tank the pump Grundfos UP 26-99F was chosen. Was not possible to experimentally calculate the real flow rate that delivers the pump, being not possible to use an ultrasonic flow meter, because it was not calibrate for the section of the system. In more was not present a pressure gauge upstream the valve and was neither possible to extrapolate the pressure difference. The flow rate is estimated indeed by a thermal equilibrium explained in section 5.1.2. Was measured by means of a power analyser, Power, Voltage and Current consumed by each pump. Indeed knowing the curves of the pump selected was easy to encounter the head and calculate the efficiency of the pump, thought the equation (XXXII):

$$P * \eta = \rho * g * Q * H$$

Where:

P is the power consumed by the pump measured by the power analyser, and in this pipe section is equal to 180W

ρ is the density of the fluid (water) at temperature and pressure inside the pipe, and in this pipe section $\rho \approx$



Figure 36: Hot water pump (used in section 1 and 2)

(XXXII)

$$974,8 \frac{kg}{m^3}$$

g is the acceleration due to gravity and it is equal to $9,8 \frac{m}{s^2}$

H is the head of the pump calculated through the pump's curve and in this pipe section is equal to 8,324 m

Q is the flow rate inside the pipe, through equation (LII) in Section 5.1.2 . It results equal to $1,93 \frac{m^3}{h}$.

η is the efficiency of the pump, calculated through equation (XXXII), resulting to be equal to 0,24.

Indeed through Bernoulli constructed in order to choose the pump was underestimate the head of the system, previously approximated equal to 7 meters. The actual flow rate, indeed resulted reduced that which was encountered into the product report of the project [21]. In the appendix the Figure 79 shows the curve and operational point of the pump - product 52722355.

2. For the construction of Bernoulli's equation for the section from the hot water storage tank to the absorption chiller in the product report was estimated a head of 5 meters column of water that together with the lost by accessories bring to a total head of 7 meters. Taking in account the nominal flow rate and temperature required by the generator of the chiller and the head required by the machine, by EES software were calculated a internal diameter of 0.032 mm (commercial pipe of 40 mm 1 ¼") Polypropylene (PP) Nominal Pressure (PN) 25. The pump Grundfous UP 26-99F was chosen, the same pump that the collector's section one. The power consumption measured was equal to 230 kW.

3. For the construction of Bernoulli's equation for the section from the chilled water storage tank to the absorption chiller was considered the nominal flow rate and temperature required by the evaporator (indeed a bigger viscosity and density) and a pressure drop in meter of water column equal to 4.10 meter; the load and minor losses increase with respect to the section 2 because the section is longer and presents more accessories; anyway the total head calculated resulted lower equal to 6 meters; a Also in this case the commercial diameter encountered was of 0.032m (commercial pipe of 40 mm 1 ¼") PP PN10. The pump Grundfous UPS 26-99 FC was chosen, that presents 3 velocity. The power P consumed by the pump measured by the power analyser is equal to 180W.



Figure 37: Chilled water tank- Chiller pump (section 3)

4. For the section from the chilled water storage tank to the water capillary mats the same manufacturer of the capillary mats, Clima Active, defined a diameter of PP tube of 2" (63 mm) and selected the pump designed to accomplish the requirements in order to water pass through the mats. Was selected pump Magna 32-80 N180, the particularity of this pump is that its speed could be regulated because pump speed is controlled by an integrated frequency converter. The pump present an analogic display showing its operational point:

The power P consumed by the pump measured by the power analyser is equal to 120W

The density ρ of the fluid (water) at temperature and pressure inside the pipe is

$$\rho \approx 997,9 \frac{kg}{m^3}$$

The acceleration g due to gravity is equal to $9,8 \frac{m}{s^2}$

The head of the pump H , showed on the digital display is equal to 2,47 m

The flow rate Q inside the pipe, showed on the digital display results equal to $7,7 \frac{m^3}{h}$

η is the efficiency of the pump, calculated through equation (XXXII), resulting to be equal to 0,43054.

In the appendix the Figure 78 shows curve and operational point of the pump 97924723.



Figure 38: Chilled water- capillary mats pump(section 4)

5. The section from the cooling tower (or better closed circuit adiabatic cooler) to the absorption chiller is the shorter, but it must to take in account the change in temperature out of the chiller. For the last section, the flow rate needed by the chiller is about $5 \frac{m^3}{h}$, and the Bernoulli equation is affected by a pressure drop

from cooling tower, the chiller and the accessories. The diameter calculated is of 0.040 (commercial pipe of 50 mm 1 ½ ") PP PN10.

Taking into account the pressure losses from the closed circuit adiabatic cooler until the absorption chiller an horizontal multistage centrifugal pump Grundfous CM5-2-ASGE-AQQE was chosen. In this case the head increases due to pressure drop in the chiller, the accessories and the tower's height to 21,72 meters column of water, including the lost by accessories. In the appendix the Figure 80 shows the operational point of the pump- product 97568429. Once measured the power in this case by the pump's curve, that provide also a power – flow rate curve was possible to encounter the real flow rate:

The power P consumed by the pump measured by the power analyser is equal to 770W

The density ρ of the fluid (water) at temperature and pressure inside the pipe is $\rho \approx 995,6 \frac{kg}{m^3}$

The acceleration g due to gravity is equal to $9,8 \frac{m}{s^2}$

The head of the pump H , calculated through the measurement is equal to 21,72 m

The flow rate Q inside the pipe is obtained on the pump's curve, once defined its head. It results equal to $5 \frac{m^3}{h}$
 η is the efficiency of the pump, calculated through equation (XXXII), resulting to be equal to 0,383.

The table below resume the operational point known of the pump selected.

Operational point	1. UP 26-99F	4. MAGNA 3 32-80 N180	5. CM5-2- ASGE-AQQE
	1 Hot water storage tank - Collectors	4 Chilled water storage tank - capillary mats	5 Cooling tower - Absorption Chiller
Cod. product	52722355	97924723	97568429
Temperature[°C]	75	8	30
H [m H2O]	8,324	2,47	21,72
ρ (density) [$\frac{kg}{m^3}$]	974,8	997,9	995,6
P (power) [W]	180	120	770
Q (caudal) [$\frac{m^3}{h}$]	1,93	7,7	5
η (efficiency)	0,24	0,43	0,38

Table 9: Operational point known of the pumps present in the system



Figure 39: Cooling water pump (section 5)

4.1.8 The coolerado

The office selected hosts about 50-80 persons and has an area of 239 m^2 , indeed, for improving the energy efficiency of the air conditioning system, a 17,6 kW indirect- evaporative air cooler responsible in renovation of the air, was installed, resulting that the air entering is provided at lower temperature than the temperature outside. Employing both system the thermal capacity needed for the office building is satisfied: the absorption chiller provide with 3 tons of cooling capacity and the Coolerado, supplying chilled fresh air with no added humidity is responsible with 5 tons in cooling capacity. The system draws a maximum of 750 watts of power at full flow[22].

Coolerado M50 air conditioner belongs to Coolerado Company, founded in 2004 by Valery Maisotsenko and Gillan brothers. Coolerado system is based on Maisotsenko cycle, a particular case of indirect adiabatic (evaporative) cooling air conditioning system, Humid working air, that constitute about half of the air that enters the heat and mass exchanger is released back into the atmosphere, carrying energy removed from the conditioned air. Chilled fresh air with no added humidity is supplied.

For the first time it was patented by Valery S. Maisotsenko and Alexandr N. Gershuni in 1987 in Soviet Union. After that they patented it in The United States of America in 1990 as "Method for indirect- evaporative air cooling". The first units were installed at Mount St. Vincent's Children's Home and Bradford Publishing. At the moment there are installed more than 1300 Coolerado air conditioners in 26 countries. [22]

Maisotsenko cycle (M-cycle) is a particular case of indirect adiabatic (evaporative) cooling (IAC) in air conditioning systems. Interest in using the technology of adiabatic cooling in air conditioning systems is caused by a number of advantages, the most important of which is a radical reduction of energy consumption. However, the efficiency of evaporative air cooling systems is strongly dependent on the state of the air. The most suitable conditions for these systems are the areas with a hot and dry climate. Determining factor in this case is the air wet bulb temperature: this is the theoretical minimum temperature to which air can be cooled.[22]



Figure 40: Model M50 Coolerado cooler system[23]

adiabatic, because it goes without heat exchange with the environment. Cooling is achieved by the fact that the particles of water take heat from the air during the evaporation process.[22] To understand the principle of Maisotsenko cycle is important to refresh the basic thermodynamic knowledge that stands to the base of this cycle: the adiabatic cooling and the indirect adiabatic cooling.

The process of adiabatic cooling

When the water evaporates into the air, it takes heat from the air. This heat is usually called latent heat. It consists of two parts. The first part is the heat, which is needed to vaporize water from liquid to vapour (phase transition from liquid phase to gas phase). The second part is the heat, which is needed to superheat water vapour to the air temperature.

The air with initial characteristics comes to the adiabatic cooler, where the particles of water are sprayed into the incoming air stream. Water particles evaporate in the stream and take the latent heat from it. The process goes with the constant enthalpy. The temperature of the air decreases, but the moisture content increases. The minimum possible temperature is the wet bulb temperature. The potential air state is the point on the saturation curve on the line with constant enthalpy. The lower the relative humidity and higher temperature of the air, the greater the potential effect of cooling. That is why dry and hot climate is the most suitable for the adiabatic cooling systems.

The process of indirect adiabatic cooling

In adiabatic cooling of the air with decreasing of the temperature, increases humidity. The higher the cooling effect, the more humid the air becomes. High humidity can cause discomfort. The most comfortable humidity level in the room varies from 40 % to 60 %. Humidity levels below 30 % and over 70 % are uncomfortable. Decrease in temperature with a simultaneous increase of humidity, using a direct evaporative cooling in a confined space, impairs the comfort especially in regions where the climate is hot and dry. High level of humidity can cause growth of microbes or microorganisms, health hazards, emissions from building materials, moisture damage and so on. Indirect adiabatic cooling helps to avoid problems associated with changes in moisture content of the incoming air. It is often so, that recirculation water is used in evaporative cooler. It may cause some problems. In systems with water recirculation there is always stagnant water. Therefore, there is high probability of formation of microorganisms. Only a regular cleaning with disinfectants (at least once a month) and regular draining (once a day) can prevent problems with hygiene. Figure 41 gives an idea of the indirect adiabatic cooling process. Warm extract air from rooms (1) comes to the evaporative cooler. There, because of the evaporation, the air cools down and becomes more humid (2). After that the air comes to the heat exchanger, where it takes heat from the incoming outdoor air (3). On the other hand, the outdoor air comes to the heat exchanger (4), where it is cooled by the exhaust air flow without increasing of the moisture content (5).

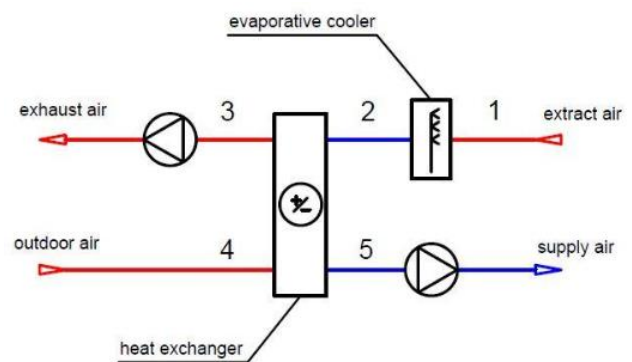


Figure 41: Schematic picture of indirect adiabatic cooling process [22]

Operation principle of Maisotsenko cycle

To understand the principle of the M-cycle we consider a simple adiabatic model (Figure 42). The incoming air comes to the dry channel, where it is cooled by the air flow from adjacent wet channels. After that the air stream comes to the wet channel, where due to evaporation it takes heat from the air in dry channels. At the exit of the wet channel the air is saturated and its temperature is equal to the wet bulb temperature. In theory, the saturated air, at temperature equal to the wet bulb temperature, is cooled to the dew point temperature of the incoming air.

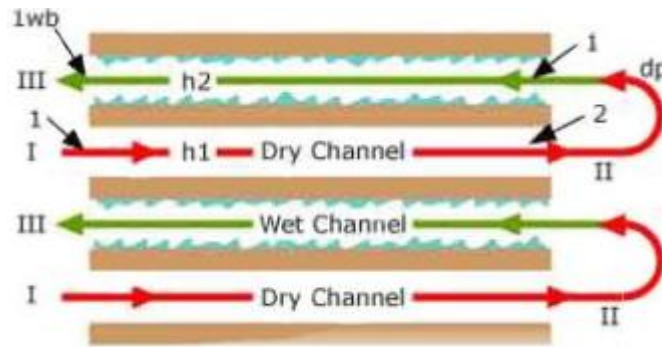


Figure 42: Heat and mass exchanger based on M-cycle [43]

These theoretical results have been achieved in the real prototypes. The air at the outlet of the second channel reached the dew point temperature, but the cooling capacity of this unit equals to zero, because there is no product stream, supply air goes to the outside. Based on this, another scheme was developed for the real air conditioner: there are dry channels for the product air and perforation in working channels. This principle was applied in Coolerado air conditioners. M-cycle diagram is shown in the Figure 44. The incoming air is divided in two streams. The working stream comes to the dry working channel, where it is cooled by adjacent wet working channel. There are also perforations between working channels, needed to significantly reduce the pressure drop. Because product channel is isolated from other channels, the air is cooled without changing of the moisture content. Due to this scheme, the product air can be cooled almost to the dew point temperature, which is the theoretical minimum achievable temperature.

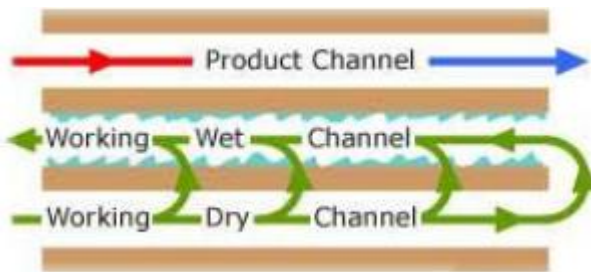


Figure 44: Perforated cross flow heat and mass exchanger [43]

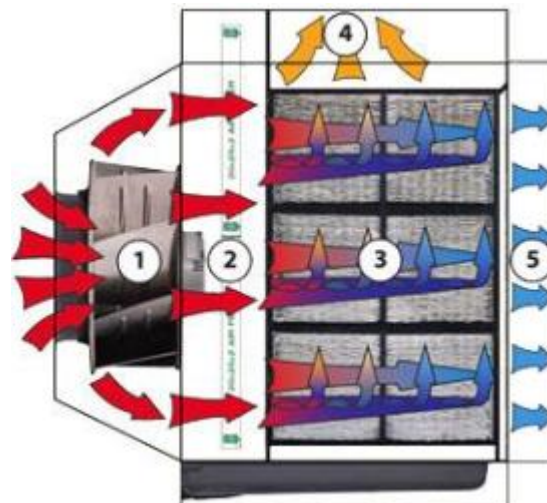


Figure 43: Schematic diagram of the Coolerado cooler [44]

Coolerado cooler has a rather simple design. It consists of a fan, filters, Heat and Mass Exchanger (HMX), air and water connections. Schematic illustration of the Coolerado cooler is shown in Figure 43. At first, fresh air enters the system (1) by a fan. After that, it is cleaned (2) by an array of air filters so to obtain air with reduced dust, pollens and allergens and enters the Heat and Mass Exchanger (HMX) (3). There, the air flow is divided into two streams. One of them, which is called Working Air Stream, takes heat from the other stream, which is called Product or Conditioned Air Stream. A small amount of excess water, used to maintain the cleanliness of the HMX, is drained away through the front drain outlet. Additionally, some water vapour in the Working Air exhaust is condensed inside the unit after cooling, and this water also runs to the drain. Humid working air, that constitute about half of the air that enters the HMX is released back into the atmosphere, carrying energy removed from the conditioned air (4). Chilled fresh air with no added humidity is supplied to the premises (5).

The main part of Coolerado air conditioners is patented Heat and Mass Exchanger (HMX). The HMX consists of plates made of a plastic-coated, cellulose blend fiber. This plastic is designed to wick water evenly on one side and pass well the heat in the transverse direction without mixing of air flows. The plates are stacked on top of each other, and a series of channels are formed between them. The diagram of the HMX is shown in the Figure 45. The air which enters the HMX is divided in the two streams previously described. Working air comes to the dry channel, where it is cooled by adjacent wet channels. In the dry channel it is split into streams which are coming to the wet channels (2). In wet channels the water evaporates and cools airflows of working air. The humid working air is exhausted to the atmosphere (4). The stream of Product air enters the dry channel (1), where it is cooled by adjacent wet channels. Coolerado air conditioners have a modular design. To meet cooling requirements buildings, they may be combined with each other. Capacities in that case are just simply summed. [22] The cooling temperature of the HMX is based on Wet Bulb Temperatures and typically produces Conditioned Air at 2-4 °F (1 – 3°C) above the Inlet Air Stream wet bulb temperature. [23]

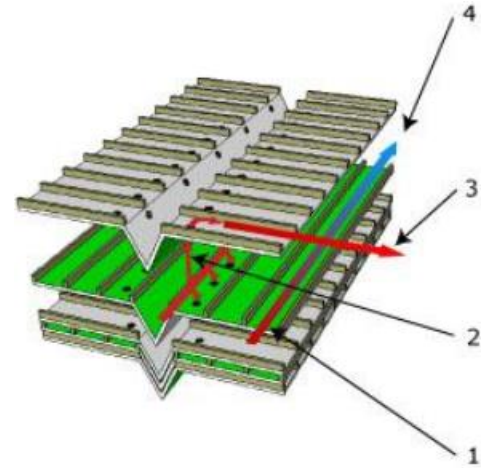


Figure 45: Design of the Heat and Mass Exchanger [43]

Coolerado M50 features and specifications

Coolerado coolers in the project is used as independent air conditioner. It is characterised by an EER 100+ (Energy efficiency Ratio)(COP 29.3+) and a (Coefficient of Performance). Cooling capacity* and efficiency increases as temperature increases. It does not add moisture to the Conditioned Air Stream, like chemical refrigerants or ozone depleting chemicals, it works in quiet conditions and vibration free operation. Delivers up to 5 tons (17.6 kw) of cooling capacity*, and draws a maximum of 750 watts of power at full flow, using up to 90% less electricity than traditional air conditioners depending on ambient air temperatures. The conditioned air is cooled without added humidity. The fan is sized to handle most ducted applications and will deliver 1350 CFM (2,294 m^3/h - 635 L/s) of conditioned air(product air). The filters in this unit are removed from the front above the fan [23]. It presents an intake airflow at 2700 CFM (4.500 m^3/h -1270 L/s), and working airflow at 1,250CFM (2.040 m^3/h - 590 L/s). Conditioned air is cooled to approximately 95 to 120% of intake air's wet bulb temperature without changing moisture content. The unit weighs 370 lbs (168 kg) dry (shipping), and approx. 420 lbs (190 kg) wet (operating). Three standard size 20" (508mm) x 25" (635mm) x2" (50.8mm).

Cooling Capacity	≤ 5 USRT	≤17.6 kW	
Electric Data	Voltaje	200-277 V	
	Frequency	50-60 Hz	
	Power requirement	input	790 W max
	Phase	1	
	Type of Motor	EC Motor	
Total Unit Weight / Shipping dimensions	Dry Install Weight	370 lbs	168 kg
	Operating Weight (wet)	420 lbs	190.5 kg
	Weidth	30"	1.524 mm
	Length	50"	1.270 mm
	High	73"	1.854 mm
Water	Minimum flow**	≥1,4 GPM	≥ 5,3 l/min
	Supply line dynamic pressure	40-80 PSI	225-500 kPa

Table 10: Specifications of Coolerado M50 [23]

*Cooling capacity depends on the ambient wet bulb and dry bulb conditions. Unit capacity indicated above is based on a very high dry bulb temperature and a very low wet bulb temperature.

**with 1/2" NTP (National Pipe Thread) Connection. The water flow rate listed is the instantaneous peak rate when the solenoid valve inside the unit is on and 0 GPM when the valve is off. The solenoid valve cycles on once every two minutes for varying lengths of time (5 to 40 second on time).[24]

From the intake air view(Figure 46) the air entered, the intake air have to be placed in open space, in order to not draw spoiled air. Working air duct (wet air) is connected to 16" (406 mm) diameter hall provided in top of the HMX section (Top view). The discharge plenum view is on the back of the cooler and connected to the product-air duct that goes in block 24. By the Figure 47 gives the idea of the installation of the Coolerado in Block 24.

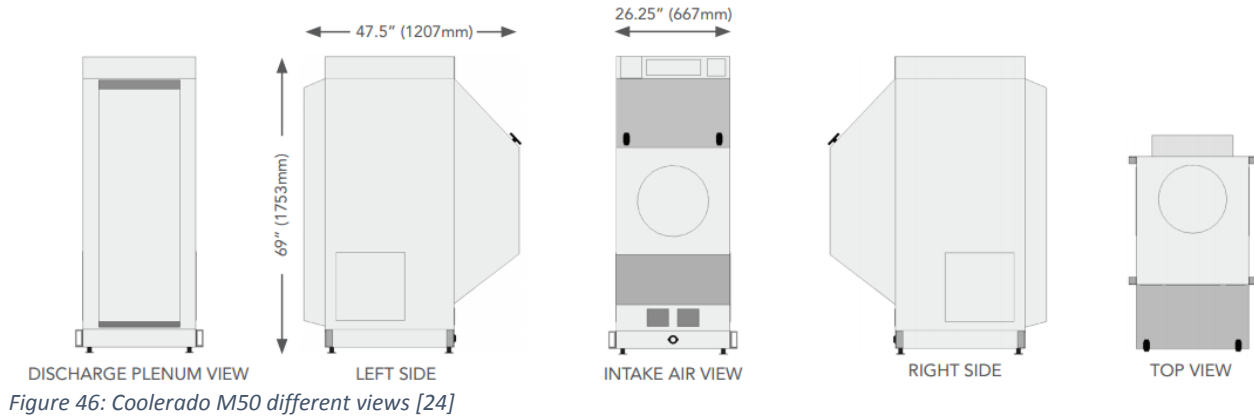


Figure 46: Coolerado M50 different views [24]

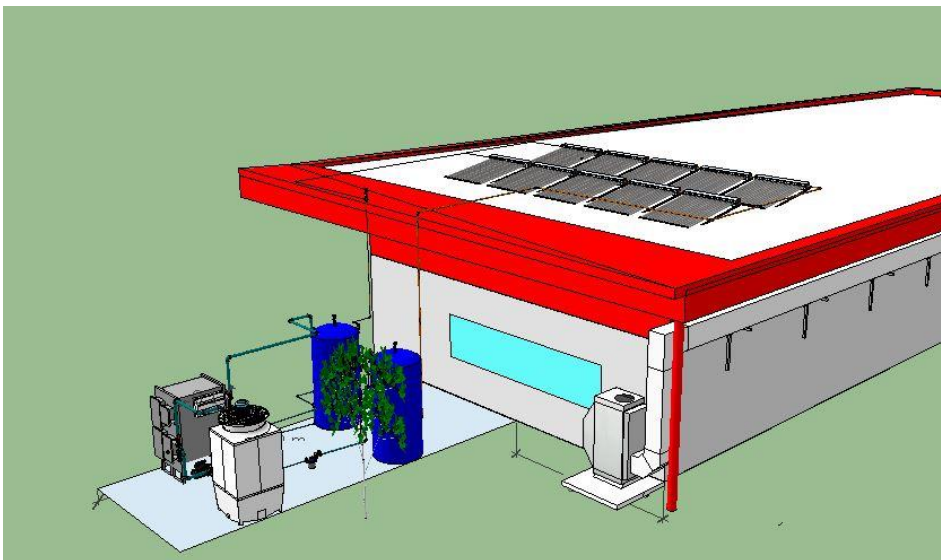


Figure 47: Installation of the coolerado at Building 24

Performance indicators at nominal conditions could be expressed by equation (XXXIII) :

$$EEF = \frac{\text{Cooling air delivered (BTUh)}}{\text{Power required (kW)}} \quad (\text{XXXIII})$$

and

$$COP_{cooling} = \frac{Q_{cold}}{Q_{hot} - Q_{cold}} = \frac{T_{cold}}{T_{hot} - T_{cold}} = \frac{|Q_C|}{W} \quad (\text{XXXIV})$$

where Q_C is the heat removed from the cold reservoir.

The performance of the machines depends from ambient temperature and in particular:

- Outdoor Design temperature (Dew bubble and Wet bubble temperature) [$^{\circ}\text{F}$; $^{\circ}\text{C}$]
- Elevation above sea Level [Ft; m]
- Intake air external static Pressure [IWG;Pa]
- Intake air Flow [CFM; l/s]

Obtaining

- Conditioned air ext. static Pressure [IWG;Pa]
- Total Conditioned air at the full speed of [CFM; l/s]
- Conditioned air temperature (+/- 2 $^{\circ}\text{C}$)
- Working air external static Pressure [IWG; Pa]
- Working air Flow [CFM, l/s]

In the appendix the air flow performance of the M50 Coolerado respect to the ambient temperature and pressure. The performance of the Coolerando could be compromised by a clogged air filter, that will increase operating costs by reducing efficiency and could potentially impact system durability: Coolerado system should never be operated without a clean air filter properly installed. For this reason is important to plan to inspect the filter monthly, since the unit uses 100% outdoor air the filters will need to be changed more often than standard HVAC(Heating and Ventilation Air Conditioning) systems that do not use 100% outdoor air.[15] Water delivery devices and piping should be inspected to insure proper water flow. This includes all pipes leading to the air conditioner as well as the internal tubes that deliver water to the heat exchanger. It is recommendable to check the water supply system for leaks, and repair if needed. Any leaks should be repaired immediately to assure proper water delivery to the unit. The procedure consider to check the internal tubes of the water distribution system for leaks, with the air filters removed. Consistent water flow is essential for efficient and proper unit operation. Water overflowing from the top of the drain pan may indicate that the drain is partially plugged. If this is the case, the procedure consider to remove the elbow from the bottom of the drain pan and clean. The water pressure must be maintained between 25 psi and 80 psi. Below 25 psi the fan will turn off automatically to prevent drying out of Heat and Mass Exchangers(HMX).[23]

4.1.9 Air duct for the coolerado

Because of the importance of the ducting system, for the pipeline of the air conditioning coming from the coolerado was chosen, instead of a classical iron laminate tube, an alternative material: the PIR-ALU®, belonging to Piruloretano sa, a Spanish company which patented it in 1965. Piralu is a panel of pure embossed aluminium pre-insulated with a Polyisocyanurate (PIR) foam, which assure high quality of air ducting, as a direct result of the combination of the aluminium and of excellent thermal insulation in all the point of the duct. It is infact used in the construction of ducting for air distribution in ventilation, heating and air-conditioning systems (HVAC). With PIR-ALU® pre-insulated panels an extremely high quality ducting can be achieved, as a direct result of the combination of the aluminium and of excellent thermal insulation in all the point of the duct. This combination also provides to an excellent internal air quality (IAQ), because the internal air is in contact only with aluminium, to which do not adhere particles. The aluminium, in more, is long-life material, lightweight and easily transported, manipulated and constructed, does not present surface corrosion, and has excellent vapour barrier and drilling technology to prevent internal condensation. So that to have less load losses and energy saving. The model PIR-ALU-20/35 was a donation. The Table 11 shows the specifications [25]

BRAND	PIR-ALU®,	
MODEL	PIR-ALU-20/35.	
GENERAL CHARACTERISTICS	Polyisocyanurate (PIR) rigid foam panel, coated with aluminium foil on both sides	
DIMENSIONS	thickness	20 mm +1.5 -1mm*
	Length	3000 m ± 7 mm*
	width	1200 mm ± 2 mm*
CHEMICAL AND PHYSICAL CHARACTERISTICS	PIR is made from the polyaddition reaction between first quality polyols and polyisocyanates. The chemical reaction involves the polymerization of the raw materials, with the transition from liquid to solid state. The polymer obtained is physiologically and chemically inert, insoluble and unable to be metabolized. The panel is a fiber-free product.	
	Nominal density	35 kg/m ³ (≥33 kg/m ³)
	Coating panel	60 µm embossed aluminium foil with a protective lacquer on both sides.
	Color	Blue
	Blowing agent	CFC, HCFC and HFC-free
MECHANICAL CHARACTERISTICS	compressive strength	3 kg/cm ² ± 0.5(2*)
THERMAL CONDUCTIVITY	0,024 W/m·K (7d, 10 °C) given by the high number of closed cells (exceeding 95%)(3*)	
FIRE REACTION	Euroclass B-s2, d0 (4*)	
SMOKE OPACITY	VOF4= 23 and DS(4)=19(5*)	
SMOKE TOXICITY	CIT=0 (6*)	
RIGIDITY	Elastic rigidity=	160*10 ³ N/m ² (7*)
WATER ABSORTION	after 28 days of total immersion in water does not increase its weight by more than 1,5%(8*)	
WATER PERMEABILITY	considered as a vapor barrier due	

	to thickness of the aluminium foil (>50 µm)	
WATER TIGHTNESS	The water tightness of the PIR-ALU® system prevents air leakage in both longitudinal and transverse joints. Both seals are perfectly sealed and secured by the use of glue and silicone inside. (9*)	
UTILIZATION TEMPERATURE	-40+80 °C without any substantial differences in the thermo-ventilating insulating specifications	
	lineal thermal expansion coefficient	$40 \cdot 10^{-6} \text{mm}/(\text{mm} \cdot \text{K})$

Table 11: Specification of Piralu Air duct for the coolerado[25]

*tolerance range (tested according to EN 823/822/824 standards)

2* tolerance range (tested according to EN 826 standard). The ducts constructed with the PIR-ALU® panels can easily withstand the stresses caused by their own weight. The deformation that can cause the internal pressure of the pipeline, both positive and negative, must be corrected by a system of reinforcements depending on the pressure and the section.[20]

3*according to EN 12667 standard. Comparisons: Wool 0,04; Fiberglass: 0,038 W/(m·K) Elastomer: 0,037 W/(m·K)

4*according to EN 13501-1 standard, reaction to fire of construction products and building elements. The PIR foam of the PIR-ALU® panel does not contribute to the propagation of the flames in a fire scenario, since it generates an intumescent layer of protection for the inner core of the foam.[20]

5*according to ISO 5659-2 standard when used in railway applications as described in EN 45545-2 standard.

6*according to ISO 5659-2 standard when used in railway applications as described in EN 45545-2 standard.

7* classified as R3 according to EN 13403 standard. With PIR-ALU® panels you can build ducts of any shape and section, aerodynamic or static[20]

8*according to EN 12087.

9*classified as C class according to EN 13403 standard for no metallic ducts.

4.1.10 Auxiliary and measurement components

Other minor component compose the air conditioning system. Here below is presented a synthetic overview.

- Three expansion tanks for both the hot and chilled water tanks and for the auxiliary heater. When water is heated in a closed system it expands. Water is not compressible, therefore, the additional water volume created has to go someplace. When an expansion tank is installed the excess water enters the pre-pressurized tank (Figure 48). As the temperature and pressure reaches its maximum, the diaphragm flexes against an air cushion (air is compressible) to allow for increased water expansion (Figure 49). When the system is opened again or the water cools, the water leaves the tank and returns to the system.[26]

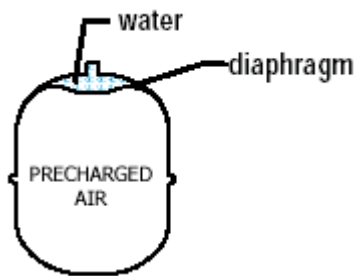


Figure 48: Expansion tank first step[26]

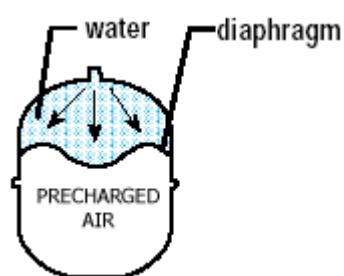


Figure 49: Expansion tank second step [26]

- Thermocouples for measure inlet and outlet temperature of collectors, water capillary mats, hot chilled and cooling part of the absorption-chiller.
- Pyrometer in order to measure the solar irradiance I [W/m^2], measuring the flux that is incident on the surface that is parallel to the sensor surface. It belongs to Kipp & Zonen®. The thermopile sensor construction measures the solar energy that is received from the total solar spectrum and the whole hemisphere (180 degrees field of view). The output is expressed in Watts per meter square. The CMP3 pyrometer (ISO 9060:1990 Second Class) is intended for shortwave global solar radiation measurements in the spectral range from 300 to 2800 nm. The thermopile detector measures irradiance up to 2000 W/m^2 with response time <18 seconds and typical sensitivity 10 $\mu V/W/m^2$ that varies less than 5 % from -10 °C to +40 °C. Operating temperature range is -40 °C to +80 °C and the stability is better than 1 % per year. The Pyrometer does not require any power; it supplies a low voltage of 0 to 20mV in relation to the amount of incoming radiation.
- Relative Humidity and Temperature Solid State Transmitter plugged into the wall, at the site of continuous monitoring of relative humidity and temperature, in the environment controlled. The transmitter belongs to Hanna Instruments Colombia®'s brand and the model is HI 8666, with an accuracy of $\pm 2\%$ for RH and $\pm 1\%$ ° C. It send a 4-20mA analogic signal, that can be sent to screens, controllers or data acquisition systems. The signals can be sent separately (or Temperature with RH or temperature with bubble point temperature) with external voltage sources of 10-20Vdc. It operates on a range from 0% (4mA) a 100% (20mA) for RH and from -20°C (4mA) to 60°C (20mA) for the temperature.

5 CHAPTER 2

5.1 PERFORMANCE ANALYSIS

Once described the system in all of its part and the nominal parameter of the main equipment defined, the further step is to evaluate its operation to evaluate the system performance in different operational conditions. In order to accomplish to that, a performance analysis for the three main subsystem that characterised the air conditioning in the Building 24 is carried out for. In particular are analysed the absorption Chiller, the Solar Collectors and the Coolerado.

5.1.1 Absorption Chiller performance analysis

In order to tests the performance of the equipment a series of test measurement (TM) in different conditions are carried out: a procedure has been followed during the TM:

1. The first “test-measurement” expect that the system works at its maximum capacity.
2. Through the temperature chart of the 1st TM, extrapolate by the thermocouples installed around the entire circuit, the thermodynamic behaviour of the system in Colombia conditions expect to be described.
3. In order to better compare the test-measurement each others, each one have to provide:
 - Table of the step followed during the measurement
 - Ambient condition registered during the measurement
 - Which parameters of the system have been modified with respect to previous measurement
 - Energy consumption registered during the whole time of the measurement (see Table 34 in the appendix)
 - Minimum temperature reached during the test measurement (see Table 34 in the appendix)
 - DT of chilled water and time in production of the chilled water before to start the air conditioning (see Table 34 in the appendix)
 - DT and time of air conditioning (see Table 34 in the appendix)

Here following the chronological thermodynamic analysis is presented.

5.1.1.1 First test-measurement (1st TM)

The day 16/03/2017 the first experimental measurement was held because the weather condition in Medellín were favourable; the following weather data was registered:

Weather data registered			
	Parameter	Value	Time of measurement
Peak data	Temperature	31,85 °C	16:00
	Radiation	995 W/m ²	12:00 a.m.
Average data	Temperature	27,9 °C	from 8:47 am to 16:06
	Radiation	608 W/m ²	
	Relative Humidity	45 %	

Table 12: Weather data registered in the 1st TM

The measurement was held by the following steps:

Equipment ON	Time	Excell number
Auxiliary heater – Collectors*	8:47	3
Auxiliary heater – Collectors – Chiller**	10:10	498
Auxiliary heater – Collectors – Chiller- Mats – Coolerado	13:57	1860/18568
Auxiliary heater – Collectors – Chiller	15:45	2510/25048
Collectors	16:06	2642/26308

NONE (end of the test-measurment)	16:30	2778 /27750
--	-------	-------------

Table 13: 1stTM steps followed

*It means that was switched on the pump from the collectors to the hot tank. This pump is activated automatically in order to avoid evaporation of the water inside the collectors.

**It means that were switched on the pumps inside the chiller (solution pump and cryogenic pump), the hot tank to the chiller's pump, the chilled tank to the chiller's pump and the cooling tower to chiller's pump and the coil inside the cooling tower.

The data collected starts from the 8:47 in the morning, at that time were switch on the auxiliary heater and the pump from the collector to the hot water storage tank. The hot water storage tank's temperature increases until the cooling chiller were switch on, indeed until the 10:10, reaching a temperature of 79°C.

When the chiller started up, the lithium bromide-water solution begin circulating between the generator and absorber. No vapour would have been evolved (the cryogenic pump would not be automatic activated) until the generator and all the solution held up in the generator have been heated to a temperature T_{min} . This temperature is the boiling point of a lithium bromide solution whose concentration corresponds to the chiller's initial charge at a pressure determined by the condenser temperature. Being the generator, sensible heat exchanger, and absorber all modelled as constant effectiveness heat exchangers during start-up, and if it is assumed that the absorber and sensible heat exchanger respond much more rapidly than the generator, then the generator temperature during start-up will vary exponentially[11]:

$$T_G = T_{G,ss} + (T_{G,o} - T_{G,ss}) \exp\left(-\frac{t}{t_H}\right) \quad (XXXV)$$

Where

T_G = the generator temperature

$T_{G,ss}$ = the steady-state generator temperature,

$T_{G,o}$ = the initial generator temperature

t_H = the generation time constant for start-up

Measurements of the time-temperature history of the generator of a 3-ton-capacity chiller (Arkla model WF-36) located at Colorado State University (CSU) Solar House I show that during start-up the generator is described well by Equation (XXXV) with a time constant t_H of about 8minutes. Being the chiller used of that same dimension could be possible to consider the $t_H = 8$ min[11]. This approximation is confirmed by the temperature trend.

More preciously in this measurement were registered after about 8 minutes later that the three valve opened, indeed from 10:16 to 10:25 (some minutes later than the chiller started up) a not steady state behaviour was registered inside the chiller: the solution pump starts a dilution between water and Li-Br reaching a $T_{min} = T_g \cong 65^\circ\text{C}$. (See "chiller hot" in Figure 50).

The Figure 50 is temperature chart history of the test done: a chart analysis is provided below.

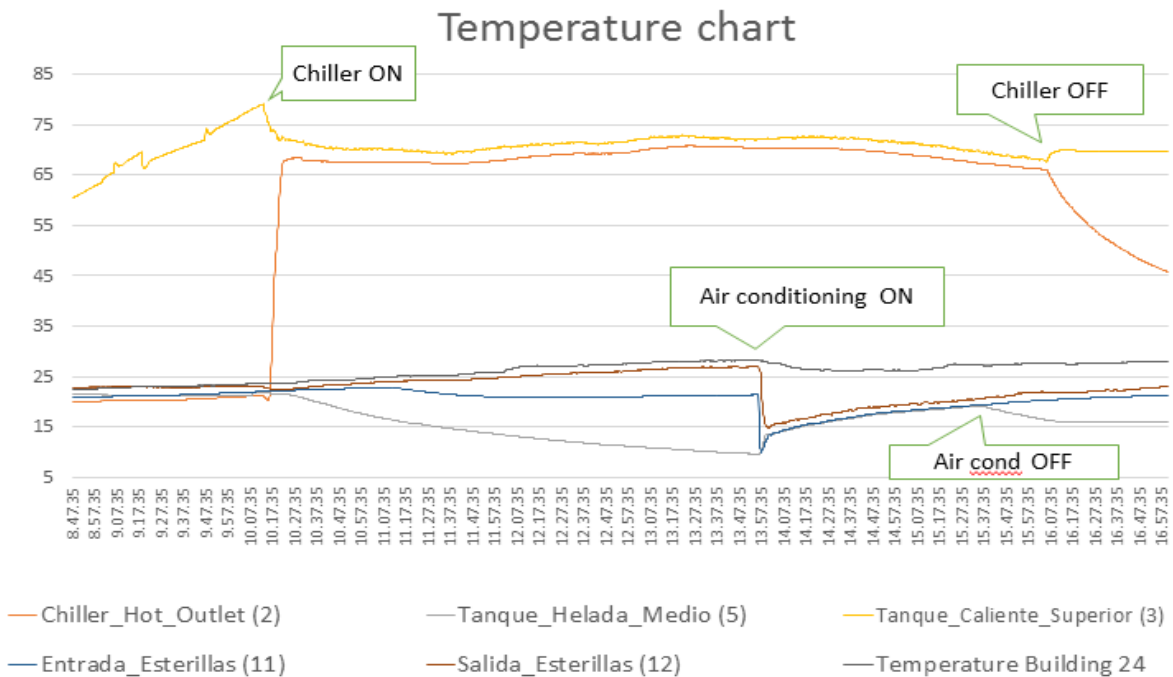


Figure 50: Temperature chart history of the 1stTM

When the chiller started on the following thermodynamic behaviour is observed inside the system:

- The temperature in the hot water storage tank starts to decrease because the chiller consume the hot water.
- The temperatures in and out of the hot part of the chiller (generator) start to increase rapidly passing from 23,5 °C to 78 °C.
- The temperatures in and out of the chilled part of the chiller (evaporator) start to decrease exponentially.

In this phase of the cycle all the pumps involved in the system are working, with the exception of the pump from the chilled water storage to the water capillary mats. This is, in fact, the period in which the chilled water is produced and stored.

When the water stored in the chilled tank reaches a temperature of about 9°C finally the air conditioning in the Building 24 through solar absorption cooling system starts. It is happen at about 14:00 the afternoon. Between the time when the chiller started on and the chilled water were produced, indeed from 10:12 in the morning to about 2:00 in the afternoon, the following thermodynamic behaviour from the system is observed:

- The temperature in the hot water storage tank is stabilized at a temperature above the 70 °C (the minimum temperature requested for the operation of the chiller)
- The temperatures in and out of the hot part of the chiller (generator) start to decrease exponentially of few degrees, from 78°C to values over 70°C.
- The temperatures in and out of the chilled part of the chiller (evaporator) passed from 24°C to 9°C. A gap of 15°C is reached in almost 4 hours.

Since when at 13:57 the pump that push water to the capillary mats installed in the building was switched on together with the coolerado air conditioning system, two degree of temperature decrease were registered in building 24, from about 28°C to 26°C in 1 hour and 45 minutes (until 15:40). The following thermodynamic behaviour is observed in the system:

- The temperature in the hot water storage tank decrease, never reaching the minimum temperature (68°C) requested for the operation of the chiller.

- The temperature in and out of the chilled part of the chiller (evaporator) rapidly increase of 2,5 degree, than increase exponentially up to reach a temperature of 16°C. That is because the water capillary mats exploiting the chilled water storage in the tank, took back to the tank (directly connected to the heat exchange of the evaporator of the chilled), a warmer water that have cooled the building. Meanwhile happen this process, the chiller continue to cool the water inside the heat exchange of the evaporator.

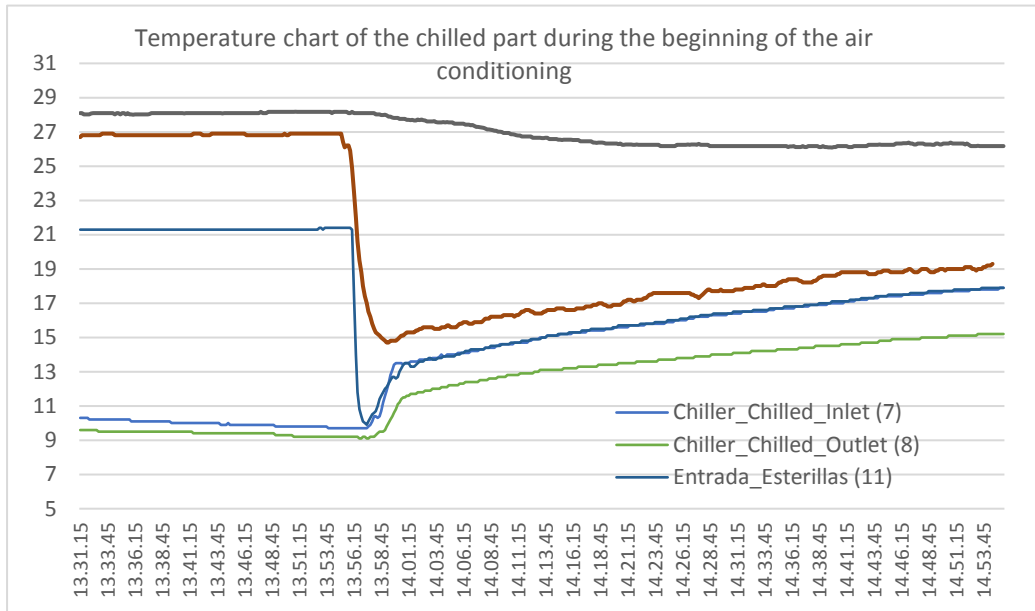


Figure 51: Temperature chart focus on chilled part of the system during the beginning of the air conditioning of the 1stTM

- Temperature in and out of the capillary mats, that before the air conditioning had a temperature gap of 6°(temperature in of the capillary mats is about 21 °C and temperature out of capillary mats is about 28°C) rapidly decrease passing from 27, 7°C to 9°C (maintaining a gap of 3°C) and then increase because of the behaviour inside the chiller, previously described (See Figure 51).

When the temperature inside the water capillary mat is not enough low to cool the building, the pump from chilled water tank to mats is switched off: at 15:40 the temperature inside the mats is at 22 °C and for this reason the air-conditioning is stopped. The chiller continue to work in order to produce chilled water, and its cooling capacity decrease because the water in the chilled tank is not used for cooling the building anymore and the temperature difference in and out to the evaporator decrease.

The minimum operational conditions required inside the chiller stop to be present at 16:06 because the temperature on the hot water storage tank, indeed on the hot part of the absorption chiller do not reach 68°C. In that moment the chiller stop to work and the temperature in the hot water storage tank start to decrease, but a very interesting fact is noticed: the chiller still has cooling capacity, because of its thermal inertia capacity, that permits the evaporator inside the chiller to still cool the water inside the heat exchange of chilled water. For this reason is not convenient to switch off the pump from the chilled part of the chiller to the tank, until the temperature difference between in and out of the chilled part is equal to zero and water at lower temperature is not possible to storage anymore.

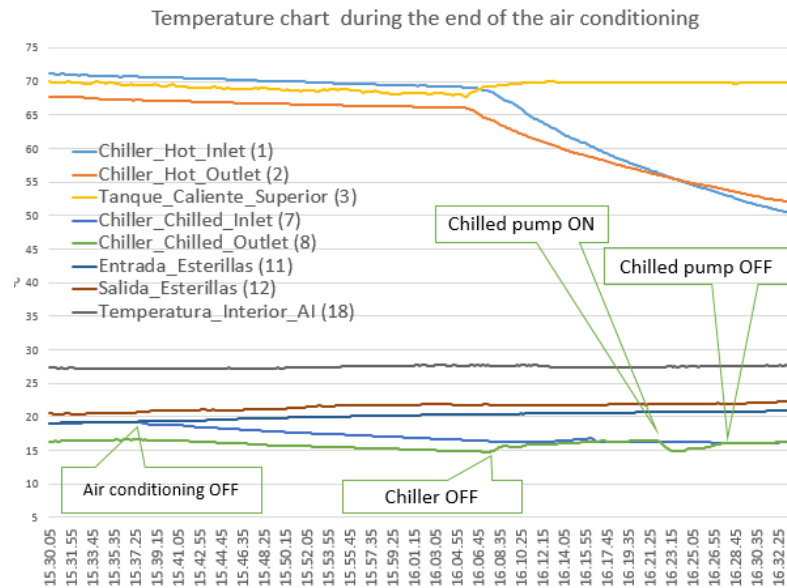


Figure 52: Temperature chart of the system during the end of the air conditioning of the 1stTM

During cooldown, after has been shut the chiller off, solution will drain to the lowest point of the chiller (usually the absorber) and lose heat to the surrounding air by conduction and natural convection because of the dilution of the solution [11]. Indeed, when in the generator the temperature of 68°C is reached, through an opening of a valve called of “regeneration” colder water will enter in order to dilute the solution in the absorber, so that when the cycle will restart the pump will inflate to the generator a solution with the right concentration of Li-Br-water. In that case:

$$T_S = T_{a'} + (T_{G,o} - T_{a'}) \exp\left(-\frac{t}{t_C}\right) \quad (\text{XXXVI})$$

Where

T_S = the solution temperature

$T_{a'}$ = the temperature of the surroundings

t_C = the cooldown constant

The cooldown constant t_C will tend to be much larger than the start-up time constant, since it depends on free rather than forced convection.

5.1.1.2 Second test measurement (2ndTM)

The day 18/03/2017 the second experimental measurement was held because the weather condition in Medellín were favourable: the following weather data was registered.

Weather data registered			
	Parameter	Value	Time of measurement
Peak data	Temperature	29,6 °C	15:20
	Radiation	984 W/m ²	11:00 a.m.
Average data	Temperature	26,7 °C	from 10:22 am to 17:00
	Radiation	539 W/m ²	
	Relative Humidity	47 %	

Table 14: Weather data registered in the 2nd TM

The measurement was held by the following steps:

Equipment ON	time	Excel number
Auxiliary heater – Collectors	10:22	3
Auxiliary heater – Collectors – Chiller	11:26	386
Auxiliary heater – Collectors – Chiller- Mats	14:21	1442/14342
Auxiliary heater – Collectors –	16:29	2209/22022

Table 15: 2ndTM steps followed

This second test-measurement was held without the use of the Coolerdo. As already said, the coolerdo is responsible first of all to renovate the air of the building and contribute to elevate the quality of the air inside the building, and exploiting the indirect evaporative cooling contribute with its cooling capacity to cool the ambient. Indeed what is expected to this measurement is that there is a reduction in the cooling effect, indeed that an higher temperature inside the building during air conditioning is established.

Respect to 1st TM the chiller was switched on when the temperature in the hot water chiller was higher, at 92°C, for these reason, and because the auxiliary heater was switched on later (10:30), the chiller starts to work 1h15m later (11:30). The pump to the capillary mat were switched on when the temperature inside the chilled tank reached 9° (14:20) and the air conditioning in the building happen until the temperature of the generator reach $T_{min} = 68^{\circ}\text{C}$ (16:29). Until about 17:00 the hot tank temperature continue to increase reaching 71°C.

The temperature inside the building, decrease of only 1,3° (from 28,1°C to 26,8°), as it was estimated, less than the previous case because was not implemented the coolerdo.

The air conditioning lasts for about 2 hours and half (from the 14:20 up to 17:00=2,67h).

The Table 16 shows the air conditioning performance between the 1st and 2nd TM characterized by the use of coolerdo. Even though the 2nd TM day was a bit more hottest, the difference in performance are relevant:

	1 st TM	2 nd TM
First 30' minutes of air cond	28,08-26,28 = 1,9 °C	28,28-26,93 = 1,35 °C
Starting from 27,67 °C after 30 min	26,176 (h 14:30) = 1,5 °C	26,73 (h 15:00) = 0,94 °C

Table 16: Comparison in air conditioning performance between 1st and 2nd TM with and without the use of coolerdo

Is not convenient in term of thermal performance to do not work with the Coolerdo, because it affects about the 30% of the air conditioning effect in the Building 24, considering only the worsening in temperature decreasing, without considering the worsening in the quality of the air. The Coolerdo contribute with about 20% of the total energy consumption during air conditioning.

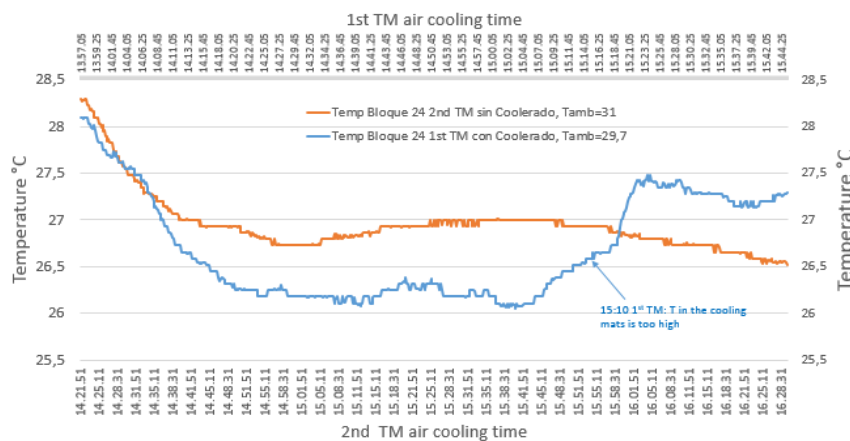


Figure 53: AiR Conditioning performance between 1st and 2nd TM

Working with an higher temperature increase the performance of producing chilled water: the Table 17 compares the 1st and 2ndTM:

Chiller Performance			
	T min °C	ΔT	Time of ΔT
1 st TM	9,2	12,5	3h 47 min
2 nd TM	8,7	14,3	2h 57min

Table 17: comparison of cooling performance of the Chiller between 1st and 2nd TM

From Figure 54 is possible to understand the consequence of using a temperature lower in the generator. In fact the 1st TM results less effective in long term because it after only one hour of air cooling it already presents insufficient thermal inertia to cool the building.

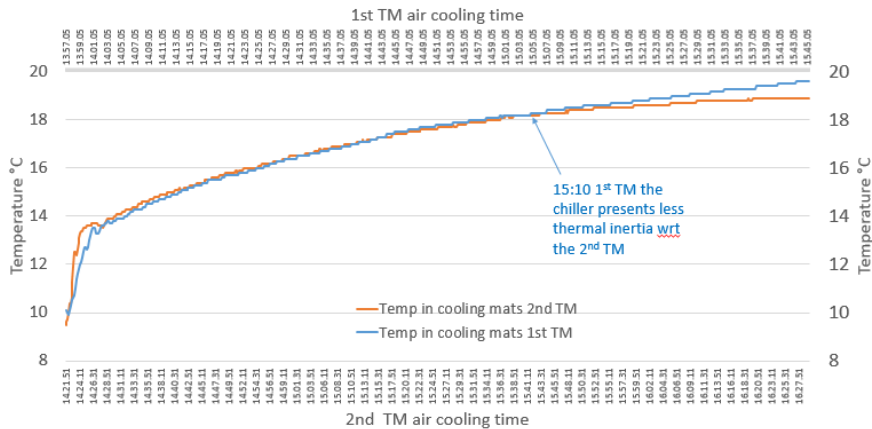


Figure 54: difference in temperature inlet the capillary mats during air cond time between 1st and 2nd TM due to difference thermal inertia.

5.1.1.3 Third test measurement (3rd TM)

The day 27/03/2017 the third experimental measurement was held because the weather condition in Medellín were favourable: the following weather data was registered.

Weather data registered			
	Parameter	Value	Time of measurement
Peak data	Temperature	29,6 °C	14:40
	Radiation	1096,5 W/m ²	14:25
Average Data	Temperature	26,7 °C	from 11:30 am to 17:30
	Radiation	583 W/m ²	
	Relative Humidity	47 %	

Table 18: Weather data registered in the 3rdTM

From these measurement, an equipment on-off indicator was added, indeed a more precise chronological steps followed could be possible to construct. The measurement was held by the following steps:

Equipment ON	time	Excell n
Auxiliary heater – Collectors	11:29:24	3
Auxiliary heater – Collectors – Cooling tower and cooling tower pump – hot and chilled water pumps** –	11:51:24	135/44502
Auxiliary heater – Collectors – Chiller***	11:53:24	147/44622
Auxiliary heater – Collectors – Chiller – Mats – Coolerado	14:28:04	1075/10706
Auxiliary heater – Chiller – Mats – Coolerado	16:20:04	1747/17422
Auxiliary heater – Chiller without Cooling tower and cooling tower pump – Mats – Coolerado	16:31:34	1816/18112
Auxiliary heater – Mats – Hot water pump – Coolerado	16:37:24	1851/18462
Auxiliary heater – Mats– Coolerado	16:40:04	1867/18622
Coolerado	17:10:54	2052/20484
NONE (end of the test-measurement)	17:25:44	2141/21383

Table 19: 3rdTM steps followed

** It means that were switched on all the pumps that goes to the chiller, except for the chiller itself, indeed the cryogenic pump and the solution pump.

***It means that were switched on the pumps inside the chiller (solution pump and cryogenic pump), the hot tank to the chiller's pump, the chilled tank to the chiller's pump and the cooling tower to chiller's pump and the fan inside the cooling tower.

In general, the performance of an absorbing machine improves at partial loads. The effect is due to the fact that the heat exchangers present in the plant operates at a lower flow rate and therefore have higher thermal efficiency: at the request of less power by the user, the machine would tend to provide cold water at lower temperatures. It could be possible for example modulating the thermal power to the generator, adjusting the input of hot water [27]. In this case could not be possible because the pump could not variate its speed indeed the 3rd TM was held working reducing the evaporator flow rate, because as Table 8 shows that pump presents three different working speed. The speed selected was the second one, the working flow in the evaporator results to be lower than the previous TM, in the generator remain equal.

In more by adding the on-off equipment indicator could be possible to experimental measure the transient behaviour of the absorption chiller, in particular was possible to recognize that:

- When the chiller is switched on (11:51), before the solution pump, and consequentially the cryogenic pump start to work, it needs 3 minutes for the dilution of the solution inside the absorber.
- When the chiller is switched off (16:31), because the generator temperature has reached T_{min} , the chiller still works for 8 minutes more without the cooling tower. That is happen in order to dilute the solution in the absorber, so that when the cycle will restart the pump will inflate to the generator a solution with the right concentration of Li-Br-water and avoid crystallization. In absorption chillers, usually the crystallization line for lithium bromide and water is very close to the working concentrations needed for practical LiBr/H₂O absorption chillers, such as Point A in Figure 55. If the solution concentration is too high or the solution temperature is reduced too low, Point A migrates to Point B and crystallization may occur, interrupting machine operation [28].

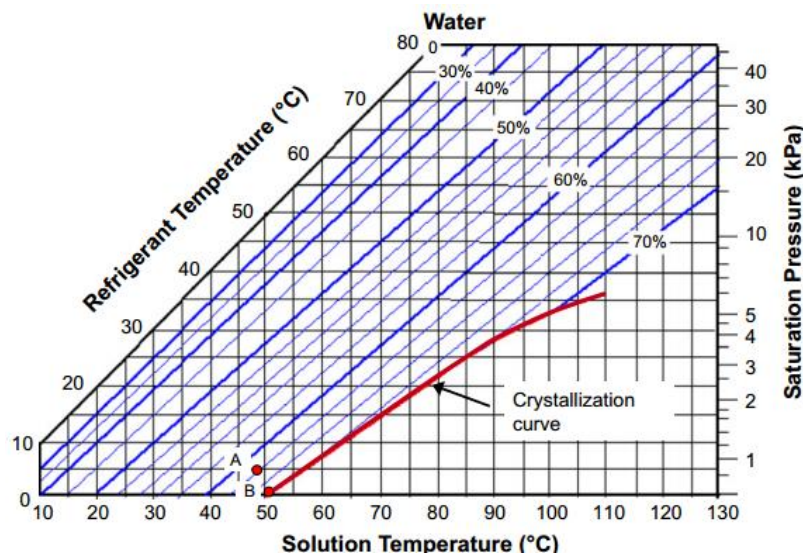
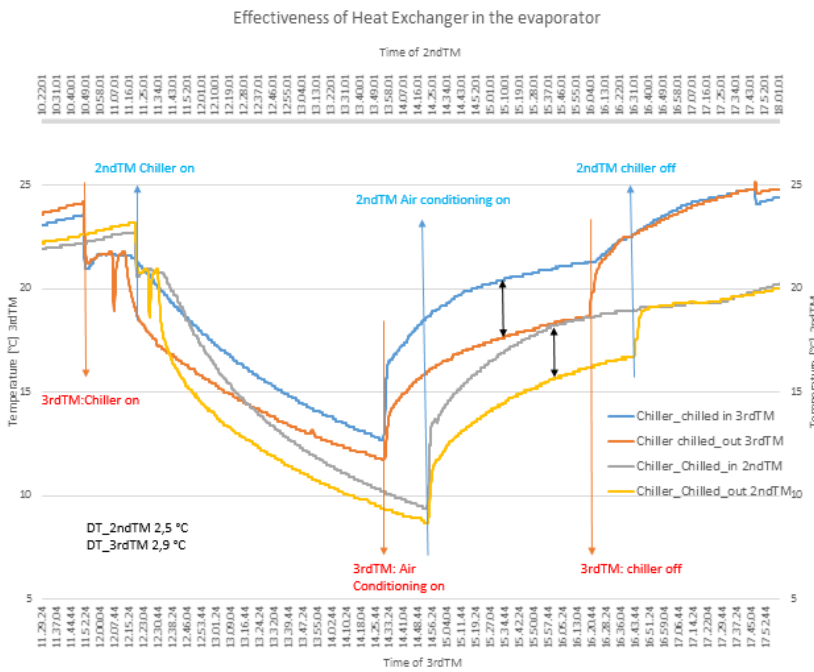


Figure 55: The property chart of LiBr/H₂O solution with crystallization curve.[28]

The chiller was switched on when temperature in the hot tank reached a temperature of about 84 °C, it caused decrease in performances. The time of cooling water production from passing from 23,8 °C to 11,7 °C (a temperature higher from the previous TM but presenting almost the same ΔT and even better if compared with the 1st TM that has the same T_{gen}) resulted reduced to 2hours and 35 minutes, against 2h 57min of the 2nd TM, because of the improvement of the heat exchange efficiency inside the absorption chiller.

The Figure 56 shows the difference in temperature in and out of the evaporator during the production of chilled water and during air conditioning of 2nd TM and 3rd TM. In the 2nd TM the slope in the decrease in chilled temperature is higher but should to be consider the fact that the temperature in the generator is higher indeed



the cooling capacity increase, but also that the cooling period is major (30 minutes more). The figure wants to show the higher difference in the 3rd TM with respect to the 2nd TM on both the period, during the production of chilled water and during the air conditioning.

Figure 56: Difference in temperature during air conditioning in 2nd TM and 3rd TM

Comparing the 3rd TM with the 1st TM that have almost the same Tgen, the Figure 57 shows the temperature difference during the air cooling period. This difference is equal during the last part only because during the 1st TM the air conditioning was stopped before than the cooling capacity of the chiller was exhausted (was switched off the pump to the collector before than the chiller switched off). Anyway, the chiller during 3rd TM presents higher thermal inertia because the thermal storage cools down more slowly, requiring the machine less power from the generator. The cooling capacity increase, against the 3h 48 minutes needed for decreasing the temperature of refrigerant water of about 12°C in the 1st TM, where needed only 2h and 35 minutes in the 3rd TM.

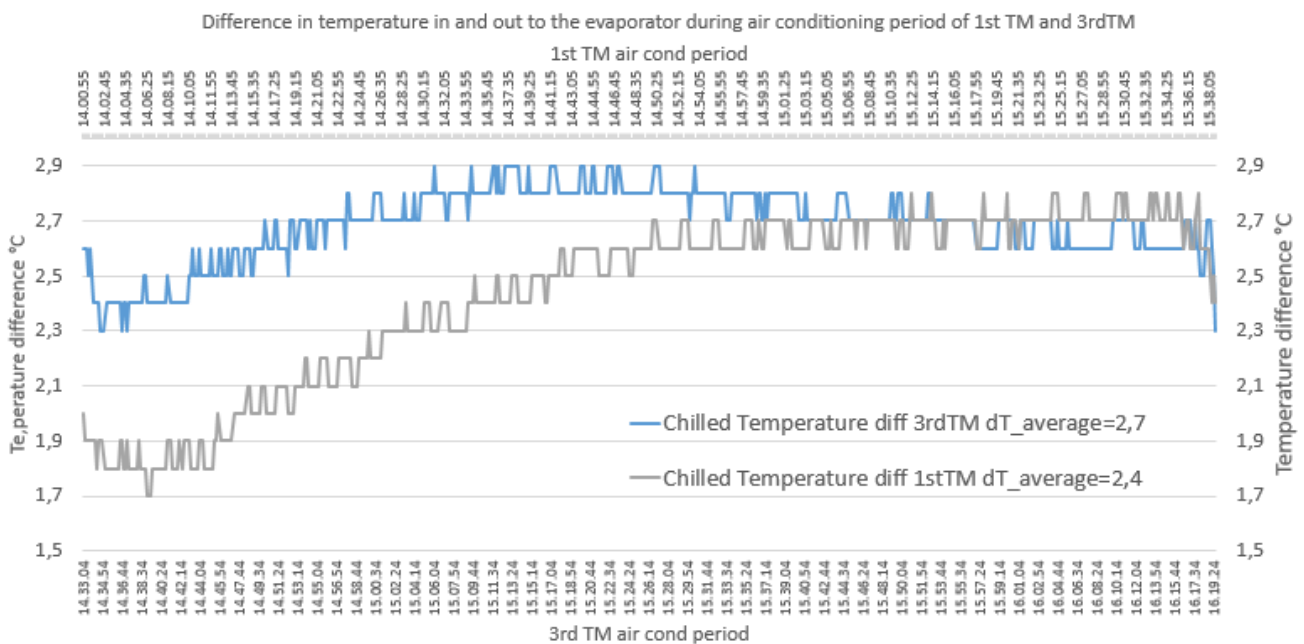


Figure 57: Comparison of the effectiveness of the heat exchange in the evaporator between 2ndTM and 3rdTM.

It could be noticed that the trend is not linear but it presents a zig-zag profile: that is explained by the behaviour of the cooling tower. The closed adiabatic circuit cooler works with a set point temperature, in this case at 30

degree. When the temperature entering to the cooler after having crossed also the absorber is up to 30 (in this case it reaches a temperature of about 33°C) the fan of the cooler switch on and regulate its speed up to the maximum and than decrease until the set point is reached. Usually this change is so rapid that in the chart is not possible to see the variable speed but only the maximum and minimum so to create a zig-zag profile (up and down between the Tset temperature). Because the performance are compromised by the cooling water inlet temperature, indeed by the condensing temperature, also the trend of the temperature in and out of the evaporator are affected by a zig-zag profile.

Is important to notice that 3rdTM was affected negatively by two different behaviour:

1. The initial generator temperature was lower that 2ndTM. In fact, because the measurement start later it was decided to start to produce chilled water when the temperature in the hot tank was at 86,5 °C.

2. The air conditioning started when the temperature in the chilled tank was about 12°C. if the temperature of water stored were lower the air conditioning performance could have been better (see later table of comparison).

A conclusion could be already extrapolate from the 3rd TM

- For reducing in energy consumption, the idea is to install pumps to the chiller, both from the chilled water tank and the hot water tank (because of the same behaviour) that could be vary them speed by a variable frequency drive. In this way is possible to improve the heat exchanger effectiveness and reduce the mass flow rate, indeed the energy consumption.
- The mean power consumption during 3rd TM registered is higher because the TM start later and during hotter hours the mean consumption of the cooling tower are higher. A reduction mean power consumption during air conditioning is present, respect to the precedent measurement, because of the lower consumption of the pump

5.1.1.4 Fourth test measurement (4th TM)

The day 28/03/2017 the fourth experimental measurement was held because the weather condition in Medellín were initially favourable, but during the air condition start to rain: the following weather data was registered.

Weather data registered			
	Parameter	Value	Time of measurement
Peak data	Temperature	28 °C	13:30
	Radiation	991,5 W/m ²	12:10 a.m.
Average data	Temperature	23,52 °C	from 7:13 am to 15:13
	Radiation	590 W/m ²	
	Relative Humidity	63,5 %	

Table 20: Weather data registered in the 4th TM

The measurement was held by the following steps:

Equipment ON	time	Excell number
Auxiliary heater	7:12:24	6
Auxiliary heater – Collectors	7:27:44	98
Auxiliary heater	8:22:54	429
Auxiliary heater – Collectors	8:47:14	575
Auxiliary heater	8:54:44	620
Auxiliary heater – Collectors	9:27:54	819
Auxiliary heater	9:41:04	898
Auxiliary heater – Collectors	10:06:04	1048
Auxiliary heater – Collectors – Hot water pump	10:13:54	1095
Auxiliary heater – Collectors– Cooling tower and cooling tower pump – hot and chilled water pumps –	10:59:24	1368
Auxiliary heater – Collectors – Chiller	11:23:44	1514

Auxiliary heater – Collectors – Chiller – Mats	13:44:14	2357/23509
NONE (end of the test-measurement)	15:13:06	2891/28853

Table 21: 4th TM steps followed

The 4th TM was held at the same operational conditions of the precedent one, with the exception that this time, being the measurement started earlier the inlet generator temperature reached 98°C. Because of the worsening in weather condition, during the production of chilled water, was decided to do not work with the Coolerado and safe 500 kW (20% power less during the air condition) because of the low thermal load request of the Building 24.

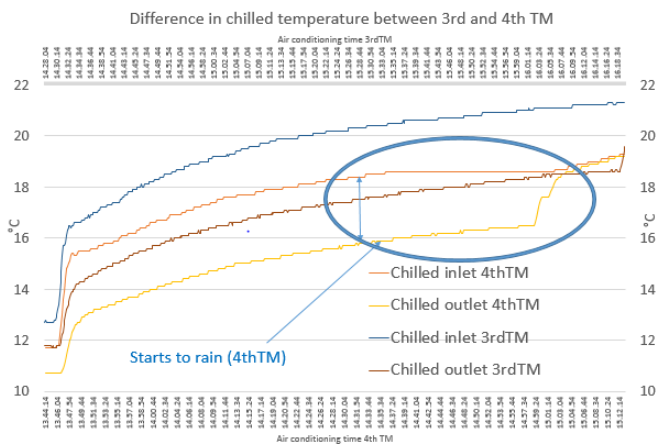


Figure 58: Difference in T_{evap} between 3rd and 4thTM

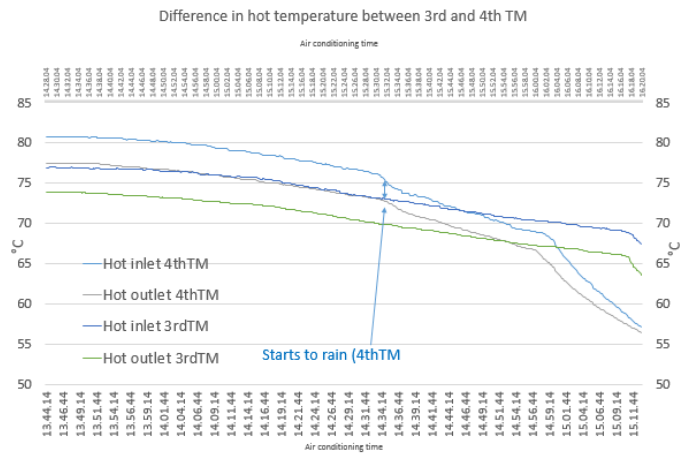


Figure 59: Difference in T_{gen} between 3rd and 4thTM

When the generator temperature reach 68 °C the chiller does not have any more the minimum temperature that get it to work, and for this reason this temperature suddenly decrease. The Figure 59 shows the difference slopes of generator temperature during the measurement. The slope decrease when it starts to rain, in the hot water storage tank the temperature decrease more rapidly because miss the collectors' contribution (first change in slope); when it is reaches the minimum temperature needed by the chiller, three way valve closed and the chiller starts to cool itself in order to avoid crystallization (second change in slope). The Figure 58 reflects the situation in the evaporator, when it starts to rain the equipment cools down and the evaporator inlet temperature receive less power and it works until finish the thermal storage.

The average instant power used by the 4th TM was the lowest registered so far, because it last less, being interrupted by the rain, because was employed the second speed of the pump connected to the chiller water storage tank, (that is equivalent of a barely reduction of 1%), and because neither the coolerado was employed, responsible of the 20% of the energy consumption during the air conditioning time. A total of 12,352 kWh of energy was consumed also because during the measurement was switched off the collector's pump in case the water temperature provided was lower than one present in the tank.

Because of the bad weather conditions, the air conditioning lasts about 1h and half (from 13:44 to 15:13) over the 8 hours of the measurement (from the 7:12 to 15:12).

The temperature difference registered in the building was the maximum reach: it passed from 28,645 to 26,08 °C in one hour and half, that because the air conditioning starts at temperature lower than usual. It permits the chiller to provide lower temperature during air conditioning, being the water returning at lower temperature: decreasing the temperature of the air on the capillary mats and consequentially in the storage tank, the efficiency of the battery increase. The chiller, in fact, since the air conditioning starts, cannot provide the energy requested to maintain the temperature of the battery constant but if the power of the user required is less because the temperature in the building is lower, the efficiency improve.

What is happen, in fact, is that the temperature in the battery gradually increase being the chiller not capable to cover the power requested and once the temperature in the building decrease, the user thermal load also decrease and it is possible to reduce this increase in temperature, indeed the air conditioning is much more efficiency.

Some conclusions could be extrapolate from the 4th TM

- It is convenient to put a on-off controller for the ignition of the pump from the collectors to the hot water storage tank, in order to switch it off when the difference between the outlet temperature of the collectors and the temperature of the hot water storage tank is minor than zero and avoid, in bad weather conditions that the water from the collectors cools down the water stored.
- If it is rain is not convenient to air conditioning with the use of Coolerado because its efficiency is highly reduced with relative humidity.
- It is always convenient to start the air conditioning before the hottest hour of the day so that the thermal charge is lower and the effectiveness of the air conditioning is higher. For these reason when a cycle of air conditioning is stopped is also convenient to produce refrigeration water for the day after in order to start the air conditioning before.

5.1.1.5 Fifth test measurement (5th TM)

Before to do the last test measurement it was observed through experimentation that the chiller was neither producing water below 15°C. After running various experiments, it was concluded that the chiller had a poor vacuum. Absorption chillers are directly dependent on how well the condensers are vacuumed, without a good vacuum the evaporative cooling will happen at a higher temperature and the water being used in the absorber will be warm; thereby, producing warmer water. Once created the vacuum of 0,3 kPa in the evaporator of the chiller the last TM was held in the 25/05/2017, and in order to improve the cooling capacity, the condensation temperature was reduce, moving the Tset of the cooling tower from 30° to 28°C. The measurement was held using the maximum speed of the pump in the evaporator, as in the 1st and 2nd TM.

The following weather data was registered.

Weather data registered			
	Parameter	Value	Time of measurement
Peak data	Temperature	31,883 °C	13:46
	Radiation	1015,6 W/m ²	13:10
Average data	Temperature	30,02°C	from 09:18 am to 13:57
	Radiation	706,3 W/m ²	
	Relative Humidity	45 %	

Table 22: Weather data registered in the 3rdTM

The measurement was held by the following steps:

Equipment ON	time	Excell n
Auxiliary heater	9:18:14	2
Auxiliary heater – Hot water pump*	10:24:11	395
Auxiliary heater – Collectors – Hot water pump	11:12:11	683
Auxiliary heater – Collectors -Collectors – Chiller**	11:14:11	695
Auxiliary heater – Collectors -Chiller – Mats – Coolerado	12:33:01	1168/11662
Auxiliary heater – Collectors -Chiller without hot water pump– Mats – Coolerado	13:50:01	1630
Auxiliary heater – Collectors - Chiller without hot and chilled water pump, Cooling tower and cooling tower pump – Mats – Coolerado	13:52:01	1642/16402
Auxiliary heater – Collectors – Hot water pump – Coolerado	13:57:31	1647/16732

Table 23: 5th TM steps followed

*The hot water pump is used in order to make the water circulating inside the tank and promote a better distribution of the hot water inside it.

**It means that were switched on the pumps inside the chiller (solution pump and cryogenic pump), the hot tank to the chiller's pump, the chilled tank to the chiller's pump and the cooling tower to chiller's pump and the fan inside the cooling tower.

During the measurement was observed a rapid production of chilled water but also a rapid arrest of the chiller (the chiller switched off after 1h and 20 minutes), once the pump to the capillary mats was switched on, that because the machine needs more power in order to furnish an higher cooling capacity, given to the lower temperature of condensation. In more was registered high energy consumption because of the cooling tower that in order to cool until the T_{set} of 28°C (see Table 34 in the Annex)

The cause of the block of the machine in all the test measurement done is due to the incapacity of the system to provide the power required to the generator by the indirect alimentation (the solar panel and the auxiliary heater).

Once understood the thermodynamic behaviour of the system in colombian condition, described in detail in the 1st TM and collected all the data provided experimentally by the tests, in which parameter were changed step by step in order to evaluate the performance in different conditions finally is possible to make a comparison and verify if the parameter modified in the system have improved or not the performance of the system. The next chart will give us the response.

5.1.1.6 Comparison

As described in section Water pipeline including five pumps 4.1.7 in which is described the hydraulic circuit that characterize the system, was not possible to measure or calculate all the flow rate involved in the closed circuits that are involved in the system, because of missing of the ultrasonic flow meter and neither pressure gauge upstream the valve. In particular was not possible to extrapolate the flow rate in the section from the hot and chilled water tank to the chiller. The pumps involved in fact do not present characteristic curve of power required with respect to the flow rate delivered, so although were measured these consumption was not possible to estimate these flux. The only power known is which provided by the cooling tower, because in that case the pump's constructor provide the curve of the delivered flow with respect to the power input. This power is so calculated:

$$\dot{Q}_{c\ tower} = \dot{m}_{c\ tower} * (T_{c\ tower,out} - T_{c\ tower,in}) \quad (XXXVII)$$

Indeed, since the flow rate measure in the generator and the evaporator miss, was not possible to experimental measure the Cooling Capacity (Q_E) and the COP.

In order to describe and compare the performance of the absorption chiller in different TMs done the performance indicators are estimated by an overall steady-state energy balance on the absorption chiller, neglecting net losses that may occur to the surroundings.

Starting from the nominal performance curve of the equipment, furnished in Figure 22, Figure 23, Figure 24 in Section 4.1.2 with respect to the chilled water outlet, cooling water inlet and hot water inlet temperature respectively, the equation curves of the cooling capacity were extrapolated. In particular, as the performance curves in Figure 60, Figure 61 and Figure 62 show, for each measure the cooling capacity with respect to the following parameter was calculated as following:

- Temperature of evaporation ("Chilled temperature" out of the evaporator, going to the chilled water tank), according to equation (XXXVIII) extrapolated by the curve

$$\dot{Q}_E = 0,2698 * T_{chilled\ out} + 9,3811 \quad (XXXVIII)$$

- Temperature of condensation ("Cooling temperature" inlet to the condenser, coming from the cooling tower), according to equation (XXXIX) extrapolated by the curve

$$\dot{Q}_E = - 0,889 * T_{cooling\ tower,out} + 37,681 \quad (XXXIX)$$

- Temperature of generation ("Hot temperature" inlet to the generator, coming from the hot water tank), according to equation (XL) extrapolated by the curve

$$\dot{Q}_E = 0,3197 * T_{hot\ water,in} - 17,482 \quad (XL)$$

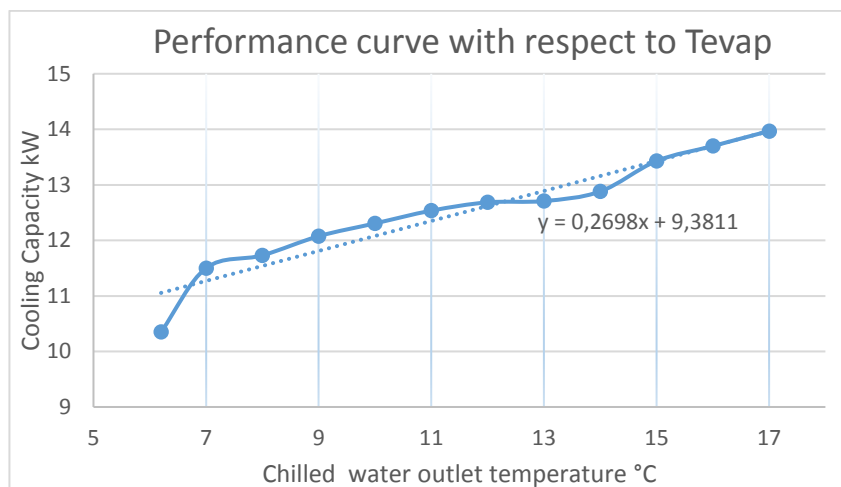


Figure 60 Performance curve extrapolated of "RXZ-11.5" wrt T evap

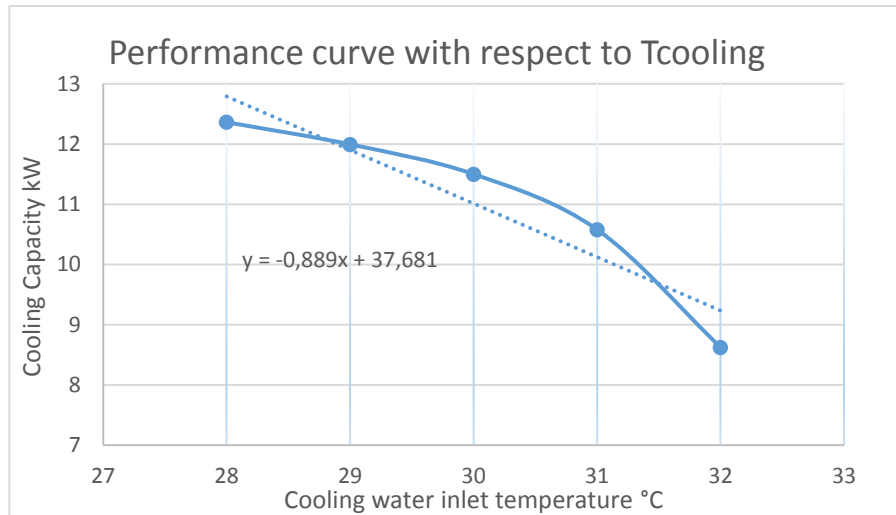


Figure 61 Performance curve extrapolated of "RXZ-11.5" wrt T cond

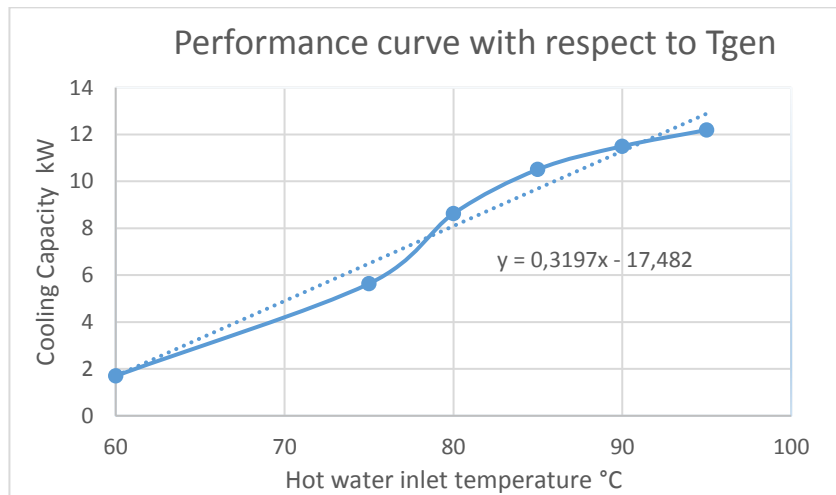


Figure 62: Performance curve extrapolated of "RXZ-11.5" wrt Tgen

Indeed for each TM three cooling capacity were find and the correction factor calculated as

$$f_1(T_{evap}) = \frac{\dot{Q}_{evap}(T_{evap})}{\dot{Q}_{nom,evap}} \quad (XLI)$$

$$f_2(T_{cooling}) = \frac{\dot{Q}_{evap}(T_{cooling})}{\dot{Q}_{nom,evap}} \quad (XLII)$$

$$f_3(T_{hot}) = \frac{\dot{Q}_{evap}(T_{hot})}{\dot{Q}_{nom,evap}} \quad (XLIII)$$

Assuming that overlap of the effect is valid the COP was find for each TM as

$$COP_{i,TM} = COP_{nom} * f_1(T_{evap}) * f_2(T_{cooling}) * f_3(T_{hot}) \quad (XLIV)$$

Where:

f_1 is the correction factor of the cooling capacity due to the influence of the chilled water outlet temperature.

f_2 is the correction factor of the cooling capacity due to the influence of the cooling water inlet temperature.

f_3 is the correction factor of the cooling capacity due to the influence of the hot water inlet temperature.

The indicators of performance (COP and cooling capacity) were analysed during a period in which the air-conditioning supplied by the transient operation of the chiller could be approximated to idealised steady-state operational conditions (the transient operation of the chiller leads to approximately 8% lower COP than would be expected if transients would neglected [11]). In order to compare the performance between each test measurement was chosen an equal period of 45 minutes.

Finally knowing the $COP_{i, TM}$ and the $\dot{Q}_{i, c\ tower}$ of each TM, the following parameters that characterize the system performance are calculated as:

$$COP_{i, TM} = \frac{\dot{Q}_{eva}}{\dot{Q}_{gen}} \quad (XLV)$$

$$\dot{Q}_{c\ tower} = \dot{Q}_{evap} + \dot{Q}_{gen} \quad (XLVI)$$

$$COP_{i, TM} = \frac{\dot{Q}_{eva}}{\dot{Q}_{gen}} \quad (XLVII)$$

$$\dot{Q}_{c\ tower} = \dot{Q}_{gen} * (COP_{i, TM} + 1) \quad (XLVIII)$$

$$\dot{Q}_{gen} = \frac{\dot{Q}_{c\ tower}}{(COP_{i, TM} + 1)} \quad (XLIX)$$

$$\dot{Q}_{eva} = \dot{Q}_{c\ tower} - \dot{Q}_{gen} \quad (L)$$

The results are shown in Table 24

	1 st TM	2 nd TM	3 rd TM	4 th TM	5 th TM
Average during 45 minutes of air conditioning (stable period)					
\overline{T}_{gen} [°C]	72,690	77,320	75,950	79,140	69,930
$\overline{\Delta T}_{gen}$ [°C]	3,484	3,28	3,166	3,380	4,560
\overline{Q}_{gen} [kW]	10,589	9,112	8,706	8,713	17,673
\overline{T}_{evap} [°C]	15,330	13,670	16,150	14,140	13,560
$\overline{\Delta T}_{evap}$	2,648	2,308	2,697	2,652	4,030
\overline{Q}_{evap} [kW]	4,273	4,473	4,240	4,698	6,699
$\overline{T}_{cooling}$ [°C]	29,530	29,520	29,460	29,430	27,600
$\overline{\Delta T}_{cooling}$ [°C]	2,56	2,340	2,230	2,310	4,198
$\overline{\dot{m}}$ [kg/s]	1,389	1,389	1,389	1,389	1,389
$\overline{Q}_{cooling}$ [kW]	14,862	13,585	12,946	12,830	24,372
COP	0,404	0,491	0,487	0,539	0,379
$\overline{P}_{air\ cond\ entire\ period}$ [kW]	2,8	2,65	2,5	2,4	3,4

Table 24: Performance results of the absorption cooling system during the five TMs

During all the TMs was never reach the nominal cooling capacity of 11,5 kW, that because of an intrinsic limit of the system that never allow to work with a temperature in the generator equal to 90°C (see Figure 62: Performance curve extrapolated of "RXZ-11.5" wrt Tgen). During the start up period, indeed the period in which no vapour would have been involved, the generator consumes a lot of power, as initial and final temperature shown in Table 25. This behaviour is more remarked during the 5th TM when working with a cooling temperature lower, and less remarked when working at partial load, during 3rd and 4th TMs.

	1TM	2TM	3TM	4TM	5TM
Initial time h	10.14	11.27	12.06.34	11.27.54	11.17.11
Finish time h	10.22	11.34	12.14.24	11.32.54	11.22.41
Start up period	00.08	00.07	00.07	00.05	00.05
Hot tank Initial T [°C]	78,5	91,4	84,4	95,5	90,4
Hot tank Final T [°C]	72,7	83,90	77,9	89	82,2
Lost in temperature	5,80	7,50	6,50	6,50	8,20

Table 25: start up period of TMs

Important improvement could lead to partially solve the problem:

- The pump that goes from the hot water storage tank to the absorption chiller take water from the bottom of the tank, indeed it is affected negatively by the thermal stratification inside the tank. It is appropriate to connect the pump to the top of the chiller. In order to minimize this problem during the collection of the thermal load, the pump was switched on in order to make the water circulating inside the tank.
- The auxiliary heater input is located directly to the hot water tank, a future simulation could be put the heater in series with the tank thereby to provide energy when the temperature is above the minimum temperature in the generator by means of a temperature controller. In this way always not only could be assured always high temperature into the generator but also the minimum temperature in the chiller and the air conditioning won't be interrupted.

The COPs in Table 24 confirm that during the TMs the performance have improved passing from the 1st TM to the 4th TM, indeed were correctly changed the parameter in the system in order to improve the performance with the actual configuration.

In particular, increasing the inlet temperature of the generator of an average of 5°C (it was necessary to heat the hot water storage tank of 13°C more, from 79°C to 92°C, see Table 34 in the annex) the COP increase of 17,7 %. Also the cooling capacity increase of 4% and the time employed in chilled water production decrease of about 48 minutes (see Table 34 in the annex).

When was reduced the flow rate in the evaporator during 3rd TM and 4th TM the improvement in the effectiveness of the heat exchange could be reflected also in the COP. If compare the indicator of the 3rd TM with which was obtained in the 1st TM, that are characterised by more similar generator temperature the COP passed from to be the 58,6 % of the nominal in the 1st TM to the 70,6 % in the 3rd TM. In this case, for almost the same cooling capacity the machine exploit much less thermal power than in the 1st TM (8,7 kW versus 10,6 kW), indeed a better COP is reached allowing the machine to work longer. This allows the machine to work longer, because the minimum conditions required in the generator are guaranteed longer, in fact the air conditioning last for more than 2 hours respect to the 1st TM in which lasts about 25 minutes less. Should also to be considered the fact that higher average temperature and lower radiation were registered during the 3rd TM, (see Table 34 in the annex), indeed more heat loss in the collectors and less power exploited in the generator have been performed with respect to the 1st TM.

The best COP is registered during the 4th TM that is characterised to high Temperature in the generator (the thermal storage temperature arrived to 98,4 °C) and better heat exchange effectiveness (the highest difference in chilled temperature), due to reduction of the mass flow rate in the evaporator, because it was working with second speed of pump. In this measurement, it was capable in reaching the 78% of the nominal COP and the cooling capacity improve of 5% with respect to the 2nd TM and the lowest time in production of chilled water was registered (1h 29 minute for more than 12° of cooling). The air conditioning performance does not improve (the air conditioning period only lasts for 1hour and 30 minutes) only because of bad weather conditions. Because the air conditioning starts when the temperature inside the building were lower the battery tank of chilled water improves its efficiency and air conditioning was more effective.

The 5th TM presented the highest cooling capacity, about equal to the 60% per cent, but present the lowest COP registered (about the 55% of the nominal one). That is because in order to provide about 7kW of cooling power consume about 17 kW of thermal power stored. Such situation provoke that the minimum condition requested from the chiller are extinguished very quickly and the air conditioning happen for only about 1h and 20 minutes (see Table 34 in the annex).

In conclusion could be said that two configuration at the actual layout of the system could be preferred: the one which is provided by the 4th TM and by the 5th TM.

Working with the second speeds of the pump in the evaporator and the highest Temperature in the generator, improves the effectiveness of the heat exchange in the evaporator and it leads to obtain the highest COP registered. That assure the longest period of work of the chiller because of its thermal inertia, consuming less instantaneous power from the generator. It was not possible to observe during the same TM because of worsening in weather condition but the prove is given by the 3rd TM, that presents the longest period of air conditioning and differs from the 4th only for the generator temperature. This could make us expect that if the weather conditions did not get worse, the TM could only give better results than the 3rd, as happen for the 2nd with respect to the 1st. In more, it is the measurement in which less power was consumed (see Table 34 in the annex), because of less power input for the ventilator of the cooling tower and also for evaporator pump.

Working with a T_{set} in the cooling tower equal to 28°C and also the maximum flow rate in the evaporator, the 5th TM proves that it possible to reach the 60% of the nominal cooling capacity. It is very useful in case the cooling demand is imminent and big; the former case it could be more suitable in case is needed only to maintain the same temperature in the building, and indeed the cooling demand is lower.

5.1.2 Collectors performance analysis

The data sheet of Solar Lucy Co. Lt does not provide the specific information about optical efficiency and coefficients c_1 and c_2 of equation (X). Although the company was been contacted never was able to reply to this question and currently we are still waiting for this information. Meanwhile, it was decided to use the data of an other tube collector, researched in SPF Institute of Solar Technology database, that has similar specifications[29].

Relative efficiency η collector's data	
Optical coefficient η_0	0,835
Loss coefficient c_1	1.56 W/m ² -K*
Loss coefficient c_2	0.0017 W/m ² - K*

Table 26: thermal efficiency's coefficients of the collectors[29]

*test of efficiency ISO9806:2013

The average of thermal efficiency during all day of the measurement when the collector's pump were switch on is evaluated, when the solar incidence radiation is recorded (from the third measurement). Figure 63 shows a plot of this efficiency during 3rd TM. Its dependence on the solar radiation is clearly evidenced and the high average temperature is responsible in reducing it of about 20 % than the optical one.

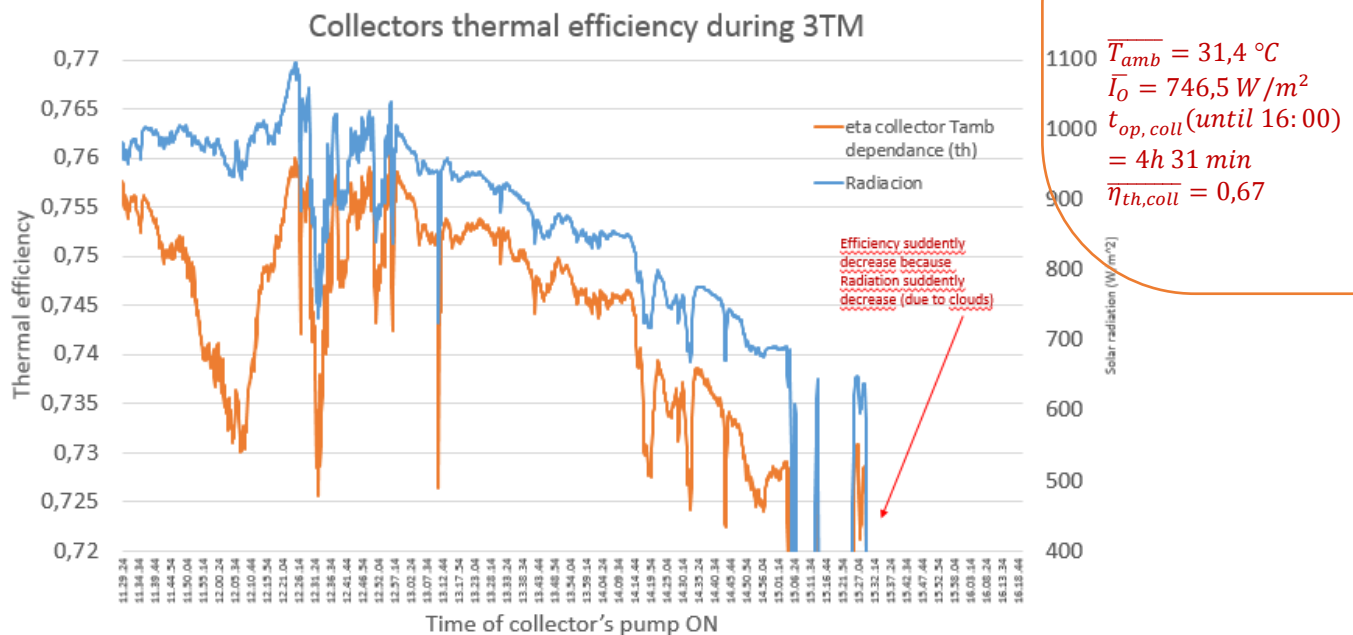


Figure 63: Collectors thermal efficiency and solar radiation during 3rd TM

The thermal efficiency has a maximum equal to the optical efficiency (a theoretical efficiency based on normal and diffuse irradiance tested by the producer [30]), and its value is related to the efficiency with respect to the designed operation. It takes in account also the influence of ambient temperature and in particular higher is the difference between collector's temperature and ambient temperature lower is the efficiency due to thermal losses. Thermal efficiency does not take in account the system condition, as the flow rate. Flow rate inherently affects performance through the average absorber temperature. If the heat removal rate is reduced, the average absorber temperature increases and more heat is lost [9]. If the flow is increased, collector absorber temperature and heat loss decrease. For measuring performance of the collector related to the flow rate, indeed a global collector efficiency is evaluated. Is defined the global coefficient, referring to the behaviour of the collector with respect to the experimental conditions and takes in account the solar cooling system performance. This solar collector efficiency is defined as the fraction of available solar power incident on the collector (Q_{solar}) that is converted into usable heat power (Q_{coll}) by the collectors[31].

$$\eta_{glob, coll} = \frac{Q_{coll}}{Q_{solar}} = \frac{\dot{m} * c_{water} * \Delta T_{col}}{I * A_{col}} \quad (LI)$$

Where

\dot{m} is the flow rate circulating in the collector, to be calculated.

c_{water} is the specific heat of water, approximated constant equal to 4,186 kJ/(kg °C).

ΔT_{col} is the temperature difference in and out to the collector, experimentally measured.

I is the radiation registered during the measured in W/m²

A_{col} is the collector's Effective lighting area installed equal to 20,4 m²

Indeed in order to calculate this parameter, the flow rate circulating inside the system was calculated. A simple balance was constructed, neglecting the heat loss from the hot water storage tank:

$$\dot{m}_{collector} * c_{water} * (T_{in} - T_{out}) = \frac{kg_{hot\ tank}}{dt} * c_{water} * (T_{final} - T_{initial}) \quad (LII)$$

Where

$\dot{m}_{collector}$ is the flow rate that have to be calculated

$(T_{in} - T_{out}) = \Delta T_{col}$

$\frac{kg_{hot\ tank}}{dt}$ is the capacity of the hot storage tank (1000 L=1000 kg) over a time in which the water is heating, during a experimented measurement. By the measurement it resulted that was convenient to work with a dt equal to 600 seconds.

$(T_{final} - T_{initial})$ is the difference in temperature after 600 seconds inside the tank, experimentally measured.

A measurement was done during a sunny day, the 17/05/2017, between the 11.40 to 13.28. During the measurement, in order to have a more homogeneous temperature inside the tank the hot water pump that goes to the absorption chiller was switched on, so that, being the chiller turned off the, the three way valve returns the water to the top of the tank. Obviously the measurement was done without switch on the auxiliary heater. Resulted an average of water flow rate given by the pump connected to the solar collector is equal to 1,93 m³/h (0,54 kg/s)(the pump has a constant flow rate, as described in section 4.1.7).

Being the 10 collectors installed in series of 5, the flow rate circulating in each collector is the middle of that, equal to 972 L/h each manifold.

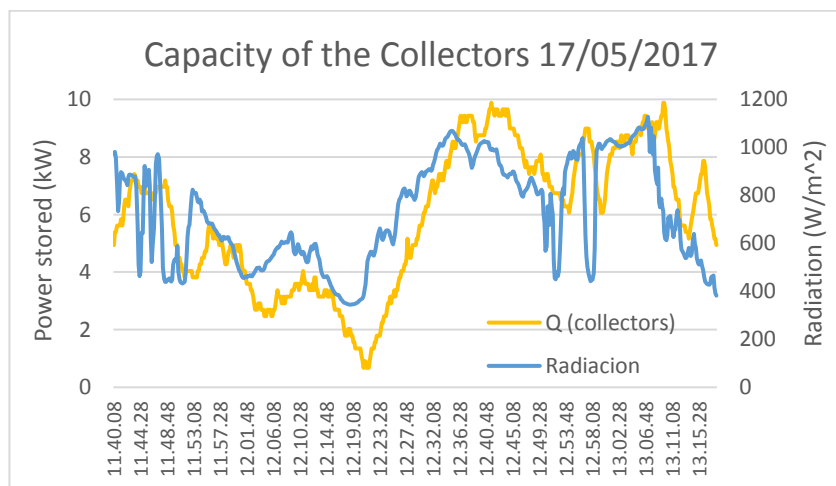


Figure 64: power stored by solar collectors in 17/05/2017

The Table 27 resume the collector's performance registered during 3rd TM, 4th TM and 5th TM (measurement for which was possible to measure the solar radiation by means of the use of pyrometer). As it could be possible to see from Figure 65, with the actual configuration of the solar panel installed on the roof of the Building 24, the radiation could be exploited only until about 16:00. It is caused for the presence of trees' shadow, as shown from the photo of Figure 66. Indeed the results referred to the whole period in which the pump from the collectors to the hot water storage tank were switched on in each measurement up to 16:00 taking into

account only values higher than zero. In Table 27 also the average of the instantaneous average power output from the collectors is indicated and the total thermal average energy provided is calculated just multiplying it with the time of the measurement.



Figure 65: Radiation incident in the Building 24 of the University in a typical sunny day of Medellín.



Figure 66: picture taken the 30/05/2017 at 16:09 showing trees shadows on the collectors

	3rdTM (27/03/2017)	4thTM (28/03/2017)	5thTM (25/05/2017)	Weighted Average**
$\overline{T_{amb}} [^{\circ}C]$	31,4	29,5	30,9	
$\overline{I} [W/m^2]$	746,5(725,08*)	723,2 (668,17*)	655,7 (775,6*)	
Collectors ON	11:29(11:53*)	10:06(11:23*)	11:12	
Collectors OFF	16:00	15:13	16:00 (13:30*)	
$\overline{\eta_{coll,th}}$	0,67	0,70	0,69	0,68
$\overline{\eta_{coll,glob}}$	0,56(0,57*)	0,50 (0,53*)	0,38 (0,50*)	0,53
$P_{max,inst}$	14,91	15,597	11,08	13,86
$P_{coll,inst} [kW]$	9,82 (9,88*)	9,34(9,79*)	6,14 (8,3*)	9,5
$\overline{E_{tot}} [kWh/day]$	44,34 (40,65*)	47,82 (37,48*)	29,5 (21,9*)	40,97

Table 27: Results of performance analysis of solar collector installed in the Building 24.

*The value is referred to the average calculated during the period in which operate also the absorption chiller

**The weighted average refers to the period in which operate also the absorption chiller, except for the energy, calculated along the whole period.

For the parameters affected by the system condition, are reported two values: the average value extrapolated during the entire period in which the pump of the collectors is switched on until 16:00, if positive, and the average value extrapolated during the time in which also the absorption chiller operates (in the table are into the parenthesis and remarked by an asterisk).

Clearly the latter values are higher because when the chiller works and exploit thermal power stored, the collectors' contribution is much more remarkable (the temperature entering the collector is lower, indeed the

collectors are much more effective, being the difference between temperature in and out of the collectors higher).

The performance of the collectors are in fact, compromise by the auxiliary heater. As example, Figure 67 shows the behaviour of the difference temperature in and out of the collector during the 4th TM, where in orange the temperature difference trend is point out and in blue the radiation on the collectors. In particular the global collector efficiency, referring also to the system condition, is affected by the auxiliary heater contribution, that heating the water inside the tank increase its temperature inlet to the collector, so to make inefficient the collector contribution in case the radiation is not enough or the temperature inlet is too high (see Condition D Figure 67). This phenomena is even worse in case the chiller does not work and the auxiliary heater is switched on in order to heat the storage faster. In fact, being this coefficient, as also the power and indeed the energy, directly proportional to the temperature difference in and out the collectors it increases when the chiller works because this difference is higher (see Condition C Figure 67), due to the fact that the generator of the chiller is consuming the power collected into the tank. When the Chiller is starting up, a not stable state persists (see Condition B Figure 67). The same happens when the hot water pump is switched on in order to make the temperature into the tank homogenous (see Condition A, Figure 67).

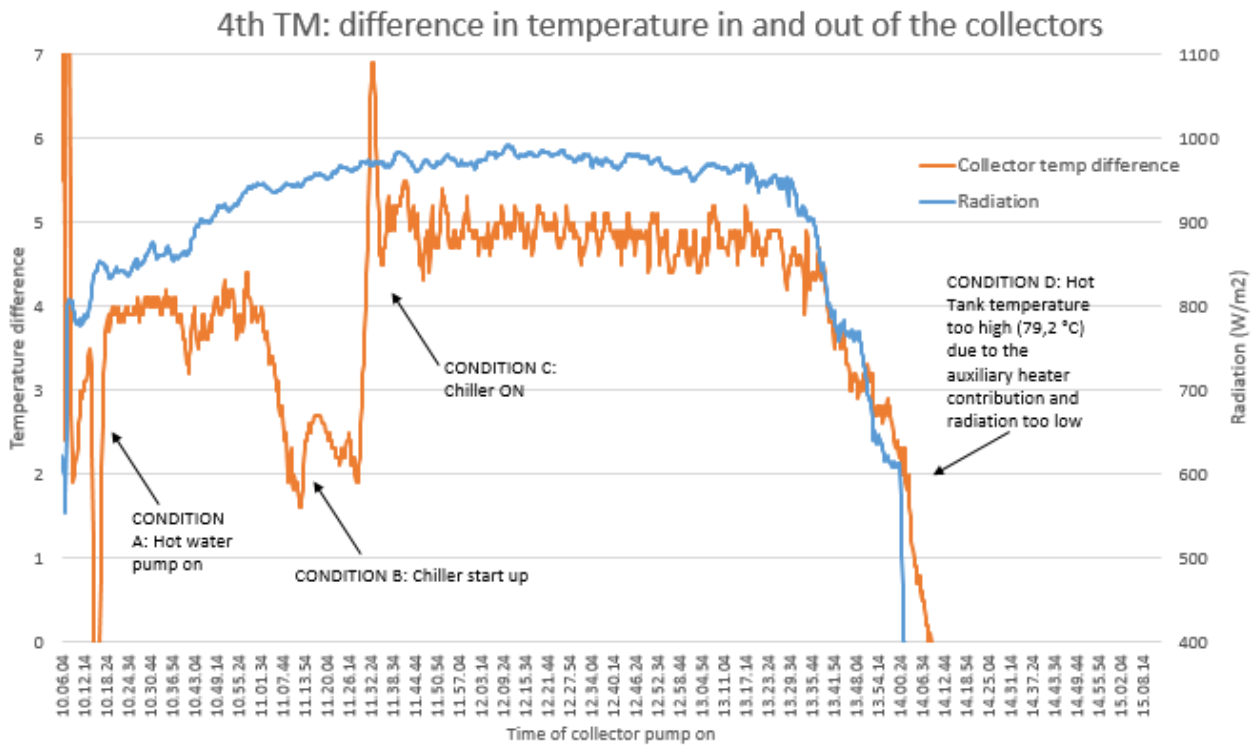


Figure 67: Collector performance analysis during 4th TM

Comparing the 3rdTM with respect the 4th TM, the former presents a value of global efficiency 10% higher. It was the longest measurement in which the collectors works simultaneously with the absorption chiller, indeed the difference in temperature in and out from the collectors was higher (Condition C). This difference with the 4th TM is reduced to 7% if referring to the period in which the chiller was switched on. It remains the measurement in which was registered the best value of global efficiency, instant power output and energy because the average generator temperature was lower (see Table 34 in the annex) and the condition D happen later: when the chiller was switched on, in fact, the water into the tank presents lower temperature. Anyway it also present an higher average radiation with respect to the 4th TM (during the lasts period of this TM starts to rain) and the start up time of the chiller was shorter.

Contrary, the 5th TM was the measurement in which the Condition C lasts less (only 2h 36min with respect to 3h and 50min of the 4th TM and 4h 22 min of the 3rd TM) and indeed the global efficiency is lower. In more the chiller during its operation required much more thermal power in order to produce a bigger cooling capacity,

and the collectors could only partially provide to it, this suppose that the average temperature difference in and out of the collector, and so the global efficiency and the power output, during absorption chiller operation was lower than in the previous cases because the chiller faster consumes the power provided by them, together with the auxiliary heater.

The ambient temperature, because of the thermal loss, negatively influences the thermal efficiency. Therefore the higher value is find for the 4th TM because present the lowest average temperature and higher average radiation with respect to the 3rd TM and 5th TM.

The values of the weighted average were calculated referring to the time of operation in which the collectors' pump and the absorption chiller operates, except for the value of the total energy, in which the entire time of operation of collectors' pump is considered, in order to include the time in which the radiation incident on the collector is considerable.

The maximum output power furnished by the solar collectors resulted to be equal to 13,86 kW and comparing it with the nominal needed by the absorption chiller equal to the nominal capacity over the nominal COP equal to 16,7 kW the capacity of the collectors resulted not enough, this justify the use of the auxiliary heater during the whole test measurments. A hypothetical solution, in order to improve the power output could be to change the arrangement of solar collectors and reduce the flow flowing in each collector by modifying the current configuration that sees a series of 5 manifolds in parallel with the same series. Besides, in order to solve the Condition D previously explained the auxiliary heater should be arragled in series with the tank so that the collector contribution could be significant also in case the radiation is low. Very reccomended is to move the collector from the actual position on differen point of the roof of the building in order to exploit the solar radiation after 4 pm, because actually the collectors resulted covered by trees' shadows.

Dimensioning the capacity collectors assuming to receive actually an instant power equal to 13, 86 kW, indeed supposing to always work with maximum solar radiation (equal about of 1000 W/m^2), in order to cover the nominal thermal power required by the absorption unit, a total of $4,2 \text{ m}^2$ of absorption area of collectors should be added, that corresponds to 4 collectors more (each collectors has 10 tube and each tubes $0,102 \text{ m}^2$ of absorbed area).

5.1.3 Coolerado performance analysis

In order to evaluate the performance of the indirect evaporative cooler known as Coolerado in Colombia conditions, the cooling capacity was measurement during two test-measurements (TM) in two different typical day of Medellín: on 21/04/ 2017 a warm day and on 24/05/2017 and a hot day (see the ambient condition of the TMs in Table 28). Already is assumed, by previous TMs, that is not convenient to work with the Coolerado when the weather condition presents high relative humidity or more in general during rainy or wet day.

Coolerado M50 Performance Table*										
External Static Pressure		Full Speed Product Air Flow			Approx. Product Air Wet Bulb Approach	Product Approx. = WB + below		Working Air Flow		
Inches H2O	Pascal	CFM	CMH	LPS		F	C	CFM	CMH	LPS
0.00	0	1350	2290	635	94%	2	1.1	1000	1700	470
0.10	24.9	1280	2170	601	95%	2	1.1	950	1610	445
0.20	49.8	1200	2050	567	95%	1	.6	890	1510	420
0.30	74.7	1140	1930	534	98%	1	.5	840	1430	395
0.40	99.5	1060	1810	500	100%	0	0	790	1340	370
0.50	124.4	990	1690	466	103%	-1	-.6	730	1240	345
0.60	149.3	920	1560	433	107%	-2	-1.1	680	1150	320
0.70	174.2	850	1440	399	110%	-3	-1.7	630	1070	295
0.80	199.1	780	1320	366	113%	-4	-2.2	570	970	271
0.90	224	710	1200	332	117%	-5	-2.8	520	880	246
1.00	248.9	630	1080	298	120%	-6	-3.3	470	800	221
*Performance at sea level: Performance increases -0.5% for every 1,000 feet / 305 m increase above sea level.										
Example: Design 98F DB / 62F WB, 0.1" ext. static, $98 - 62 = 36$, $36 * 0.95 = 34.2$, $98 - 34.2 = 63.8$ °F Product Air Temperature = Design WB + 2 = 64 °F										
Example: Design 36C DB / 16C WB, 0.1" ext. static, $36 - 16 = 20$, $20 * 0.95 = 19$, $36 - 19 = 17$ C Product Air Temperature = Design WB + 1.1C = 18.1 °C										

Figure 68: Nominal performance of the Coolerado in different external condition

The first test measurement was held by the use of a digital anemometer and manometer and the speed and the dynamic pressure respectively that going out from the four section inside the building were measured. For more precious results, three measurements were done for the section of the inlet product air of the building (each approximately for the hole in the sketches of the Figure 69).

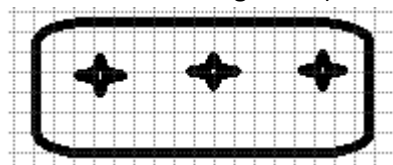


Figure 69: Sketch of point of measurements in the sections at the outlet of the Coolerado's duct.

The second measurement was held by the "Testo" multifunctional equipment model 400 [32] (the equipment through Pitot Tube read the velocity) and also in this case were measured the speed and the pressure of the air flow at the discharge of the fan, by inserting the pitot tube inside the duct just out of the fan. In this way the measurement of the "product air (volume) flow rate" Q could be estimate without considering minor or load losses due to the accessories and length of the duct, and the measurement of the external static pressure could be more accurate. In that case five measurement were done as the sketch in Figure 70 shows with respect the cubic section of the duct of the Coolerado.

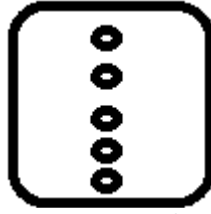


Figure 70: Sketches of point of measurements in the sections of the Coolerdo's duct

Simply multiply the average speed registered for the respectively section area, the volume flow rate in CFM and referring to the nominal performance given by the constructor (Figure 68), the correspondent external static pressure (inches H2O or Pa) were calculated, as equation (LIII) shows:

$$Q = A * v \quad (LIII)$$

Q is the air flow rate of the cooling flow that enter to the Building.

A is the section area of the grating through enters the product air flow of the coolerdo.

v average velocity of the product air flow measured from the grating.

Should be noted that in the first measurement the flow rate is given by the sum of flow rate measured in each grating, being them in series; meanwhile an average is done in the second measurement.

The specific volume \dot{v} (ρ^{-1}) was calculated for both case in each point of the measurement using the approximation of ideal gases for the inlet air was used and the indeed the equation of state was used:

$$P * \dot{v} = \frac{R * T}{M} * 1000 \quad (LIV)$$

Where

\dot{v} is the specific volume in m^3/kg

M is the molecular mass of the air approximated to the constant value of 29 kg/kmol

R is the universal gas constant in $\text{J}/(\text{mol} * \text{K})$

T is the temperature experimentally measured in the duct of the Coolerdo

P is the dynamic pressure experimentally measured in the duct of the Coolerdo in Pa (in the second case by the use of Pitot Tube were measured the static and total pressure and calculated the dynamic one)

In the Annex, the Table 35 shows the measurements done in order to obtain the Full Speed Product (volume) air flow Q and the specific volume (reported as density). As was expected, the volume flow rate in the second measurement resulted higher because the product air speed does not resulted affected by the losses in the duct, and also because of different ambient condition, that in the 24/05, shows an higher temperature and lower humidity.

In order to obtain the air flow expressed in kg/s the equation (LV) was employed (in the first case using the average of the specific volume and the sum of the flow rate; in the second case using the average of both the parameters of the equation)

$$\dot{m} = Q / \dot{v} \quad (LV)$$

Where

Q is the volume flow in m^3/s

\dot{v} is the specific volume in m^3/kg

Finally the cooling capacity (Output Cooling Power) was estimated as:

$$\dot{Q}_{cooling} = \dot{m} * c_{p,air} * (T_{dry,bulb} - T_{product\ air\ flow}) \quad (LVI)$$

and as it was expected, the two measurement reflects the fact that cooling capacity increase (from 4,18 kW of the first test to 7,1 kW the second test) as temperature increases, and as relative humidity decreases. They both resulted highly reduced with respect to the maximum nominal capacity (17,6 kW) because the cooling capacity depends on the ambient wet bulb and dry bulb conditions. Unit capacity indicated by the constructor

are based on a very high dry bulb temperature and a very low wet bulb temperature[24], that corresponds to a weather characterized by a very dry and particularly high temperature. In more also the heights of Medellin decrease its performance of a minimum of 2,5 %, as reported in datasheet in Figure 68.

The average power required by the Coolerado was experimentally measured and resulted 550,6 kW for the first and 681,3 kW for the second one, according to the fact that a bigger flow rate and indeed an higher average speed of the ventilator inside the Coolerado was registered, during the second test measurement. It never exceed the maximum input power required according to the datasheet, where it is spoken of a maximum power required of 790 Watts.

In order to compare it with an air conditioning system also the COP and EER are introduced, so the COP cooling and the EER were estimated. The nominal performance of Coolerado speaks of an EER of 100+ (COP of 29+).

$$EEF = \frac{\text{Cooling air delivered (BTUh)}}{\text{Power required (kW)}} \quad (LVII)$$

According to the previous results, the experiments shows a EER higher for the second test measurement with respect to the first one, and lower to the nominal one. In Table 28 below the results of the measurements of the performance tests.

	21/04/2017	24/05/2017	Unit
Section Area	0,285x0,135	(0,45-0,02) ²	m ²
Full Speed Product (volume) Air Flow	1358,17	1447,24	Ft ³ /min (CFM)
Correspond external static Pressure	0.1	0.1	" H20
Tamb (Dry bulb Temperature)	27,8	30,5	°C
Ambient H.R.	53	39	%
Cp air	1,006	1,006	kJ/(kg*°C)
Dew Point Temperature*	16,62	14,95	°C
Wet bulb temperature*	19,76	19,44	°C
T out the coolerado	21,5	20,5	°C
H.R. % salida coolerado	64,7	40	%
Cooling Air mass flow rate	0,66	0,71	Kg/s
Output Cooling Power	4,18	7,1	kW
Input electrical power	550,36	578,7	W
Output cooling power	14,25x10 ³	24,18x10 ³	BTU/h
COP	7,6	12,25	-
EER	25,9	41,8	BTU/(Wh)

Table 28: Results of the performance analysis of the Coolerado

* calculated by means of <http://www.meteorivierapicena.net>

These results shows clearly that the Coolerado performance improve during hotter day because the power consumption increase relatively less if compared to the improvement of the Cooling Capacity.

In more, a comparison between the nominal temperature of the product air flow and the experimental one was calculated using the equations provided by the constructor: with respect to the external static pressure, the air product temperature should approach at 94% to the wet bulb temperature. In equation (LVIII) also is considered 2,5% of worsening in performance because of the height of Medellín of 1538 meters:

$$(T_{amb} - T_{wb}) * 0,94(0,95 \text{ for the first measure}) * (1 - 0,005 * 1538/305) = X \quad (LVIII)$$

$$(T_{amb} - X) = \text{Design } T_{wb} \quad (LIX)$$

$$\text{Product air temperature} = \text{Design } T_{wb} + 1,1 \quad (LX)$$

		Experimental	Theoretical	Deviation(%)
21/04/2017 (warm day)	T product air flow	21,5	21,53	0,15
	Cooling Capacity	4,18	4,15	0,52
24/04/2017 (hot day)	T product air flow	20,5	21,47	4,7
	Cooling Capacity	7,1	6,4	9,7

Table 29: Experimental and nominal air product temperature of the Coolerado

The higher error in the second measurement is given by the fact that the temperature measured through the digital anemometer by Pitot Tube inside the duct just after the Coolerado was more oscillating than which was registered at the end of the duct.

The results shows a Cooling capacity much reduced with respect the nominal maximum (17,6). Indeed the performance of the equipment were plotted for different weather condition for the city of Medellín. Being the Coolerado performance depending on temperature and relative humidity two different cases were simulated, assuming a constant volume air flow equal to $Q = 0,76 \text{ m}^3/\text{s}$ (maximum value registered in the previous measurement, assuming the ventilator of the coolerado works always at the same speed). The product air temperature was calculated through equations (LVIII) (LIX) (LX). Were chosen two favourable working condition:

- Relative Humidity equal to 30%
- Dry bulb temperature equal to 33°C

The Figure 71 and Figure 72 show the results obtained and in the Annex the calculus done are shown in Table 36 Table 37.

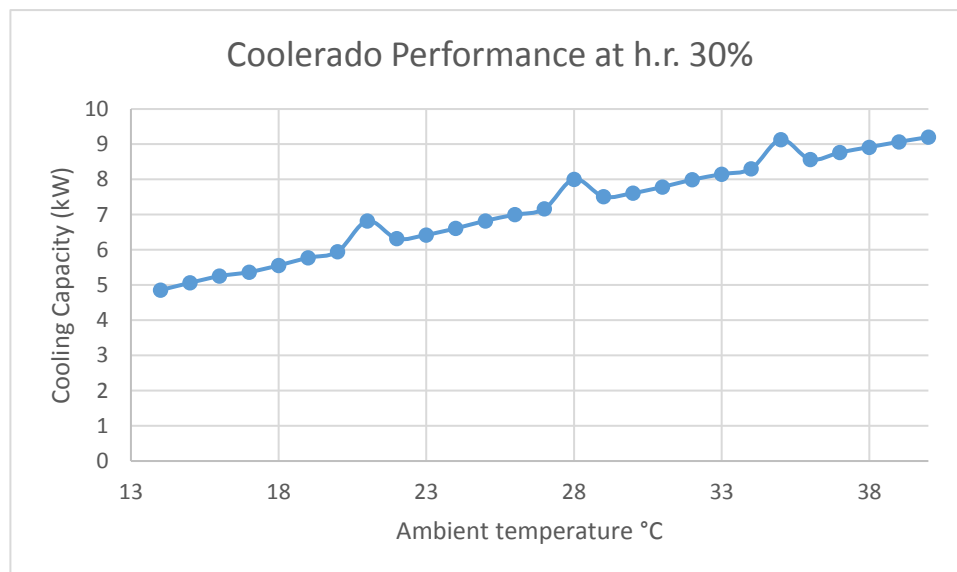


Figure 71: Coolerado Performance at a defined dry bulb temperature

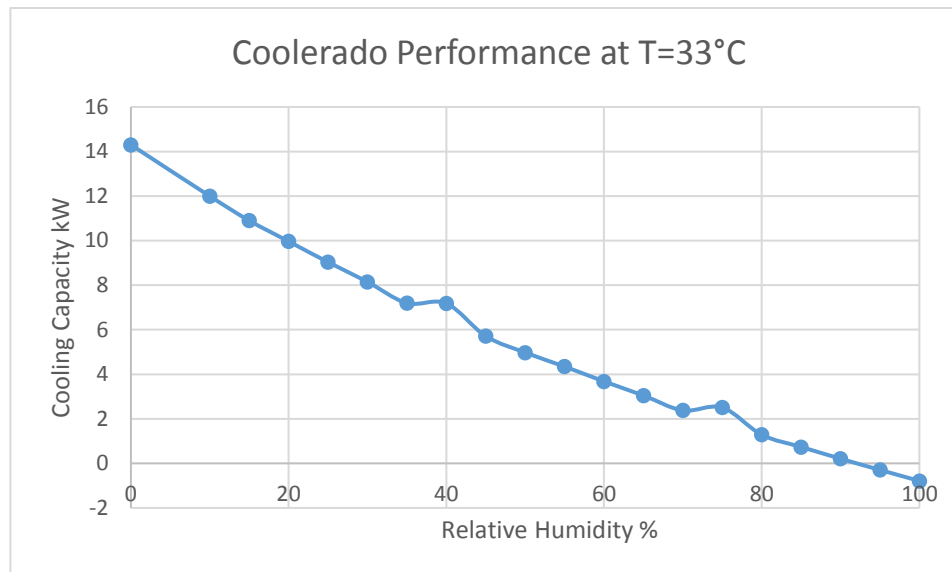


Figure 72: Coolerado Performance at a defined dry bulb temperature and relative humidity

By these plots it could be seen that in these conditions it is never reach the maximum nominal capacity (17,6 kW): in the first simulation (at r.h.=30%) about 9,2 kW of cooling power is reach at the temperature equal to 40 °C and at temperature above 35°C the capacity is halved. At the ambient temperature of 21, 28 and 35 °C the capacity improve because the difference in wet and ambient temperature is higher. Instead, in the second case (at T=33°C) the cooling capacity reaches a maximum of 14,3 kW but decrease really rapidly at relative humidity few lower.

Considering all the tests measurement done so far, from the Table 34 in the annex, it could be said that the air conditioning with the use of Coolerado at Building 24 happen when the temperature oscillates between 33 °C to 23°C and relative humidity between 30% to 72%, without take in account the day in which rain, because in that case is not convenient to work with the Coolerado.

Indeed taking in account these ambient condition, and the maximum flow rate registered experimentally, the maximum cooling capacity of the M50B Coolerado is more than 8 kW (a cooling capacity of 8,2 kW was obtained at the best ambient conditions of the air cooling, T=33°C, r.h.= 30%) and an energy consumption of maximum 681,3 W (the maximum experimentally registered).

In Table 30 a comparison between nominal and in Medellín condition performance.

COOLERADO M50B	Nominal	Medellín Condition
PERFORMANCE		
Height	Sea level	1538
T dry bulb	“Very high”	33°C (average 24,8 °C)
T wet bulb	“Very low”	19,57 ° (average 16,7°C)
Max capacity [kW]	17,6	8 (at average cond. 4,5 kW)
Max Power input [W]	790	681,3 (at average cond 550,3 kW)
EER (COP) [BTU/(Wh)]	76 (22,3)	40 (12,76) [at average cond 27,9 (8,18)]

Table 30: Comparison between datasheet capacity and actual capacity in Medellín condition of Coolerado

One observation should be done, performance of the Coolerado could be compromised by a clogged air filter, that will reduce the product air flow rate or increase the product air temperature, increasing operating costs by reducing efficiency and could potentially impact system durability. By datasheet is recommended to inspect the filter monthly, since the unit uses 100% outdoor air the filters will need to be changed more often than standard HVAC (Heating and Ventilation Air Conditioning) systems that do not use 100% outdoor air: last documented check up dated back to 27th September of 2016.

5.2 ECONOMIC ANALYSIS

In order to analyse the economic effort and justify the initial capital cost of the system a comparison with an air cooled Chiller, the most used conventional refrigeration system is done. An analysis of fixed and annual cost was done, taking in account only the purchased equipment costs(PEC) in the fixed capital investment (FCI). The simple payback period was calculated as[33]:

$$\text{Simple Payback}[\text{years}] = \frac{\text{Cost}}{\text{Benefit}} \quad (\text{LXI})$$

Where

the *Cost* are represent by the fixed cost difference between solar and conventional [€]

the *Benefit* are represented by the variable (annual) cost savings, in primary energy consumption and Operational and Maintenance(O&M) costs, represented by the variable cost difference between conventional and solar systems [€/year].

The analysis was carried on for different size of the system (indeed for different cooling capacity), from the actual case (about 30 kW_{fr}) up to 500kW_{fr} , and assuming that the expenditure is justified over a long period of cooling demand, the analysis was also done for different operational hours (*t_{op hours,year}*) from 3000 h/year up to 1000 h/year. The former cooling demand reflects Colombian climate, but it can also reflects the demand of big users, as malls or hospitals in South of Italy, when sunlight hours arrives up to 15h hours/day in summer season.

Two different cases were analysed: Colombian and Italian case, differentiating only for the specific cost of Electrical Energy (EE).

All the price furnished by the constructors in US\$ or COP were converted in € with the rate exchange of June 20th 2017 and tax free.

5.2.1 Fixed Costs

The PEC of the solar cooling system is given by the costs of the following equipment:

1. Absorption refrigeration Chiller, whose cost is given by the same constructor, Shandong LucyNew Energy Technology Co. for the actual size of the system. The specific costs in
2. Table 31 were used for higher size of the system.

	p < 50 kW	50 kW < p < 100 kW	100 kW < p < 350 kW	350 kW < p
€ / kW	732	535	323	121

Table 31: Specific Cost of Absorption refrigeration Chiller[27].

The cost was calculated as:

$$C_{\text{abs chiller}}[\text{€}] = \dot{c}_{\text{abs,chill}} * P_{\text{cooling}} \quad (\text{LXII})$$

Where

$\dot{c}_{\text{abs chill}}$ is the specific cost associated with respect to the size, shown in Table 31

P_{cooling} is the cooling capacity of the absorption chiller

3. The solar collectors, whose cost was estimated from the cost per tube (c_{tubes}) furnished by the constructor Shandong LucyNew Energy Technology Co. Since the conclusion in the Section 5.1.2, the capacity of the collectors to be installed should increase in order to cover the thermal power required by the absorption chiller. The sizing (number of tube) of the collectors with respect to the cooling capacity installed was estimated assuming also an increase of the size for the thermal storage, by means of a solar multiple, which suppose for an optimal technical-economical balance an installed capacity of the collector 1 times and half bigger with respect to which is needed by the machine. Indeed, the number of tube per installed capacity was adjusted by a corrective facto given by:

$$n_{\text{tubes, corrected}} = n_{\text{actual,tubes}} * \frac{P_{\text{nominal input,abs chiller,actual}}}{\text{Actual CapacityCollectors}} * \text{Solar Mutliplier} \quad (\text{LXIII})$$

Where

$n_{actual,tubes}$ is the actual number of collector installed equal to 200

$$P_{nominal\ input,abs\ chiller,actual} = \frac{Nominal\ Capacity_{abs\ Chiller,actual}}{Nom\ COP_{abs\ Chiller}}$$

$Nominal\ Capacity_{abs\ Chiller,actual}$ is the actual cooling capacity of the absorption chiller (11,5 kW)

$Nom\ COP_{abs\ Chiller}$ equal to 0,69 for every size of the chiller

$Actual\ Capacity_{Collectors}$ is the average maximum power output from the collector equal to 13,86 kW (See Table 27 in Section 5.1.1.6)

$Solar\ Mutliplier$ equal to 1,5.

Indeed the Cost of the collectors were calculated

$$C_{coll}[\text{€}] = \dot{c}_{tubes} * n_{tubes,corrected} * R \quad (LXIV)$$

Where

\dot{c}_{tubes} is the specific cost per tube (€/tube) of collector furnished by the constructor , Shandong LucyNew Energy Technology Co. sized for an expenditure equal to 200 tubes; for bigger quantity of tube a discount rate with respect to that price was estimated. As Table 38, in the appendix shows, a 10%, 15% and 20% of discount is applied for quantities of pieces higher than 1000,2000 and 6000 respectively.

$R = \frac{P_{nom\ input,abs\ chiller}}{P_{nominal\ input,abs\ chiller\ actual}}$ is the ratio between the cooling capacity of the absorption chiller with respect to the actual one (11,5 kW).

4. The thermal storage, whose cost is given by the same constructor, Lapesa© for the actual size of the system. The specific costs in Figure 73 were used for higher size of the system.

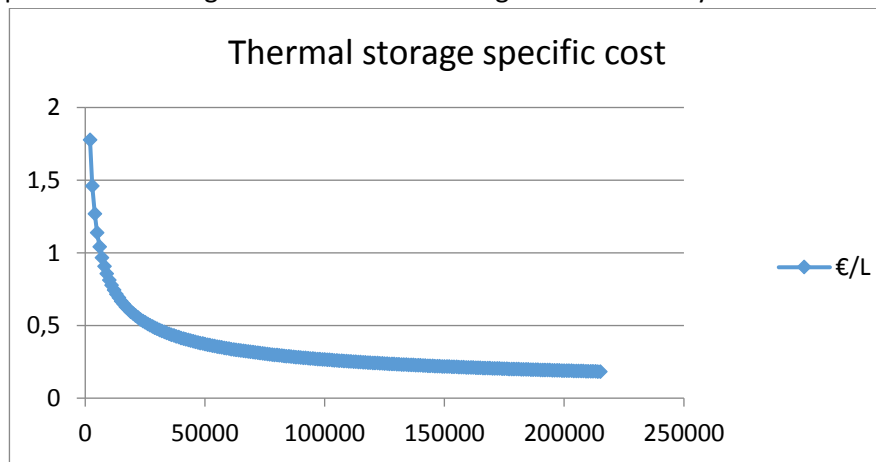


Figure 73: thermal storage specific cost per €/litre[27]

Indeed the cost were calculated as equation

$$C_{storage}[\text{€}] = \dot{c}_{storage} * L_{storage\ actual} * R \quad (LXV)$$

Where

$\dot{c}_{storage}$ is the specific cost per litre with respect to the size, shown in Figure 73

$L_{storage\ actual}$ is the actual thermal storage installed equal to 2000L.

5. The Cooling tower
6. The Radiant Ceiling
7. The Coolerado.

For these equipment, for which was not been possible to use a specific cost with respect to the size, the equation (LXVI)[34] was used.

$$C_{PE,Y} = CE_{PE,W} \left(\frac{X_y}{X_w} \right)^\alpha \quad (LXVI)$$

Where

$C_{PE,Y}$ is the purchased equipment cost of the equipment at the specific size, given by the constructor

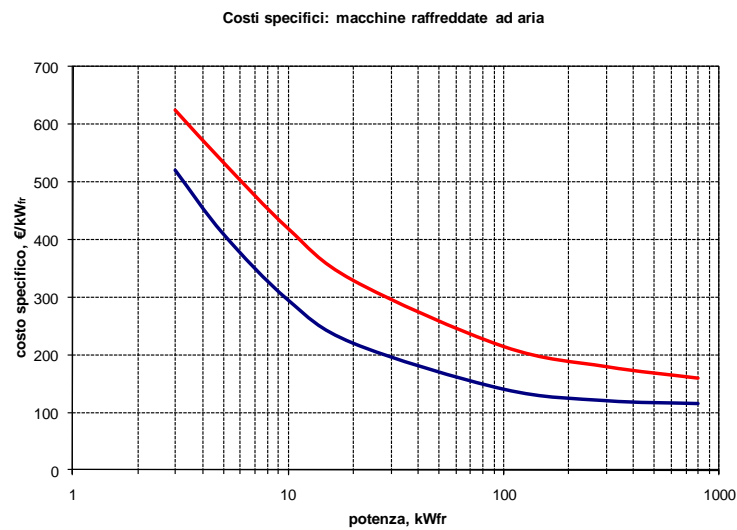
$CE_{PE,W}$ is the purchased equipment cost of the equipment installed in the system.

X_y and X_w are the equipment's capacity at the specific size of the system and at which is installed in the system respectively.

α is a coefficient equal to 0,6.

The PEC of conventional refrigeration system is represent by the costs of the following equipment:

1. The air cooled chiller, whose cost presents a certain variability depending on components and the technology.[35] Were assumed the costs represented by the red curve in As for the solar system, the equation (LXII) was used in order to calculate the cost.



2. Figure 74, that indicates the maximum values of the average specific costs (€/kW_{fr}). Indeed for the actual case (11,5 kW_{fr}) a cost equal to 300 €/kW_{fr} was used. As for the solar system, the equation (LXII) was used in order to calculate the cost.

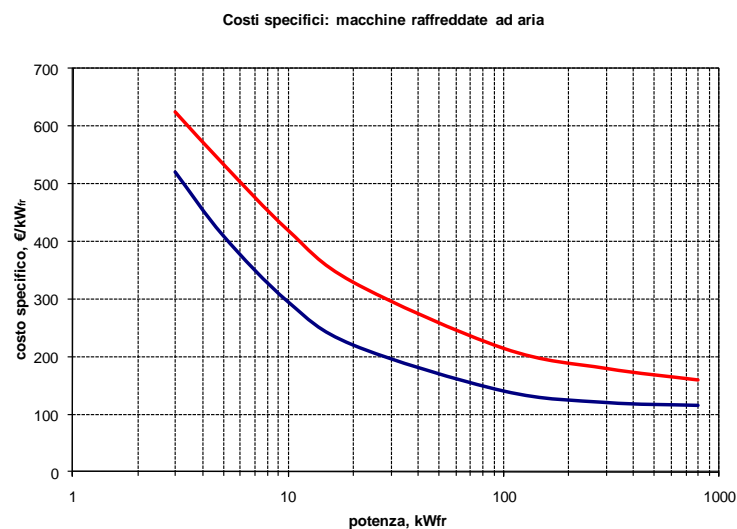


Figure 74: Specific costs of Air cooled Chillers [35]

3. The fun coil units, for which the same procedure of the equipment 4, 5 and 6 of the solar system was used.

The Balance of Plant (BOP), constituting minor and auxiliary equipment's costs of the system, that make the entire plant operate have been accounted in the fixed costs for both solar and conventional system. This indicator represents the costs of the accessories, like water pipes and fittings and all the equipment that put all the cooling system together. It account for a 10 % and a 30% of the PEC of the solar and conventional respectively. This difference is given by the fact that the equipment costs of the solar system is much more relevant.

5.2.2 Variable Costs

The annual energy resources used by the solar system are constituted by:

1. Sun Radiation, totally free
2. The electrical energy (EE) used by auxiliaries in the solar cooling system. In the actual case it was calculated as

$$EE_{annual,solar\ system} \left[\frac{kWh}{year} \right] = \bar{P}_{air\ cond\ period} * t_{op\ hours,year} \quad (LXVII)$$

Where

$\bar{P}_{air\ cond\ period}$ is the average instant power consumed during air conditioning period (during the whole period is clearly less, see Table 34 in the annex), experimentally measured equal to 2,5 kW., as in section 5.1.1.6 in Table 24 is shown, during the 3rd TM, in which the best operational point of the system was encountered (best COP) and also the Coolerado operates.

In order to estimate this consumption for bigger size was assumed that a 40% of this consumption does not depend on the size of the cooling system, and the rest increase linearly.

3. Primary energy source, the Natural Gas, used by the auxiliary heater. A good dimension of the solar system suppose that the cooling system works for the half time of its operational hours by thermal energy coming from the auxiliary heater and half by the solar collector; indeed the annual consumption was estimated for the half operational hours. The annual electrical energy input by the auxiliary heater is so calculated:

$$EE_{annual,LGP} \left[\frac{kWh}{year} \right] = P_{input,nom\ abs\ chiller} * \eta_{heater} * \frac{t_{op\ hours,year}}{2} \quad (LXVIII)$$

Where

$P_{input,nom\ abs\ chiller}$ is the thermal power required from the absorption chiller, depending on the size considered.

η_{heater} is the efficiency of the heater assumed constant and equal to 0,92 [16].

The annual energy resources used by the conventional system is constituted by

1. Electrical Energy(EE) consumption used by the compressor of the air cooled Chiller and auxiliaries, that suppose consume a 10 % of which required the Chiller is calculated as

$$EE_{annual,conv\ system} \left[\frac{kWh}{year} \right] = (P_{input,conv\ Chiller} + \frac{P_{input,conv\ Chiller}}{10}) * t_{op\ hours,year} \quad (LXIX)$$

Where

$P_{input,conv\ Chiller}$ is the power requested by the compressor Chiller and it is calculated as the Cooling capacity output over the COP of the machine, as equation (LXX) shows:

$$P_{input,conv\ Chiller} = \frac{P_{cooling,output}}{COP_{air\ cooled\ Chiller}} \quad (LXX)$$

$COP_{air\ cooled\ Chiller}$ is assumed improving at bigger size, as table shows

	p<100 kW	100 kW<p<300 kW	300 kW< p < 1000 kW	1000 kW < p
COP	3	3,5	3,75	4

Table 32: improvement in performance of an air cooled Chiller

Indeed the annual cost of energy resource was calculated for both system by the equation:

$$C = \sum C_i = C_{LPG} + C_{EE}(\text{€/year}) = E_{annual,i}[\text{kWh/year}] * \dot{c}_i[\text{€/kWh}] \quad (LXXI)$$

Where

\dot{c}_i is the specific cost per kWh of the LPG and EE , in particular:

\dot{c}_{LPG} was assumed equal to 0,3 €/Smc (tax free) indeed was converted into €/kWh assuming a LHV of 34,5 MJ/Smc and 3,6 MJ/kWh and indeed equal to 0,031 €/kWh for both Colombian and Italian case.

\dot{c}_{EE} is equal to 0,16 €/kWh for Colombian case and to 0,21 €/kWh for Italian case.

The O&M costs where assumed equal to 4% of the investment cost of the conventional cooling system and the middle for the solar one.

Table 33: payback period of actual configuration of the solar cooling air conditioning system with respect to a conventional one Table 33 shows the results for the actual configuration, in both Country. The payback period in this case from Colombian to Italian case shifts of 2 years. It could be said that for a solar system that has a duration of almost 20 years the expenditure is acceptable until the payback period is equal to 6 years. Indeed it is considered quite high for Colombia, that has a very low cost of electrical energy; that is due to the high expenditure of purchased equipment costs; in the appendix the Table 39 shows the calculus done for the payback period of the actual configuration of the solar cooling system.

	Solar cooling system	Conventional Cooling System
Fixed Costs [€]	44'419,1	15'600
ITALIAN CASE		
Annual Costs [€/year]	2'689,1	7'554
Payback [years]	5year and 11 months	
COLOMBIAN CASE		
Annual Costs [€/year]	2'314,1	5'904
Payback [years]	8 years	

Table 33: payback period of actual configuration of the solar cooling air conditioning system with respect to a conventional one

The Figure 75 shows the results of the analysis for the Colombia case. It is very clear the dependence in size of the equipment: the benefit, indeed the annual primary energy savings in term of money increase so that the ratio to the benefit over the cost decrease exponentially, increasing the size of the system. In Colombia, because of the very low cost of electric energy (0,16 €/kWh), this technology resulted economically convenient (payback period less than 6 years) from capacity few lower than 200 kW if the cooling demand is minimum of 3000 h/years. For cooling capacity bigger than 850 kW the payback period resulted lower to 6 years also for cooling demand halved. The minimum period of payback registered is of 2 years and less of 9 months for a cooling capacity equal to 1300 kW. For the same size even a cooling demand of 1000h /year, considering a reduce use of the auxiliary heater of about 350 h/year over the whole period and assuming that the gas price is equal to Italian one, results convenient with Colombian price: the period of return of the investment in this case is barely over the which is considered convenient, less than 6 years and half.

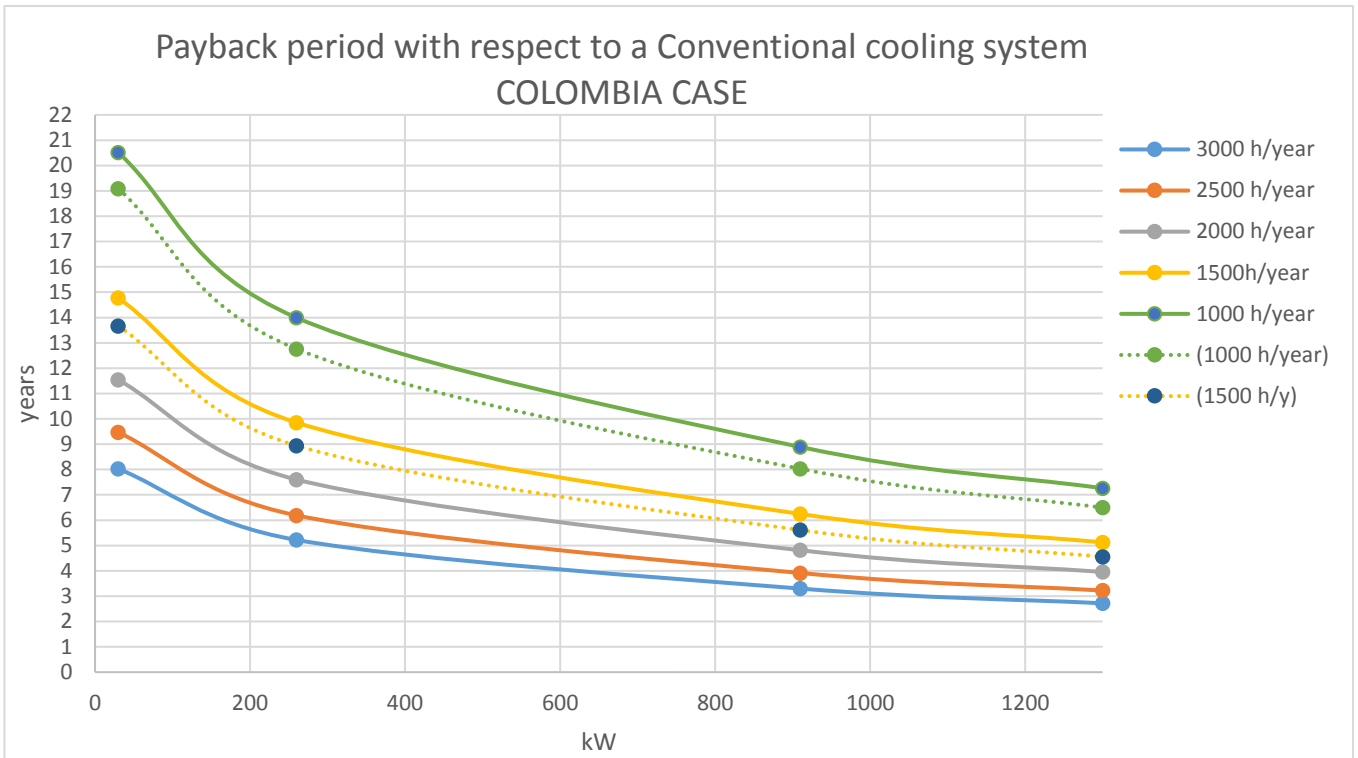


Figure 75: Results of the payback period between Solar and Conventional cooling system for Colombia case

The situation seems much more convenient for our Country, where the price of electrical energy is 25% higher. The dotted lines represents the payback period for different size of the solar cooling system in case in which it operates 2/3 of the operational hours by sun radiation and 1/3 by thermal energy given by the auxiliary heater, indeed at different share in primary energy consumption. This assumption is done only when the operational hours are lower and indeed is enough to suppose that are present these conditions for Italian weather (1000 and 1500 h/year, indeed supposing 3 or 5 months of cooling demand, in which the sun radiation on the collectors can contribute for more time, as summer period). With the Italian situation the simple payback period does not overcome for an absurd case, of an investment for installing 260 kW of cooling power having a cooling demand of 1000h/year, the 10 years and it becomes very convenient for size over 500 kW also for cooling demand of 1500 h/year. The best results shows a period lower of 2 years for investments in capacity higher of 1300 kW if cooling demand is minimum equal to 3000 h/year.

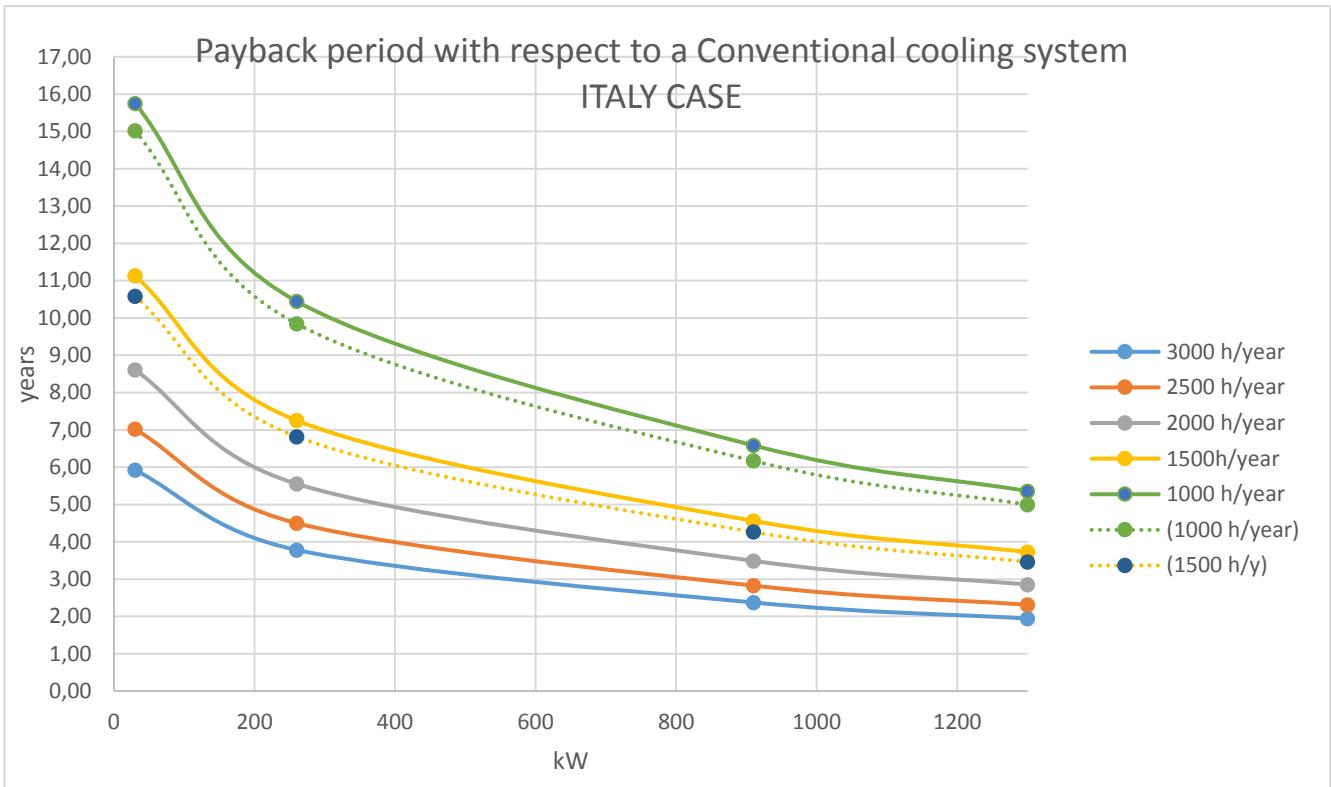


Figure 76 Results of the payback period between Solar and Conventional cooling system for Italy case

For both cases a remarkable improvement in payback period passing from 1000 h/year to 1500 and always less perceptible increasing the cooling demand up to 3000 h/year. That because the electric energy consumption is much more heavy for high cooling demand, and the savings are more remarkable with respect to the cost of the investment, that might be not justifiable if the electric energy consumption is not so elevated. In more should also be noticed that for the electrical energy consumption of the conventional system was assumed a COP that improves with the size (see Table 32); it is not always verified as true, even more if considered that over time the machine is affected by a drop in performance due to wear. Therefore, an even more inclined trend could present the payback period curve with respect to the size, that is traduced with the fact that even shorter period in return of the investment could be expected.

6 CONCLUSIONS

During this work a performance analysis of a cooling system installed in the office building of the Bolivarian Pontifical University, in the eternal Spring City of Medellín was carried out by analysing its main sub-systems. In particular the three main sub-system analysed are:

- The 11,5 kW absorption chiller, whose performance were tested at different operational conditions
- The evacuated heat pipe tube collectors, which are coupled to the absorption chiller in order to provide to thermal power needed
- The 17,9 kW indirect evaporative cooler, known as Coolerado, which is responsible to improve the energy efficiency of the air conditioning and to renovate the air inside the building

Important conclusions could be inferred after having analysed them.

The absorption chiller evidenced a cooling capacity lowered of more than the 50 % of the nominal capacity, essentially due to impossibility of the system to maintain an high temperature in the generator. The machine, in fact cannot exploit the nominal thermal power required by the generator (that should be equal to 16,7 kW). Starting from the performance curve provided by the constructor and assuming a linear overlapping of the effects of the generator, evaporator and condenser temperature in the performance of the machine, a lower power was registered furnished by the generator, if working at normal capacity (were registered values between 10,5 to 8,7 kW). The problem could be solved doing some modification of the layout:

- The pump that goes from the hot water storage tank to the absorption chiller takes water from the bottom of the tank, indeed it affectes negatively the generator operation due to the thermal stratification inside the tank. It is appropriate to connect the pump to the top of the hot water storage tank, in order to bring into the generator always the hottest water stored.
- The auxiliary heater input is located directly to the hot water tank. A future simulation could be to connect the auxiliary heater in series with the thermal storage. It could lead to provide always the nominal temperature required by the machine, and to avoid the stoppage of the machine, assuring the minimum temperature required in the absorption chiller.
- The pump that goes from the chilled water storage tank to the absorption chiller takes water from the bottom of the tank, indeed it always sent the coolest water to the evaporator, affecting negatively the heat exchange effectiveness in the evaporator. Move the downstream handle of the chilled water pump to the top part of the tank will increase the difference between inlet and outlet temperature of the heat exchange of the evaporator, increasing the cooling capacity.

By the analysis carried out working with the actual layout, starting from the performance curves provided by the constructor of the absorption unit and assuming a linear overlapping of the effect of the generator, evaporator and condenser temperature in the performance of the machine, two different operational conditions of the system could be preferred: the one which could lead to highest COP registered so far, and another that provides the highest cooling capacity, at a cost of higher energy consumption.

These two different configuration are obtained by the lasts two TMs, the 4th and the 5th, proving indeed that during the experimental tests, the right directions in varying operational conditions has being followed.

The operational conditions, which lead to optimize the COP, have been reached at 4th TM. Working with the second speeds of the chilled water pump to the evaporator and at the highest temperature that actually could be possible to maintain in the generator, heating the thermal storage up to the limit that avoid the boiling (about 98°C), the effectiveness of the heat exchange in the evaporator improves and the machine produce chilled water exploiting less thermal power in the generator, indeed obtaining the highest values of COP so far registered, equal to 0,54 that is only 20% less of the nominal value. This configuration assure the longest period of work of the chiller because consumes less instantaneous power from the generator. In more, it is assure the lowest value of energy consumption, because both the cooling tower and the pump required less power input.

The operational conditions, which lead to optimize the Cooling capacity, have been reached at 5th TM. As the performance curves of the absorption unit shows, lowering the condensation temperature up to the limit that avoid crystallization of the refrigerant flow, increase the cooling capacity of the machine. In particular, it was working with a T_{set} in the cooling tower equal to 28°C and at maximum capacity in the evaporator, indeed with the third speed of the chilled water pump. It was possible to reach the 60% of the nominal cooling capacity, once have heated the thermal storage up to the boiling limit. This configuration is very useful in case the cooling demand is imminent and big; the former case it could be more suitable in case is needed only to maintain the same temperature in the building, and indeed the cooling demand is lower, and energy could be saved.

The average maximum collectors capacity registered during the TMs done, resulted equal to 13,86 kW, indeed the actual capacity of the collectors does not resulted enough in order to furnished the nominal thermal power required by the absorption chiller and this justify the use of the auxiliary heater during the whole test measurements. In order to improve the capacity of the collectors some improvement have been proposed.

- The actual arrangement of solar collectors sees a series of 5 manifolds in parallel with the same series. In this way the flow rate provided by the pump is separated into two flux. Neglecting the heat loss from the hot tank, the flow rate resulted by the energy balance into the hot tank, is equal to 972 L/h per manifold. Reducing the flow rate, that referring to the datasheet of similar collectors could be even three times lower, the ΔT of the collectors could improve and indeed the power output. Indeed positioning the collectors in series of two, indeed five in parallel could increase their performance.
- The actual arrangement of the auxiliary heater provoke that in case the radiation is low and the temperature inside the storage tank already high (due to the auxiliary heater contribution) the collectors contribution is not effective. The problem could be solved arranging the auxiliary heater in series with the hot water storage tank, so that the thermal storage is completely dependent by the solar energy contribution.
- The actual position of the collectors does not permit to exploit the solar radiation after 4 pm, because the collectors resulted covered by trees' shadows. Very recommended is to move the collector to a different point of the roof of the building.

Dimensioning the capacity collectors assuming to receive always an instant power equal to 13,86 kW, indeed supposing to always work with maximum solar radiation (equal about of 1000 W/m²), in order to cover the nominal thermal power required by the absorption unit, a total of 4,2 m² of absorption area of collectors should be added, that corresponds to 4 collectors more (each collectors has 10 tube and each tubes 0,102 m² of absorbed area).

From the Coolerado performance analysis, responsible in renovate the air in the building, is evinced that the machine in Medellín condition, and at the actual state of cleaning of filters could furnish a cooling capacity equal to 8 kW, the capacity should again tested just after a cleaning of the filter and checked if it improves.

From the economic analysis, is evinced the very strong dependence of the simple payback period on the size of the solar cooling system: increasing the size of the system the benefit, indeed the annual primary energy savings in term of money, increase, so that the ratio of the benefit over the cost decrease exponentially, also due to the lower specific cost of the machine. E.g. the payback period is strongly reduced passing from the solar cooling system of a capacity of 30kW to a system of 250 kW. For installed capacity higher than the system analysed, the technology resulted very convenient not only for a typical Colombian cooling demand (3000 h/year) but also for demand halved, indeed also for an Italian case. Actually in Italy, where the electric energy cost is very high the payback period of the investment resulted in general, much reduced than in Colombia, where the electric energy cost 35% less, due to the wealth of rivers that allows low-cost hydroelectric power production. E.g. considering a cooling demand that could be realistic for both Colombian and Italian weather, equal to 1500 h/year, the technologies proposed resulted convenient already for system of the cooling capacity equal to 600 kW in Italy and equal to 850 kW in Colombia.

The lowest return period of investment is registered for solar absorption cooling system with a cooling capacity about equal to 1300 kW, for which is enough a period between 2 and not higher than 3 years to recover the expenditure. In more should also be noticed that the economic analysis was carried out considering for the electrical energy consumption of the conventional system a COP that improves with the size; it is not always verified as true, even more considering that over time the machine is affected by a drop in performance due to wear. Therefore, even shorter period in return of the investment could be expected. Anyway, the very good news is that installing an air conditioning system that uses these technologies could make the user richer not only in term of money but also in term of sustainability, because the conditioned ambient in which he will live won't be responsible in remarkable CO₂ emissions and won't use any type of refrigerant that impacts the ozone. The user will live not only on a cheap air-conditioned but also environmental-friendly room.

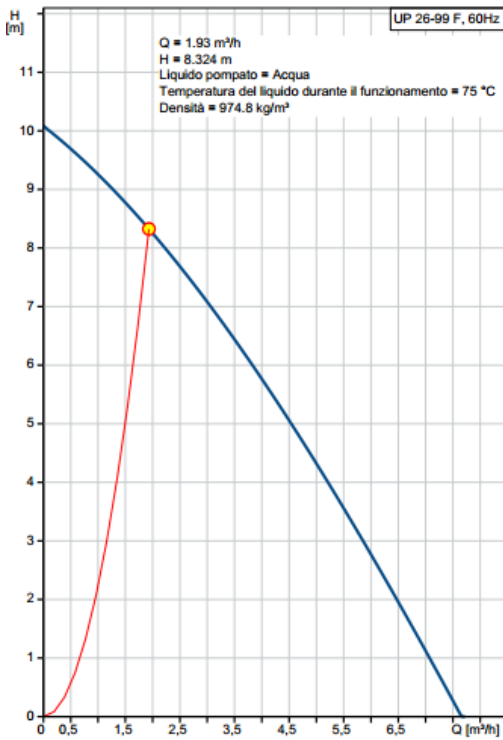


Figure 79: Operational point of section from the collectors to the hot water storage tank (Section 1)

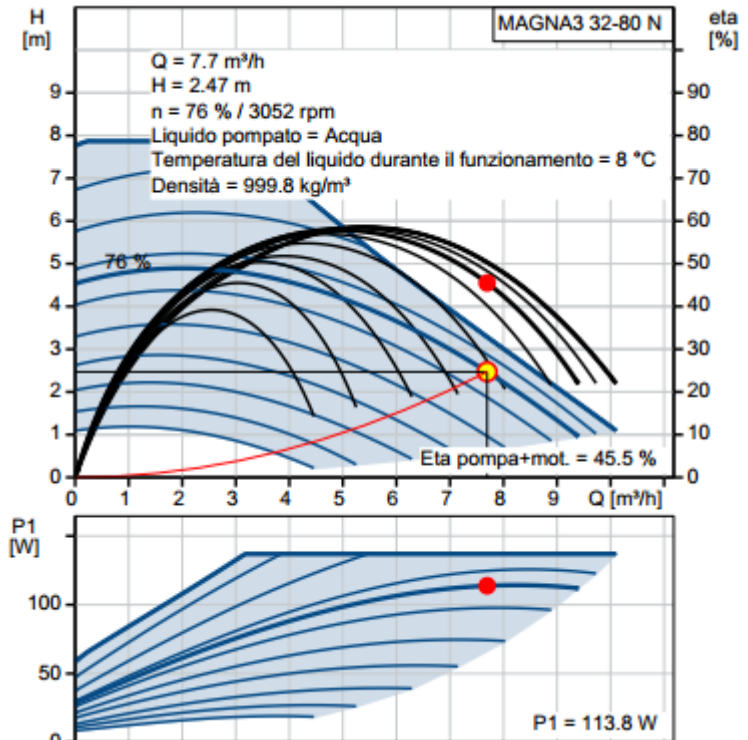


Figure 78: Operational point of section from the chilled water storage tank to the capillary mats (Section 4)

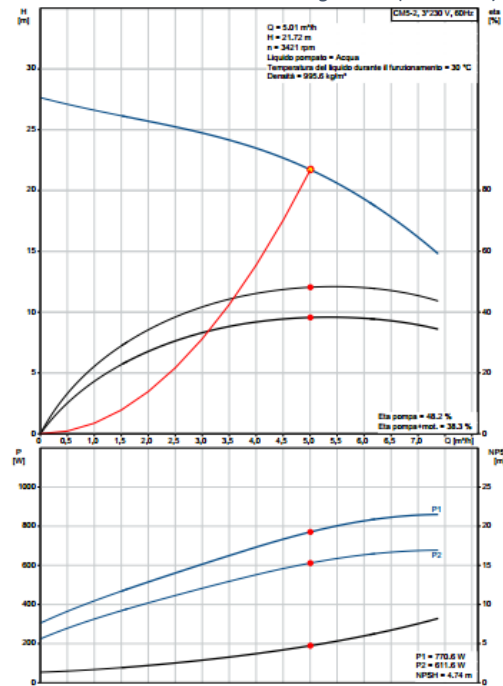


Figure 80: Operational point of the section from the cooling tower to the chiller (Section 5)

		1 st TM	2 nd TM	3 rd TM	4 th TM	5 th TM
	Day	16/03/2017	18/03/2017	27/03/2017	28/03/2017	25/05/2017
Time of measurement	Start time	8:47	10:22	11:29	7:12	9:21
	Finish time	16:06	16:29	17:10	15:13	13:50
Ambient Condition	Average T [°C]	27,9	26,7	26,7	23,5	30
	Average Rad [W/(m ²)]	608	539	583	590	706,3
	Average H.R [%]	45	47	47	63,5	45
	T max [°C]	31,85	32	32,97	28	31,9
	T min [°C]	25,1	25	27,9	20,76	27
	Rad max [W/(m ²)]	995	984	1096,5	991	1015,9
	h.r. max	71,6	54,3	58,9	91,2	55,12
	h.r. min	29,7	38,4	39,7	44,3	37,7
System Condition	T max hot tank [°C]	79	92,6	83,7	98,4	98,6
	\bar{T}_{gen} [°C]	72,73	74,9	72,47	74,3	70,7
	Tset-real cooling[°C]	29,52	29,5	29,4	29,3	27,6
	Peculiarities		Without use of Coolerado	Chilled flow rate reduced-Once refrigerator water finished, only the use of the Coolerado was experimented	Chilled flow rate reduced-Bad weather conditions and rain. Without use of Coolerado	Tset cooling reduced to 28°C
Air conditioning performance	TM effectiveness air cond operational hours	1h 48min	2h	2h 11min +15min coolerado only	1h 29 min	1h 17min
	DT max °C Building 24	2,014	2,07	2,13+ 0,5 coolerado only	2,56	2,2
Chiller performance	T min [°C]	9,2	8,7	11,7	10,7	8,3
	Chilled water ΔT	12,1	12,3	12,5	12,6	13,6
	Time of ΔT	3h 48 min	2h 57 min	2h 35 min	1h 29 min	1 h 20 min
Electrical energy consumption	Mean power during air cond (kW)	2,8	2,65	2,5 and 0,594 only coolerado	2,4	3,6
	Mean Power	2,25	2,25	2,36	1,54	2,25
	Total Energy (kWh/TM)	16,5	13,8	13,4 and 0,15 only coolerado	12,35	10,46

Table 34: Data registered and calculated during all test measurement

TM1	Duct 1	Duct 2	Duct 3	Duct 4	Average Speed (m/s)	Q volume flow rate (m³/s)	Average Dinamic Pressure	density kg/m³
1 out	4,25	4,25	4,35	3,95	4,35	0,17	84168,67	1,03
2 out	4,45	4,5	4,25	4,05	4,1	0,16	84172,07	1,03
3 out		3,65	4	4,05	4,19	0,16	84170,75	1,03
4 out					4,02	0,16	84170,95	1,03
Tot out						0,64 (=1358,17 ft³/min)		1,03

TM 2	Speed	P TOT	Static P	Dynamic P	Pa	density kg/m³	Q volume flow rate m³/s	mass flow rate kg/s
1	3,51	16,50	8,14	8,36	84171,23	1,03	0,65	0,67
2	3,78	16,64	9,38	7,26	84170,13	1,03	0,70	0,72
3	3,49	12,85	8,02	4,83	84167,70	1,03	0,65	0,67
4	3,72	12,85	9,15	3,70	84166,57	1,03	0,69	0,71
5	3,97	12,10	10,46	1,64	84164,51	1,03	0,73	0,76
average	3,69					1,03	0,68	0,704
						ft³/min	1447,24	

Table 35: data of measurements for Coolerado performance (upper table refers to 21/04 and bottom table to 24/05)

densità kg/m³	flusso m³/s	m	h.R.	T wet corrispondente	dewpoint	Tdry	33	33	correzio	designed wet	T product air flow
0,9579	0,76	0,728	0	10,49		14,30022702	22,51	20,626	12,37409438	13,4741	
0,9556	0,76	0,7263	10	13,88	-2,64	11,99641835	19,12	17,52	15,48035027	16,5804	
0,9545	0,76	0,7254	15	15,5	2,95	10,89933084	17,5	16,035	16,96475574	18,0648	
0,9534	0,76	0,7246	20	16,88	7,08	9,965040879	16,12	14,771	18,22924929	19,3292	
0,9523	0,76	0,7237	25	18,26	10,38	9,032877835	14,74	13,506	19,49374283	20,5937	
0,9512	0,76	0,7229	30	19,57	13,14	8,149488201	13,43	12,306	20,6940954	21,7941	
0,9501	0,76	0,7221	35	20,99	15,53	7,194900737	12,01	11,005	21,99524094	23,0952	
0,9491	0,76	0,7213	40	21	17,62	7,180678882	12	10,996	22,00440393	23,1044	
0,948	0,76	0,7205	45	23,2	19,5	5,711255917	9,8	9,9797	24,02026321	25,1203	
0,9469	0,76	0,7196	50	24,3	21,21	4,974926312	8,7	7,9718	25,02819285	26,1282	
0,9458	0,76	0,7188	55	25,24	22,7	4,34630734	7,76	7,1105	25,88951454	26,9895	
0,9447	0,76	0,718	60	26,24	24,21	3,679427652	6,76	6,1942	26,80581422	27,9058	
0,9436	0,76	0,7171	65	27,19	25,55	3,04741917	5,81	5,3237	27,6762989	28,7763	
0,9426	0,76	0,7164	70	28,2	26,8	2,376955524	4,8	4,3982	28,60176157	29,7018	
0,9415	0,76	0,7155	75	28	27,98	2,506098245	5	4,5815	28,41850164	29,5185	
0,9404	0,76	0,7147	80	29,85	29,09	1,284367422	3,15	2,8863	30,11365603	31,2137	
0,9393	0,76	0,7139	85	30,68	30,14	0,736690453	2,32	2,1258	30,87418476	31,9742	
0,9382	0,76	0,713	90	31,48	31,14	0,210010851	1,52	1,3928	31,6072245	32,7072	
0,9371	0,76	0,7122	95	32,25	32,09	-0,29574074	0,75	0,6872	32,31277525	33,4128	
0,9361	0,76	0,7114	100	33	33	-0,787275078	0	0	33	34,1	

Table 36: Coolerado Performance calculation at a defined dry bulb temperature

densità kg/m³	flusso m³/s	m	T dry	T wet corrispondente	dewpoint	r h	30	30	correzio	designed wet	T product air flow
0,927	0,76	0,7045	40	24,63	19,16	9,202036632	15,37	14,084	25,91647404	27,0165	
0,9305	0,76	0,7072	39	23,89	18,3	9,067292077	15,11	13,845	25,15471195	26,2547	
0,9339	0,76	0,7098	38	23,17	17,45	8,91723108	14,83	13,589	24,41127586	25,5113	
0,9374	0,76	0,7124	37	22,45	16,59	8,766771426	14,55	13,332	23,66783977	24,7678	
0,9408	0,76	0,715	36	21,8	15,73	8,567886578	14,2	13,011	22,98854466	24,0885	
0,9443	0,76	0,7177	35	20	14,87	9,128996793	15	13,744	21,25550492	22,3555	
0,9478	0,76	0,7203	34	20,29	14	8,306277435	13,71	12,562	21,4375315	22,5375	
0,9512	0,76	0,7229	33	19,57	13,14	8,149488201	13,43	12,306	20,6940954	21,7941	
0,9547	0,76	0,7256	32	18,85	12,28	7,992202232	13,15	12,049	19,95065931	21,0507	
0,9582	0,76	0,7282	31	18,2	11,42	7,786553385	12,8	11,729	19,2713642	20,3714	
0,9617	0,76	0,7309	30	17,5	10,56	7,61287487	12,5	11,454	18,5462541	19,6463	
0,9652	0,76	0,7336	29	16,69	9,69	7,512105668	12,31	11,28	17,72035104	18,9204	
0,9687	0,76	0,7362	28	15	8,83	8,007606469	13	11,12	16,08810426	17,1881	
0,9722	0,76	0,7389	27	15,28	7,97	7,164743034	11,72	10,739	16,26096784	17,361	
0,9757	0,76	0,7415	26	14,56	7,1	6,999144848	11,44	10,482	15,51753175	16,6175	
0,9792	0,76	0,7442	25	13,85	6,24	6,82531361	11,15	10,217	14,78325866	15,8833	
0,9828	0,76	0,7469	24	13,2	5,37	6,609425956	10,8	9,986	14,10396354	15,204	
0,9863	0,76	0,7496	23	12,5	4,51	6,425673301	10,5	9,6211	13,37885344	14,4789	
0,9899	0,76	0,7523	22	11,69	3,64	6,317363873	10,31	9,447	12,55295038	13,653	
0,9935	0,76	0,7551	21	10	2,77	6,2058698	11	10,079	10,92070361	12,0207	
0,997	0,76	0,7577	20	10,28	1,91	5,950580813	9,72	9,9064	11,09356719	12,1936	
1,001	0,76	0,7608	19	9,56	1,04	5,778100098	9,44	8,6499	10,3501311	11,4501	
1,004	0,76	0,763	18	8,9	0,17	5,556271845	9,1	8,3383	9,661672984	10,7617	
1,008	0,76	0,7661	17	8,2	-0,7	5,366557204	8,8	8,0634	8,936562885	10,0366	
1,012	0,76	0,7691	16	7,39	-1,57	5,253148221	8,61	7,8893	8,110659823	9,21066	
1,015	0,76	0,7714	15	6,68	-2,44	5,06250917	8,32	7,6236	7,376386728	8,47639	
1,019	0,76	0,7744	14	6	-3,31	4,854019358	8	7,3304	6,669602623	7,7696	

Table 37: Coolerado Performance calculation at a defined relative humidity

	p<1000	1000<p<2000	2000<p<6000	p>6000
€/piece	26,3	23,67	22,355	21,04

Table 38: Collectors price per tube with respect to the quantity of tube

Fixed Costs	Solar cooling	Conventional €	Power	
Absorption Chiller	9997,98		30	
Solar Collectors	8167,58			
Cooling Tower	6655,46			
Radiant Ceiling	3071,73			
Storage Tank	5658,82			
Coolerado	6829,41			
Air Compression Chiller		9000		
Fan coil distribution		3000		
BOP	10%	30%		
BOP	4038,1	3600		
TOT FIXED	44419,09	15600	COST	28819,09
			10	
Annual Costs				h/year
EE, kW	2,5	11		3000
EE, kWh	7500	33000		€/kWh
EE, €	1200	5280		0,16
GAS, €	802,05			
O&M	312	624		
TOT Annual	2314,05	5904	BENEFIT	3589,95
Payback (anni)				8,03
ITALIAN CASE				
Annual Costs				h/year
EE, kW	2,50	11,00		3000,00
EE, kWh	7500,00	33000,00		€/kWh
EE, €	1575,00	6930,00		0,21
GAS, €	802,05			
O&M	312,00	624,00		
TOT Annual	2689,05	7554,00	BENEFIT	4864,95
TOT				
Payback (anni)				5,92

Table 39: Colombian and Italian Case of economic analysis for the cooling system

8 FIGURE LIST

Figure 1: Irradiation on collector surface and cooling demand over a day.	6
Figure 2: Worldwide distribution of the cooling power assisted by solar energy and	7
Figure 3: Map of UPB with a focus on Building 24 [8]	10
Figure 4: Schematic view of the roof of Building 24 [8].....	10
Figure 5: LabView Control screen of the system	11
Figure 6: Schematic diagrams of an evacuated tube collector[9]	12
Figure 7: Comparison of the efficiency of various collectors a two irradiance levels: 500 W/m ² and 1000 W//m ² [10].....	13
Figure 8: direction and inclination of the collectors	13
Figure 9: Manifold and heat pipe sketch[41].....	14
Figure 10: Heat pipe dimensions[41]	14
Figure 11: Heat pipe details [41].....	14
Figure 12: Manifold and support component of the collectors[41]	14
Figure 14: Radiation input and heat loss from a collector[10]	16
Figure 13: Energy losses in a solar collector (Peter Lund, 2016)	16
Figure 15: Carnot cycles for a combined heat pumping facility such as an absorption heat[12].....	18
Figure 16: The theory of absorption and evaporation[13]	20
Figure 17: Flow chart of absorption chiller[13].....	20
Figure 18: Hot water lithium bromide absorption chiller [13].....	20
Figure 19: Pressure-temperature diagram of a single effect, libr-water absorption[42]	21
Figure 20 : Duhring chart of the water–lithium bromide absorption cycle[10]	21
Figure 21: Availability flow balance of the absorption system [10].	23
Figure 22: Cooling Capacity versus Chilled Water Outlet Temp [13].....	25
Figure 23: Cooling Capacity versus Cooling Water Inlet Temp [13].....	25
Figure 24 : Cooling Capacity versus Hot Water Inlet Temp [13].....	25
Figure 25: Gaiser inertia buffer tank [15].	26
Figure 26: Glaciar Closed circuit cooling tower [17]	28
Figure 27: Evaporative cooling process[18]	28
Figure 28: Schematic picture of closed circuit adiabatic cooler[17].....	29
Figure 29: Celdek series[17].....	29
Figure 30: Cooling tower's water distribution[17].....	29
Figure 31: Water-air heat exchange[17]	29
Figure 32: Dimensions of the cooling tower[17].....	30
Figure 33: Cooling capacity chart of the Closed adiabatic cooler wrt the ambient conditions and outlet water temperature[17]	31
Figure 34: Radiation cooling technology of the water capillary mats [19]	32
Figure 35: Capillary mats assembled in a superimposed form on the “false ceiling”, of the top of Building 24	33
Figure 36: Hot water pump (used in section 1 and 2)	34
Figure 37:Chilled water tank-Chiller pump (section 3)	35
Figure 38: Chilled water-capillary mats pump(section 4)	35
Figure 39: Cooling water pump (section 5).....	36
Figure 40: Model M50 Coolerado cooler system[23]	37
Figure 41: Schematic picture of indirect adiabatic cooling process [22]	38
Figure 42: Heat and mass exchanger based on M-cycle [43]	39
Figure 43: Schematic diagram of the Coolerado cooler [44]	39
Figure 44: Perforated cross flow heat and mass exchanger [43].....	39

Figure 45: Design of the Heat and Mass Exchanger [43]	40
Figure 46: Coolerado M50 different views [24]	41
Figure 47: Installation of the coolerado at Building 24.....	41
Figure 48: Expansion tank first step[26]	45
Figure 49: Expansion tank second step [26]	45
Figure 50: Temperature chart history of the 1stTM	48
Figure 51: Temperature chart focus on chilled part of the system during the beginning of the air conditioning of the 1stTM.....	49
Figure 52: Temperature chart of the system during the end of the air conditioning of the 1stTM.....	50
Figure 53: AiR Conditioning performance between 1 st and 2 nd TM.....	51
Figure 54: difference in temperature inlet the capillary mats during air cond time between 1 st and 2 nd TM due to difference thermal inertia.	52
Figure 55: The property chart of LiBr/H ₂ O solution with crystallization curve.[28]	53
Figure 56: Difference in temperature during air conditioning in 2nd TM and 3rd TM.....	54
Figure 57: Comparison of the effectiveness of the heat exchange in the evaporator between 2ndTM and 3rdTM.....	54
Figure 58: Difference in T _{evap} between 3 rd and 4 th TM	56
Figure 59: Difference in T _{gen} between 3 rd and 4 th TM	56
Figure 60 Performance curve extrapolated of “RXZ-11.5” wrt T _{evap}	59
Figure 61 Performance curve extrapolated of “RXZ-11.5” wrt T _{cond}	60
Figure 62: Performance curve extrapolated of “RXZ-11.5” wrt T _{gen}	60
Figure 63: Collectors thermal efficiency and solar radiation during 3 rd TM	64
Figure 64: power stored by solar collectors in 17/05/2017.....	65
Figure 65: Radiation incident in the Building 24 of the University in a typical sunny day of Medellín.	66
Figure 66: picture taken the 30/05/2017 at 16:09 showing trees shadows on the collectors.....	66
Figure 67: Collector performance analysis during 4 th TM.....	67
Figure 68: Nominal performance of the Coolerado in different external condition	69
Figure 69: Sketch of point of measurements in the sections at the outlet of the Coolerdo’s duct.	69
Figure 70: Sketches of point of measurements in the sections of the Coolerdo’s duct	70
Figure 71: Coolerado Performance at a defined dry bulb temperature.....	72
Figure 72: Coolerado Performance at a defined dry bulb temperature and relative humidity	73
Figure 73: thermal storage specific cost per €/litre[27]	75
Figure 74: Specific costs of Air cooled Chillers [35]	76
Figure 75: Results of the payback period between Solar and Conventional cooling system for Colombia case	78
Figure 76 Results of the payback period between Solar and Conventional cooling system for Italy case.....	79
Figure 77: Plant distribution mats – UPB.....	83
Figure 78: Operational point of section from the chilled water storage tank to the capillary mats (Section 4)	84
Figure 79: Operational point of section from the collectors to the hot water storage tank (Section 1).....	84
Figure 80: Operational point of the section from the cooling tower to the chiller (Section 5).....	84

9 TABLE LIST

Table 1: Specifications of the evacuated tube collectors (ECTs)	15
Table 2: Energy and Mass Balance Equations of Absorption System Components [10]	22
Table 3: Specifications of RXZ absorption chiller [14].....	24
Table 4: Specifications of water storage tank [15]	26
Table 5: Specifications of the auxiliary heater [16].....	27
Table 6: Closed circuit adiabatic cooling tower specifications[17]	30
Table 7: Specification of capillary mats installed [20].....	33
Table 8: Pipeline specifications	34
Table 9: Operational point known of the pumps present in the system.....	36
Table 10: Specifications of Coolerado M50 [23]	40
Table 11: Specification of Piralu Air duct for the coolerado[25]	44
Table 12: Weather data registered in the 1 st TM.....	46
Table 13: 1stTM steps followed	47
Table 14: Weather data registered in the 2 nd TM.....	50
Table 15: 2ndTM steps followed.....	50
Table 16: Comparison in air conditioning performance between 1 st and 2 nd TM with and without the use of coolerado	51
Table 17: comparison of cooling performance of the Chiller between 1 st and 2 nd TM	51
Table 18: Weather data registered in the 3 rd TM	52
Table 19: 3rdTM steps followed	52
Table 20: Weather data registered in the 4 th TM	55
Table 21: 4th TM steps followed.....	56
Table 22: Weather data registered in the 3 rd TM	57
Table 23: 5 th TM steps followed.....	57
Table 24: Performance results of the absorption cooling system during the five TMs.....	61
Table 25: start up period of TMs.....	61
Table 26: thermal efficiency's coefficients of the collectors[29].....	64
Table 27: Results of performance analysis of solar collector installed in the Building 24.....	66
Table 28: Results of the performance analysis of the Coolerado	71
Table 29: Experimental and nominal air product temperature of the Coolerado.....	72
Table 30: Comparison between datasheet capacity and actual capacity in Medellin condition of Coolerado.	73
Table 31: Specific Cost of Absorption refrigeration Chiller[27].	74
Table 32: improvement in performance of an air cooled Chiller.....	77
Table 33: payback period of actual configuration of the solar cooling air conditioning system with respect to a conventional one	78
Table 34: Data registered and calculated during all test measurement.....	85
Table 35: data of measurements for Coolerado performance (upper table refers to 21/04 and bottom table to 24/05)	86
Table 36: Coolerado Performance calculation at a defined dry bulb temperature.....	86
Table 37: Coolerado Performance calculation at a defined relative humidity	86
Table 38:Collectors price per tube with respect to the quantity of tube	87
Table 39: Colombian and Italian Case of economic analysis for the cooling system.....	87

10 GLOSSARY

1. Absolute humidity: Absolute humidity is the actual mass of water vapor in the air water vapor mixture. Absolute humidity may be expressed in pounds of water vapor (lbs). [3]
2. BTUs: The British Thermal Units is a traditional unit of heat; it is defined as the amount of heat required to raise the temperature of one pound of water by one degree Fahrenheit. It is part of the British Imperial system of units.[1] Its counterpart in the metric (SI) system is the calorie or Joules: 1btu= 1055,06 Joules=2521.64 cal
3. CFM: cubic feet per minute is a flow rate unit. $1\text{CFM} \approx 1.699 \text{ m}^3/\text{h} \approx 0.471947 \text{ l/s}$
4. COP: The coefficient of performance (sometimes CP or CoP) of a heat pump, refrigerator or air conditioning system is a ratio of heat removed from the cold reservoir or cooling provided to work required. Higher COPs equate to lower operating costs. The COP usually exceeds 1, especially in heat pumps, because, instead of just converting work to heat (which, if 100% efficient, would be a COP_hp of 1), it pumps additional heat from a heat source to where the heat is required.[36]
5. Dewpoint: The Dew Point is the temperature at which water vapor starts to condense out of the air and becomes completely saturated. Above this temperature the moisture will stay in the air. The dew point temperature is an indicator of the actual amount of moisture in air. The dew-point temperature is expressed in degrees and like humidity ratio; it represents an absolute measure of the moisture in the air at a constant pressure. If the dew-point temperature is close to the air temperature, the relative humidity is high, and if the dew point is well below the air temperature, the relative humidity is low [3].
6. Dry Bulb Temperature (DBT): The Dry Bulb Temperature refers to the ambient air temperature measured using a normal thermometer freely exposed to the air but shielded from radiation and moisture. It is called "Dry Bulb" because the air temperature is indicated by a thermometer not affected by the moisture of the air. The dry bulb temperature is an indicator of heat content of the air. As the DB temperature increases, the capacity of moisture the airspace will hold also increases. The dry bulb temperature is usually given in degrees Celsius (°C) or degrees Fahrenheit (°F). [2]
7. EER: Energy Efficiency Ratio. This is the ratio of cooling capacity in BTUs per hour to the power input in watts, or how well it cools compared to how much energy it needs. The higher the EER, the more efficient the unit.[37]
8. External Static Pressure (ESP): It is the pressure that the fan has to overcome due to ducts and fitting losses to give the required space ventilation and cooling requirements at least equal to the designed flow. It is a function of the length, equivalent diameter, velocity, frictional losses and density of the media flowing, commonly air. Fan manufacturers also rate the fans static pressure minimum requirements that the fan will operate normally. ESP is the static pressure created downstream of the air handling unit that the fan must overcome- this includes duct friction losses, room static pressures, etc. This could included a negative static pressure on the pull side of the fan and a positive pressure on the push side, or any combination of pressures the fan must overcome. ESP is different from total static pressure in that TSP adds the pressure losses of all internal units such as filter banks, heating coils and dampers to the ESP value to give you the total pressure the fan/s must overcome.
9. GPM: gallon per minute (flow rate unit) $1 \text{ GPM} = 0.0630902 \text{ l/s}$
10. Heat of combustion: The heating value (or energy value or calorific value) of a substance, usually a fuel or food (see food energy), is the amount of heat released during the combustion of a specified amount of it. The energy value is a characteristic for each substance. It is measured in units of energy per unit of the substance, usually mass, such as: kJ/kg, kJ/mol, kcal/kg, Btu/lb. Heating value is commonly determined by use of a bomb calorimeter. The quantity known as lower heating value (LHV) (net calorific value (NCV) or lower calorific value (LCV)) is determined by subtracting the heat of vaporization of the water vapor from the higher heating value (HHV). This treats any H₂O formed as a vapor. The energy required to vaporize the water therefore is not released as heat. LHV calculations assume that the water component of a combustion process

is in vapor state at the end of combustion, as opposed to the higher heating value (HHV) (gross calorific value or gross CV) which assumes that all of the water in a combustion process is in a liquid state after a combustion process.

11. Humidity: The term humidity describes the quantity of water vapor in air. If the air holds 50% of its capacity, the humidity would be 50%. If the humidity is low, then the capacity to hold more water is higher, and a greater amount of evaporation takes place. It can be expressed as an absolute, specific or a relative value.[38]

12. IWC: Inches of water column (inch WC), inAq, Aq, or in H₂O is a non-SI unit for pressure. It is used for measuring small pressure differences across an orifice, or in a pipeline or shaft. Inches of water can be converted to a pressure unit using the formula for pressure head. An inch of water column (iwc) is synonymous with an inch of water gauge (iwg). It is defined as the pressure exerted by a column of water of 1 inch in height at defined conditions. For example, 39 °F (4 °C) at the standard acceleration of gravity; 1 inAq is approximately equal to 249 pascals at 0 °C [39].

13. Latent heat: Latent heat is the heat energy involved in the phase change of water. The latent heat will only change the structure or phase of the material without change to temperature.[3]

14. Lineal expansion thermal coefficient: describes how the size of an object changes with a change in temperature. Specifically, it measures the fractional change in size per degree change in temperature at a constant pressure. Unit [K⁻¹]

15. Lbs: The acronym stands for pound-mass, is a unit of mass used in the imperial, United States customary and other systems of measurement: 1 lbs = 0.453592 kg.

16. PEC: Purchased Equipment Cost

17. PP: The acronym of PP stands for polypropylene. Polypropylene is a thermoplastic "addition polymer" made from the combination of propylene monomers. It is the world's second-most widely produced synthetic plastic, after polyethylene. [40]

18. LPG: Liquefied petroleum gas or liquid petroleum gas (LPG or LP gas), also referred to as simply propane or butane, are flammable mixtures of hydrocarbon gases used as fuel in heating appliances, cooking equipment, and vehicles.

19. PN The acronym of PN stands for "nominal pressure". It indicates the maximum pressure of the fluid that can be carried by the pipe when the fluid is at 20 °C, expressed in bar.

20. Psychrometric Chart: The psychrometric chart is a graphical representation that describes the relationships between the air temperature and relative humidity. Although complicated in appearance, this chart can be used to establish state points and is used to calculate specific humidity, dew point and vapor pressure.[38]

21. Relative humidity: Relative Humidity or RH is the actual amount of moisture in the air compared to the total or maximum moisture the air can hold at a given temperature. When air has 50 percent relative humidity (RH), we say it is 50 percent saturated (the terms are numerically so close that we use them interchangeably). Obviously, as air approaches 100 percent saturation, it can take on less and less water until at 100 percent RH, the air cannot hold more water. Relative humidity is determined by comparing the "wet-bulb" and "dry-bulb" temperature readings. Dry bulb and wet bulb temperatures are taken simultaneously and then plotted on a psychrometric chart. Relative humidity is determined by the value at the intersection of two temperature lines. [2]

22. Sensible Heat: The heat used to change the temperature of the air. Sensible heat will always cause a change in the temperature of the substance. [3]

23. Specific heat capacity: The specific heat capacity of a substance is the amount of energy needed to change the temperature of 1 kg of the substance by 1°C. In SI the unit is J/(kg*K); anyway for engineering purposes is often used in KJ/(kg* °C). It generally depends on temperature.

24. Specific humidity or (humidity ratio): is the ratio between the actual mass of water vapor present in moist air - to the mass of the dry air. The humidity ratio is very useful inn evaporative cooling because it provides the measure of the amount of moisture absorbed by the air stream and is useful in determining the

spray water requirements. Specific Humidity is normally expressed in grains of water vapor /lb of dry air and may also be expressed in the units of pounds of water vapor/lb of dry air or grams of water vapor /kg of dry air. [38]

25. USRT: United State Refrigeration Tons (capacity/power of refrigeration unit $1\text{USRT}\approx 3.5\text{ kW}$)

26. Wet Bulb Temperature: The Wet Bulb temperature is the temperature measured by using a thermometer whose glass bulb is covered by a wet wick/cloth. The wet bulb temperature is indicator of moisture content of air. Wet bulb temperature is very useful in evaporating cooling processes as the difference between the dry bulb and wet bulb temperature is a measure of the cooling efficiency. At 100% relative humidity, the wet bulb temperature equals dry bulb temperature. [3]

27. Wrt: with respect to (abbreviation).

11 REFERENCES

- [1] O. Uribe, J. Martin, M. Garcia-Alegre, M. Santos, and D. Guinea, "Smart Building: Decision Making Architecture for Thermal Energy Management," *Sensors*, vol. 15, no. 11, pp. 27543–27568, Oct. 2015.
- [2] COLCIENCIA Colombia, "Presentacion del proyecto," 2011.
- [3] "LEED v4 for BUILDING DESIGN AND CONSTRUCTION LEED v4 Building Design and Construction Addenda," 2017.
- [4] M. Rodríguez-Becerra, G. Espinoza, and D. Wilk, "Gestión ambiental en América Latina y el Caribe Evolución, tendencias y principales prácticas."
- [5] "→ Refrigerants Environmental Data. Ozone Depletion and Global Warming Potential. 2 of 2," *Ozone Deplet. Potential*, vol. 1, 2006.
- [6] P. J. Wilbur and C. E. Mitchel, "Solar absorption air conditioning alternative," *Sol. Energy*, vol. 17, pp. 193–199, 1975.
- [7] W. Sparber, A. Napolitano, and P. Melograno, "OVERVIEW ON WORLD WIDE INSTALLED SOLAR COOLING SYSTEMS," 2007.
- [8] U. Centro de Investigación en refrigeración y climatización CIRCLI, "Proyecto Aire acondicionado Solar," 2011.
- [9] S. Kalogirou, *Solar Energy Engineering - Processes and Systems*, 1st editio. Academic Press - Elsevier, 2009.
- [10] S. Kalogirou, *Processes and System*, 1st ed. 2009.
- [11] J. A. Duffie and W. A. Beckman, *Solar_Engineering_of_Thermal_Processes.pdf*, Second. John Wiley & Sons, INC, 1980.
- [12] K. E. Herold, R. Radermacher, and S. Klein, *Absorption Chillers and Heat Pumps*, CRC Press. United State of America, 1996.
- [13] S. Lucy, N. Energy, and T. Co, "Operation Manual of Hot Water Operated 目录 Content."
- [14] L.-C. I. U. Shandong Lucy New Energy Technology Co., "Especificaciones RXZ11." .
- [15] Lapesa, "Domestic Hot Water Production and storaga Tanks," 2016.
- [16] OKA grupo empresarial, "CALDERA MURAL MIXTA OKA," 2016.
- [17] G. I. S.a.s., "Adial cool Cweek - Enfriador Adiabático de Circuito Cerrado." pp. 3–6, 2016.
- [18] Y. A. Cengel and M. A. Boles, *Thermodynamics an engineering approach*, 5th ed. 2006.
- [19] JSC Wasserkabel Baltic, "Water capillary mats – energy-efficient one system technology for heating and cooling."
- [20] S. Werner, "Cotización ClimaActive – Esterillas de Agua, Instalación en el proyecto Trigeneración en el Bloque 24 de la Universidad UPB en Medellín," 2016.
- [21] desarrollo y calidad en refrigeración y climatización C. Grupo de energía y termodinamica - Centro de investigación, "Informe Producto No. 2 del Proyecto: Integración de tecnologías energéticamente eficientes en sistemas de climatización operados con energía térmica," no. 2, pp. 1–22, 2016.
- [22] G. Viacheslav, "SYSTEMS BASED ON MAISOTSENKO CYCLE Coolerado Coolers," 2012.
- [23] Corporation Coolerado, "Coolerado Owner ' s Manual YOUR INSTALLATION AND SERVICE PROVIDER," pp. 1–20, 2013.
- [24] J. O. B. Name and C. Fan, "M50 Submittal Data Sheet," pp. 1–3.
- [25] piralu.com, "PiR-ALU." [Online]. Available: <http://www.piralu.com/web-i/presentacion-i.htm>. [Accessed: 21-Feb-2017].
- [26] Watts, "Thermal Expansion - Learn About." [Online]. Available: <http://www.watts.com/pages/learnabout/thermalExpansion.asp>. [Accessed: 15-Feb-2017].
- [27] P. Silva, *Macchine ad Assorbimento*. 2017.
- [28] X. Liao and R. Radermacher, "Absorption chiller crystallization control strategies for integrated cooling heating and power systems," 2007.
- [29] Enertech GmbH, "Solar Collector Factsheet C1207," *Solartechnik Prufung Forsch.*, pp. 2–3, 2010.
- [30] H. Marie, "Efficient Solar Cooling : First Ever Non-tracking solar collectors powering a double effect absorption chiller," *Univ. California, Merced*, 2011.
- [31] B. Widjolar, "Performance Analysis of XCPC Powered Solar Cooling Demonstration Project," UC

Merced Electron. Theses Diss., 2013.

- [32] "Portable Reference Technology."
- [33] J. R. Turner, *The Handbook of Project Based Management*. McGraw Hill, 2009.
- [34] E. Colombo, "Thermoeconomics: economic analysis," 2016.
- [35] P. Silva, "Macchine frigorifere," 2017.
- [36] "A new era of Seasonal Efficiency has begun," *Daikin.co.uk*.
- [37] J. Orloff, "Energy Efficiency Ratio of Room Air Conditioners," *Frugal Living*, 2016.
- [38] I. A. Bhatia, "Principles of Evaporative Cooling System," vol. 231, 2012.
- [39] National Physical Laboratory, "My pressure gauge is scaled in 'inches' - what does this mean? (FAQ - Pressure) : FAQs : Reference : National Physical Laboratory," 2007. [Online]. Available: [http://www.npl.co.uk/reference/faqs/my-pressure-gauge-is-scaled-in-'inches'-what-does-this-mean-\(faq-pressure\)](http://www.npl.co.uk/reference/faqs/my-pressure-gauge-is-scaled-in-'inches'-what-does-this-mean-(faq-pressure)). [Accessed: 20-Feb-2017].
- [40] "DISCOVERY OF POLYPROPYLENE AND THE DEVELOPMENT OF A NEW HIGH-DENSITY POLYETHYLENE."
- [41] L. Shandong Lucy New Energy Technology Co., "Especificaciones Colectores Solares S-HSC-70-20.pdf."
- [42] M. Motta, D. Energetica, and P. Milano, "Technology Status , including latest developments."
- [43] "A Technical Description of the Maisotsenko cycle.," 2012. [Online]. Available: http://www.idalex.com/technology/how_it_works_-.
- [44] C. Company, "How coolerado air conditioners work.," 2011. [Online]. Available: <http://www.coolerado.com/products/how-coolerado-works/>. [Accessed: 14-Apr-2017].